BENCHMARKING AND APPLICATION OF DENSITY FUNCTIONAL METHODS IN COMPUTATIONAL CHEMISTRY

by

BRIAN N. PAPAS

(Under Direction the of Henry F. Schaefer III)

ABSTRACT

Density Functional methods were applied to systems of chemical interest. First, the effects of integration grid quadrature choice upon energy precision were documented. This was done through application of DFT theory as implemented in five standard computational chemistry programs to a subset of the G2/97 test set of molecules. Subsequently, the neutral hydrogen-loss radicals of naphthalene, anthracene, tetracene, and pentacene and their anions where characterized using five standard DFT treatments. The global and local electron affinities were computed for the twelve radicals. The results for the 1-naphthalenyl and 2-naphthalenyl radicals were compared to experiment, and it was found that B3LYP appears to be the most reliable functional for this type of system. For the larger systems the predicted site specific adiabatic electron affinities of the radicals are 1.51 eV (1-anthracenyl), 1.46 eV (2-anthracenyl), 1.68 eV (9-anthracenyl); 1.61 eV (1-tetracenyl), 1.56 eV (2-tetracenyl), 1.82 eV (12-tetracenyl); 1.93 eV (14-pentacenyl), 2.01 eV (13-pentacenyl), 1.68 eV (1-pentacenyl), and 1.63 eV (2-pentacenyl). The global minimum for each radical does not have the same hydrogen removed as the global minimum for the analogous anion. With this in mind, the global (or most preferred site) adiabatic electron affinities are 1.37 eV (naphthalenyl), 1.64 eV (anthracenyl), 1.81 eV (tetracenyl), and 1.97 eV (pentacenyl). In later work, ten (scandium through zinc) homonuclear transition metal trimers were studied using one DFT functional. Electronic ground states and bond lengths for equilateral triangles were: $Sc_3$ ($^2A_1'$, 2.83 Å), $Ti_3$ ($^7E'$, 2.32), $V_3$ ($^2E''$, 2.06), $Cr_3$ ($^{17}E'$, 2.92), $Mn_3$ ($^{16}A_2'$, 2.73), $Fe_3$ ($^{11}E''$, 2.24), $Co_3$ ($^6E''$, 2.18), $Ni_3$ ($^3A_2''$,

2.23), $Cu_3$ ($^2E'$, 2.37), $Zn_3$ ($^1A_1'$, 2.93). Vibrational frequencies, several low-lying electronic states, and trends in bond lengths and atomization energies are discussed. The predicted dissociation energies $\Delta E$ ($M_3 \rightarrow M_2 + M$) are 49.4 kcal $mol^{-1}$ ($Sc_3$), 64.3 kcal $mol^{-1}$ ($Ti_3$), 60.7 kcal $mol^{-1}$ ($V_3$), 11.5 kcal $mol^{-1}$ ($Cr_3$), 32.4 kcal $mol^{-1}$ ($Mn_3$), 61.5 kcal $mol^{-1}$ ($Fe_3$), 78.0 kcal $mol^{-1}$ ($Co_3$), 86.1 kcal $mol^{-1}$ ($Ni_3$), 26.8 kcal $mol^{-1}$ ($Cu_3$), and 4.5 kcal $mol^{-1}$ ($Zn_3$).

INDEX WORDS: Density Functional Theory, precision, G2-97, Polycyclic Aromatic Hydrocarbon, PAH, electron affinity, transition metal trimers, $M_3$.

# BENCHMARKING AND APPLICATION OF DENSITY FUNCTIONAL METHODS IN COMPUTATIONAL CHEMISTRY

by

BRIAN N. PAPAS

B.S., Michigan State University, 2002

A Dissertation Submitted to the Graduate Faculty of The University of Georgia in Partial Fulfillment of the Requirements for the Degree

DOCTOR OF PHILOSOPHY

ATHENS, GEORGIA

2006

# BENCHMARKING AND APPLICATION OF DENSITY FUNCTIONAL METHODS IN COMPUTATIONAL CHEMISTRY

by

BRIAN N. PAPAS

Major Professor: Henry F. Schaefer III

Committee: Geoff Smith
Nigel Adams

Electronic Version Approved:

Maureen Grasso
Dean of the Graduate School
The University of Georgia
May 2006

TABLE OF CONTENTS

Page

LIST OF TABLES ..... vi

LIST OF FIGURES ..... vii

CHAPTER

1 INTRODUCTION AND BACKGROUND MATERIAL ..... 1

1.1 Introduction ..... 1

1.2 Theory and Implementations ..... 1

1.3 Prospectus ..... 3

1.4 References ..... 3

2 CONCERNING THE PRECISION OF STANDARD DENSITY FUNCTIONAL PROGRAMS: GAUSSIAN, MOLPRO, NWCHEM, Q-CHEM, AND GAMESS .4

2.1 Abstract ..... 5

2.2 Introduction ..... 5

2.3 Methods ..... 5

2.4 Results ..... 7

2.5 Conclusions ..... 10

2.6 Acknowledgements ..... 10

2.7 Tables and Figures ..... 10

2.7 References ..... 21

3 THE NAPHTHALENYL, ANTHRACENYL, TETRACENYL, AND PENTACENYL RADICALS, AND THEIR ANIONS ..... 23

3.1 Abstract ..... 24
3.2 Introduction ..... 24
3.3 Methods ..... 25
3.4 Results and Discussion ..... 27
3.5 Conclusions ..... 31
3.6 Acknowledgments ..... 32
3.7 Tables and Figures ..... 32
3.8 References ..... 37
4 HOMONUCLEAR TRANSITION METAL TRIMERS ..... 40
4.1 Abstract ..... 41
4.2 Introduction ..... 41
4.3 Methods ..... 42
4.4 Results ..... 44
4.5 Conclusions ..... 61
4.6 Acknowledgements ..... 62
4.7 Tables and Figures ..... 62
4.7 References ..... 67
5 CONCLUSIONS ..... 79

# LIST OF TABLES

Page

Table 2.1: G2/97 subset of neutral molecules considered in the present research.. .....10

Table 2.2: Specification of the numerical integration grids used in this study.....11

Table 2.3: "Exact" energies (Hartrees), computed as averages of energies from all programs with the "Large" grid quadratures.....12

Table 3.1: Ipso C-C-C angles (in degrees) for the radicals and their anions.. .....33

Table 3.2: C-C bond lengths (in Å) adjacent to the removed hydrogen atom. .....34

Table 3.3: EAs (in eV) with ZPVE corrected values in parentheses. .....35

Table 3.4: ZPVE corrected energies (kcal/mol) relative to lowest energy species.. .....36

Table 3.5: Global AEAs (eV), with ZPVE corrected values in parentheses.. .....36

Table 4.1: Low-lying electronic states of first row transition metal trimers.. .....62

Table 4.2: Harmonic vibrational frequencies (in $cm^{-1}$) for transition metal trimers.....63

Table 4.3: Summary of electronic ground states for the transition metal trimers in $D_{3h}$ symmetry.....64

# LIST OF FIGURES

Page

Figure 2.1: Gamess error curves. ....14

Figure 2.2: Molpro error curves. ....15

Figure 2.3: NWChem error curves ....16

Figure 2.4: QChem error curves. ....17

Figure 2.5: Gaussian 94 error curves.. ....18

Figure 2.6: BLYP results by molecule type. ....19

Figure 2.7: B3LYP results by molecule type. ....20

Figure 3.1: IUPAC numbering scheme for (a) naphthalene, (b) anthracene, (c) tetracene, and (d) pentacene. ....32

Figure 3.2: EAs vs Number of Rings ....33

Figure 4.1: Bond lengths (Å) of $D_{3h}$ transition metal trimers computed with the BP86 method ..64

Figure 4.2: Atomization energies (eV) of $D_{3h}$ transition metal trimers computed with the BP86 method ....65

Figure 4.3: $M_3 \rightarrow M_2 + M$ dissociation energies (eV) of $D_{3h}$ transition metal trimers computed with the BP86 method. ....66

# CHAPTER 1

# INTRODUCTION AND BACKGROUND MATERIAL

## 1.1 INTRODUCTION

"Errors using inadequate data are much less than those using no data at all."

-Charles Babbage

With infinite computational capabilities, all chemical questions could be answered through *ab inito* methods. While modern computers have made significant progress over the Analytic Engine designed by Charles Babbage, they have not yet reached this point. As a result, compromises must be made, and all answers found must be understood within the framework of these compromises.

This delicate balancing act between accuracy and attainability is the paramount challenge faced by computational chemists. With small and well-behaved systems, it is often possible to describe physical quantities to a high degree of accuracy. Describing more complicated systems necessitates a loss in accuracy. It is in this paradigm where Density Functional Theory (DFT) really shines.

## 1.2 THEORY AND IMPLEMENTATIONS

The fundamental precept of DFT is that the ground state electronic energy is determined, in a one-to-one manner, by the electronic density ρ. This was first proven by Hohenberg and Kohn.[1] The beauty of this result lies in the resultant reduction of variables compared to orbital-based theories. Systems with N electrons have 4N variables (three spatial and one spin for each electron) if each orbital is described. Energies computed directly from the density only require three coordinates.

Such computations require the definition of an energy functional, $E[\rho]$. From the perspective of wave mechanics, it is clear that this can be divided into three terms: the kinetic energy $T[\rho]$; the electron-nuclei attraction $E_{ne}[\rho]$; and the electron-electron repulsion $E_{ee}[\rho]$. Taking further convention from

Hartree-Fock theory, $E_{ee}[\rho]$ can be divided into Coulomb and Exchange parts, $J[\rho]$ and $K[\rho]$ , respectively. Equations (1.1) and (1.2) show the straightforward expressions for $E_{ne}[\rho]$ and $J[\rho]$. In $E_{ne}[\rho]$ the summation is over the atoms present in a molecule,

$$E_{ne}[\rho] = \sum_a \int \frac{Z_a \rho(\mathbf{r})}{|\mathbf{R}_a - \mathbf{r}|} d\mathbf{r} \tag{1.1}$$

$$J[\rho] = \frac{1}{2} \iint \frac{\rho(\mathbf{r})\rho(\mathbf{r}')}{|\mathbf{r} - \mathbf{r}'|} d\mathbf{r} d\mathbf{r}' \tag{1.2}$$

while in both equations the integrations are over all space. This leaves the kinetic energy and exchange terms the only unknowns.

It is here that modern DFT methods depart from the ideal proposed by Hohenberg and Kohn.[1] This occurs with a partial return to oribital based theory as described by Kohn and Sham.[2] At its core, modern DFT methods split the kinetic energy into two terms, one which can be computed exactly and another which is a small correction. Consider a Hamiltonian in which the potential has been split into two parts, $\mathbf{V}_{ext}(\lambda)$ and a scaled $\mathbf{V}_{ee}$ (Eq. 1.3). With $\lambda = 1$, $\mathbf{V}_{ext}(\lambda)$ will be $\mathbf{V}_{ne}$, the electron nuclei attraction

$$\mathbf{H}_\lambda = \mathbf{T} + \mathbf{V}_{ext}(\lambda) + \lambda \mathbf{V}_{ee} \tag{1.3}$$

potential. As l is scaled down to zero, the external potential $\mathbf{V}_{ext}(\lambda)$ is adjusted such that the density resulting from finding the solution is always the same, the density of the true system. When $\lambda = 0$, the potential corresponds to a system with no electron-electron interaction. Since $\mathbf{V}_{ext}(\lambda)$ is assumed to not depend upon inter-electron distance, the exact solution to the Schrödinger equation is a Slater determinant of molecular orbitals, $\varphi_i$. For such a system, the kinetic energy is easily defined as equation 1.4. This is, however, only an approximation for the real kinetic energy, which would correspond to the $\lambda = 1$ case.

$$T_S = \sum_i^N \left\langle \varphi_i \left| -\frac{1}{2} \nabla^2 \right| \varphi_i \right\rangle \tag{1.4}$$

The remaining kinetic energy is absorbed into an exchange-correlation term.

It is thus that we are left with the definition of the DFT energy (Eq. 1.5). Te remaining unknown term is $\underline{E}_{xe}[\rho]$, the exchange-correlation functional. It is this functional which is the Holy Grail of DFT

$$E_{DFT} = T_S + E_{ne}[\rho] + J[\rho] + E_{xc}[\rho] \tag{1.5}$$

developmental research. Rather than go into excessive detail, it suffices to say that numerous functionals have been developed, to date.

Some of these functionals have been developed with general use in mind, while others are more specialized. There is one commonality between most: they result in non-analytic integrals when solving for the molecular orbitals. As a result, a grid quadrature must be chosen for numerical integration.

## 1.3 Prospectus

It is within this DFT framework that the research presented within this dissertation is performed. In Chapter 2 the implications of the choice of grid quadrature upon the precision of computed energies is evaluated. This particular aspect of the approximations used in DFT methods is often overlooked, yet must be considered when determining error-bars. Chapter 3 presents the results of applying several different functionals to dehydrogenated linear polycyclic aromatic hydrocarbons and their anions, with the intent of determining their electron affinities. Finally, Chapter 4 discusses the application of DFT to one particularly onerous set of molecules: homonuclear transition metal trimers.

## 1.4 References


1 P. Hohenberg and W. Kohn, *Phys. Rev.* **136**, B864 (1964).

2 W. Kohn and L. J. Sham, *Phys. Rev.* **140**, A1133 (1965).

# CHAPTER 2

## CONCERNING THE PRECISION OF STANDARD DENSITY FUNCTIONAL PROGRAMS: GAUSSIAN, MOLPRO, NWCHEM, Q-CHEM, AND GAMESS[*]

[*] B. N. Papas and H. F. Schaefer. To be submitted to *THEOCHEM.*

## 2.1 ABSTRACT

The density functionals BLYP and B3LYP in five major quantum chemistry packages have been applied to 83 molecules found in the G2/97 test set. The goal of this research is to provide guidelines for researchers concerning the precision to be expected for the various integration grid quadratures implemented within those codes. This work also tests the compatibility of the different methods. These program packages are: GAUSSIAN, MOLPRO, NWCHEM, Q-CHEM, and GAMESS.

## 2.2 INTRODUCTION

Since its advent, Density Functional Theory (DFT) has found its way to the top of the list of methods of choice for the quantum mechanical study of very large molecular systems. A particular aspect of DFT, namely choice of integration grid quadrature, is often neglected by novice users. As discussed by Martin, Bauschlicher, and Ricca,[1] the choice of integration grid quadrature can affect DFT results, and in rare cases can result in convergence to incorrect orbital occupations. The effects of this precision are often amplified when computing numerical derivatives and anharmonic force fields.[2] As such, it is important to understand which integration grid quadratures can be used in different programs, and what precision should be expected from them.

## 2.3 METHODS

Two popular DFT functionals and five computational software packages are tested within this study. The correlation functional of Lee, Yang, and Parr (LYP)[3] was combined with either Becke's pure exchange functional (B)[4] or the three-parameter hybrid exchange functional (B3)[5]. The five programs used are Gaussian 94,[6] Molpro,[7] NWChem,[8] and Q-Chem,[9] and Gamess.[10] The B3LYP version implemented[6,11] in Gaussian 94 was used here when available. However, Molpro[7] and Gamess[10] are currently only capable of producing results for the B3LYP functional in its originally recommended Becke form[5] (part of the functional referred to as B3PW91 and now referred to as B3LYP5 in Gaussian and Q-Chem). Therefore only BLYP results will be reported from Molpro[7] and Gamess.[10]

Two standard basis sets were used on each of the molecules examined. These are Dunning's correlation consistent basis sets, denoted cc-pVDZ[12] and cc-pVTZ.[12] In every case spherical harmonics were used to describe the angular properties of the basis functions. Analysis was carried out on a subset of the well established G2/97[13,14] test set of molecules. Cartesian geometries used are the database results from the MP2(full)/6-31G(d) level of theory. The subset used consisted of 83 molecules, listed in Table 1. Molecules omitted from the full set (noted in the footnote) were those for which technical difficulties were encountered with one or more of the five programs during the computations.

Three sets of input parameters are examined. In the first, each program is left to its "default" settings for both integration grid quadrature and self-consistent-field (SCF) convergence criteria. This was done as it is the setting most likely to be chosen by users. In the "medium" grid scenario the SCF iterative procedure is expected to be converged to at least $10^{-10}$ hartree ($E_h$) in conjunction with the largest grid which can be entered with a simple keyword. Finally, "large" integration grids are used, also with SCF iteration convergence set to $10^{-10}$ hartrees.

For the Gaussian[6] program, the "default" grid is taken to be 75 radial points with 302 angular points, while default SCF energy convergence is to 0.000159 hartrees. The "medium" grid is the UltraFine grid found in later versions of the Gaussian[6] code, with 99 radial and 590 angular points. The "large" Gaussian[6] grid was chosen to have 141 radial points and 974 angular points.

NWChem[8] has a slightly smaller "default" grid, with 49 radial points and 434 angular points for Li – F and 88 with 434 for Na – Cl, but an SCF iteration energy convergence criteria of $10^{-6}$ hartree. The "medium" NWChem[8] grid comes from the xfine keyword, and has 100 radial points with 1202 angular points for Li – F, and 125,1454 for Na – Cl. While larger grids could be entered, one with 205 radial and 1454 angular points was considered sufficient for the "large" grid.

In Q-Chem[9] the "default" integration grid is the SG-0 grid, with only 23 radial and 170 angular points. SCF iteration convergence is achieved when the wavefunction error is below $10^{-5}$ hartree (so the energy should be converged to a higher degree). The "medium" grid is the SG-1 grid, which includes 50 radial and 194 angular points. Once again, much larger grids can be entered, but the grid with 205 radial

and 1454 angular points was considered large enough for the "large" integration grid. In addition to this, the cut-off for two-electron integrals was changed to $10^{-13}$ hartree for the "medium" and "large" grids, so that all integrals with smaller values are considered to be zero.

The grids in Molpro[7] are adaptive, and not so easily defined. As a "default", the grid is created to ensure that the Slater-Dirac functional is integrated to $10^{-5}$ $E_h$ accuracy. The SCF iterative procedure is converged to $10^{-6}$ hartree. For the "medium" and "large" grids, these grid integration convergence thresholds were chosen to be $10^{-8}$ and $10^{-13}$, respectively.

The "default" grid in Gamess[10] has 96 radial functions, 12 theta and 24 phi functions. The "medium" and "large" grids use a heightened convergence criteria of $10^{-10}$ on the density matrix. The "medium" grid consists of 110 radial, 24 theta, and 48 phi points while the "large" grid has 200, 28, and 56. It should be noted that Gamess[10] uses the most recent value for the angstrom to bohr conversion. The necessary minor conversions were done to ensure the equivalency of Gamess geometries with the other programs.

It should be noted that most of these grids are automatically "pruned," and thus even choosing the same grid in different programs may result in different actual integration grids. Table 2 summarizes these grid choices. The resulting energies are compared to the energy obtained by averaging the values from the five programs with the largest grids. These values, hereafter referred to as the "exact" values are listed in Table 3. In some instances, the energy from one program was significantly different from those found by other programs. Since this did not occur consistently, it is likely not a consequence of the implementation of the functionals, but instead a consequence of some unknown phenomena. These values were thrown out when "exact" values were computed. Most of the energies used to compute the exact values agreed to within 5 nano-Hartrees.

## 2.4 RESULTS

Figures 1-5 plot the absolute errors compared to "exact" values for each program, basis set, functional, and grid quadrature choice. In each plot the lines are labeled with a three element code

defined in the following manner: the first is a letter designating the grid quadrature choice (D=default, M=medium, L=large); the second denotes the basis set (D=cc-pVDZ, T=cc-pVTZ); and the third denotes the functional (0=BLYP, 3=B3LYP). The lines are also coded by style and color. Red colors indicate default settings, green colors the medium grid quadrature, and blue the large grid quadrature. Lighter colors are for the cc-pVDZ basis set while darker colors are for the cc-pVTZ basis set. Solid lines are for BLYP results and dotted lines are for B3LYP results. Lines plot the relation between an energy error (on the x-axis, plotted logarithmically) and the percentage of computations within the particular data set which had absolute errors of that magnitude or less. For example, if every total energy in a set had a precision of $10^{-5}$ Hartrees, the plot would show a vertical line at $10^{-5}$. A data set with perfect precision would generate a vertical line which crosses the x-axis at $10^{-\infty}$.

There are several things to keep in mind while analyzing these graphs. The number of computations with a particular error is related to the slope of the curve at a given point. A gentle slope indicates widely spaced errors, while a steep slope is a sign of a large number of data points with similar errors. In most cases examined here, the ten percent best and ten percent worst error data points exhibit the widely-spaced character, while the middle eighty percent tend to have a more consistent error, leading to a steep slope. Long plateaus at the top of the graph indicate that there were species which produced particularly bad precision; this is most often the case with the large grids, where energies from some programs differed from those produced in other programs by significant amounts, indicative of a poorly behaved result. Each program had at least one system where this occurred. Needless to say, lines towards the right represent lower overall errors. Keeping this in mind, the spread of errors between the three different grids indicates the relative quality of the grid quadrature. In Molpro, the control of the precision was comparatively straight-forward, leading to the spacing between the default and medium grid lines being roughly equal to the spacing between the medium and large grid lines. In Q-Chem, the SG-0 and SG-1 grids are similar, so the spacing between them is small. Since the large grid comes with a significant increase in point density, it is far away from both default and medium in precision.

Several observations can be made. Overall, the cc-pVDZ basis set provided more precise values than the cc-pVTZ basis. In some instances, this difference is on the order of half an order of magnitude, but in general it is a small difference, on average changing the median error by about 20%. This is likely a result of the larger grid which is required to describe integrals of the cc-pVTZ basis functions, as they involve higher angular momentum and a wider range of gaussian exponents. This effect is best observed by comparing the results of $CH_4$ with $SiCl_4$: the first shows higher precision in cc-pVDZ results while the second has slightly more precise cc-pVTZ results. It should also be noted that for the default grid, BLYP and B3LYP produce about the same precision results. Similarly, for the medium grid the errors in the BLYP and B3LYP energies are comparable. It is only with the largest grid that the analytic exchange terms present in B3LYP make the energy more precise.

Figures 6 and 7 depict the behavior of some subsets of the G2/97 neutral molecules examined here, for the BLYP and B3LYP functionals, respectively. These subsets are: molecules with large dipole moments (red); amines and amides (pink); alcohols and thioalcohols (dark green); molecules with atoms which do not obey the octet rule (light green); unsaturated compounds (light blue); molecules with non-Abelian symmetry (dark blue); and the full set of molecules (black). Data from all programs and both basis sets were combined in the creation of these two graphs. The three sets of lines are, from left to right, for the default, medium and large grid quadratures, respectively.

Each subset behaves in a different way. The high dipole-moment molecules show better precision than the full set. Amines and amides show worse precision in BLYP, but appear to benefit greatly from analytic exchange terms; with B3LYP they behave better than the full set. Alcohols and thioalcohols tend to follow the full set errors well, though for the large grid BLYP computations the errors do not go down nearly as far as the full set, suggesting that few of these molecules could be computed precisely. Results for the non-octet rule obeying systems are difficult to analyze, as the set was very small. Unsaturated compounds have error curves strongly matching the behavior of the whole set. The non-Abelian subset shows the most grid dependent behavior. When higher precision is sought

through use of a larger grid quadrature, there is an increase in the number of pathological cases with poor precision.

## 2.5 CONCLUSIONS

Energetic behavior for the G2/97 neutral set of molecueles has been determined for every combination of five computational chemistry packages, two functionals, and two one-particle basis sets. The graphical data presented in this research is intended to be a guide to future researchers. Figures 1-5 present a means for estimating likely precision given a particular computational chemistry package and grid quadrature. Figures 6 and 7 show how well different types of chemical systems behave for BLYP and B3LYP given a grid quadrature.

## 2.6 ACKNOWLEDGEMENTS

This research was supported by the U. S. Department of Energy Chemical Physics Program.

## 2.7 TABLES AND FIGURES

Table 2.1: G2/97 subset of neutral molecules considered in the present research.

| # | Sym | Molecule | # | Sym | Molecule |
|---|---|---|---|---|---|
| 0 | $D_{3h}$ | $BF_3$ | 47 | $C_s$ | Formic Acid (HCOOH), HOCO cis |
| 1[a] | $D_{3h}$ | $BCl_3$ | 48 | $C_s$ | Methyl formate ($HCOOCH_3$) |
| 2 | $D_{3h}$ | $AlF_3$ | 49 | $C_1$ | Acetamide ($CH_3CONH_2$) |
| 3 | $D_{3h}$ | $AlCl_3$ | 50 | $C_{2v}$ | Aziridine (cyclic $CH_2$-NH-$CH_2$ ring) |
| 4 | $T_d$ | $CF_4$ | 51 | $D_{\infty h}$ | Cyanogen (NCCN) |
| 5 | $T_d$ | $CCl_4$ | 52 | $C_s$ | Dimethylamine, $(CH_3)_2NH$ |
| 6 | $C_{\infty v}$ | O=C=S | 53 | $C_s$ | Trans-Ethylamine ($CH_3$-$CH_2$-$NH_2$) |
| 7 | $D_{\infty h}$ | $CS_2$ | 54 | $C_{2v}$ | Ketene ($H_2C$=C=O) |
| 8 | $C_{2v}$ | $COF_2$ | 55 | $C_{2v}$ | Oxirane (cyclic $CH_2$-O-$CH_2$ ring) |
| 9 | $T_d$ | $SiF_4$ | 56 | $C_s$ | Acetaldehyde ($CH_3CHO$) |
| 10 | $T_d$ | $SiCl_4$ | 57 | $C_{2h}$ | Glyoxal (O=CH-CH=O), Trans |
| 11 | $C_s$ | $N_2O$ | 58 | $C_s$ | Ethanol (trans, $CH_3CH_2OH$) |
| 12 | $C_s$ | ClNO | 59 | $C_{2v}$ | DimethylEther ($CH_3$-O-$CH_3$) |
| 13 | $C_{3v}$ | $NF_3$ | 60 | $C_{2v}$ | Thiooxirane (cyclic $CH_2$-S-$CH_2$ ring) |
| 14 | $C_{3v}$ | $PF_3$ | 61[a] | $C_s$ | Dimethylsulfoxide $(CH_3)_2SO$ |
| 15 | $C_{2v}$ | $O_3$ (Ozone) | 62 | $C_s$ | ThioEthanol ($CH_3$-$CH_2$-SH) |
| 16 | $C_{2v}$ | $F_2O$ | 63 | $C_{2v}$ | Dimethyl ThioEther ($CH_3$-S-$CH_3$) |
| 17 | $C_{2v}$ | $ClF_3$ | 64 | $C_s$ | Vinyl fluoride ($H_2C$=CHF) |
| 18 | $D_{2h}$ | $C_2F_4$ ($F_2C$=$CF_2$) | 65 | $C_s$ | Ethyl chloride ($CH_3$-$CH_2$-Cl) |
| 19 | $D_{2h}$ | $C_2Cl_4$ ($Cl_2C$=$CCl_2$) | 66 | $C_s$ | Vinyl chloride, $H_2C$=CHCl |
| 20[a] | $C_{3v}$ | $CF_3CN$ | 67 | $C_s$ | CyanoEthylene ($H_2C$=CHCN) |

| | | | | | |
|---|---|---|---|---|---|
| 21[a] | $C_{3v}$ | Propyne ($C_3H_4$) | 68 | $C_{2v}$ | Acetone ($CH_3$-CO-$CH_3$) |
| 22 | $D_{2d}$ | Allene ($C_3H_4$) | 69 | $C_s$ | Acetic Acid ($CH_3COOH$), Single bonds trans |
| 23 | $C_{2v}$ | Cyclopropene ($C_3H_4$) | 70 | $C_s$ | Acetyl fluoride ($CH_3COF$), HCCO cis |
| 24 | $C_s$ | Propene ($C_3H_6$) | 71 | $C_s$ | Acetyl,Chloride ($CH_3COCl$), HCCO cis |
| 25 | $D_{3h}$ | Cyclopropane ($C_3H_6$) | 72 | $C_s$ | Propyl chloride ($CH_3CH_2CH_2Cl$) |
| 26 | $C_{2v}$ | Propane ($C_3H_8$) | 73 | $C_1$ | Isopropyl alcohol, $(CH_3)_2$CH-OH, Gauche isomer |
| 27 | $C_{2h}$ | Trans-1,3-butadiene ($C_4H_6$) | 74 | $C_s$ | Methyl ethyl ether ($CH_3$-$CH_2$-O-$CH_3$), Trans |
| 28[a] | $D_{3h}$ | Dimethylacetylene (2-butyne, $C_4H_6$) | 75 | $C_{3v}$ | Trimethyl Amine, $(CH_3)_3N$ |
| 29 | $C_{2v}$ | Methylenecyclopropane ($C_4H_6$) | 76 | $C_{2v}$ | Furan (cyclic $C_4H_4O$) |
| 30 | $C_{2v}$ | Bicyclo[1.1.0]butane ($C_4H_6$) | 77 | $C_{2v}$ | Thiophene (cyclic $C_4H_4S$) |
| 31 | $C_{2v}$ | Cyclobutene ($C_4H_6$) | 78 | $C_{2v}$ | Pyrrole (Planar cyclic $C_4H_4NH$) |
| 32 | $D_{2d}$ | Cyclobutane ($C_4H_8$) | 79 | $C_{2v}$ | Pyridine (cyclic $C_5H_5N$) |
| 33 | $C_{2v}$ | Isobutene ($C_4H_8$), Single bonds trans | 80 | $D_{\infty h}$ | $H_2$ |
| 34 | $C_{2h}$ | Trans-butane ($C_4H_{10}$) | 81[a] | $C_{\infty v}$ | SH radical |
| 35[a] | $C_{3v}$ | Isobutane ($C_4H_{10}$) | 82 | $C_{\infty v}$ | CCH radical |
| 36 | $D_{2d}$ | Spiropentane ($C_5H_8$) | 83 | $C_s$ | $^2$A' $C_2H_3$ |
| 37 | $D_{6h}$ | Benzene ($C_6H_6$) | 84 | $C_s$ | $^2$A' $CH_3CO$, HCCO cis |
| 38 | $C_{2v}$ | Difluoromethane ($H_2CF_2$) | 85 | $C_1$ | $H_2COH$ radical |
| 39 | $C_{3v}$ | Trifluoromethane ($HCF_3$) | 86 | $C_s$ | $^2$A' $CH_3O$ |
| 40 | $C_{2v}$ | Dichloromethane ($H_2CCl_2$) | 87[a] | $C_s$ | $^2$A" $CH_3CH_2O$ |
| 41[a] | $C_{3v}$ | Chloroform ($HCCl_3$) | 88 | $C_s$ | $^2$A' $CH_3S$ |
| 42 | $C_s$ | Methylamine ($H_3C$-$NH_2$) | 89 | $C_s$ | $^2$A' $C_2H_5$, Staggered |
| 43 | $C_{3v}$ | Acetonitrile ($CH_3$-CN) | 90 | $C_s$ | $^2$A' $(CH_3)_2CH$ |
| 44 | $C_s$ | Nitromethane ($CH_3$-$NO_2$) | 91[a] | $C_{3v}$ | t-Butyl radical, $(CH_3)_3C$ |
| 45 | $C_s$ | Methylnitrite ($CH_3$-O-N=O), NOCH trans, ONOC cis | 92 | $C_{2v}$ | $^2A_1$ $NO_2$ |
| 46 | $C_{3v}$ | Methylsilane ($CH_3$-$SiH_3$) | | | |

[a]These systems were omitted due to technical difficulties with one or more of the chosen programs.

Table 2.2: Specification of the numerical integration grids used in this study. In parentheses are the number of radial quadrature points, followed by the number of angular points.

| | "Default" | "Medium" | "Large" |
|---|---|---|---|
| GAUSSIAN | (75,302) | (99,590) | (141,974) |
| MOLPRO[b] | $10^{-5}$ | $10^{-8}$ | $10^{-13}$ |
| NWCHEM | (49,434) – (88,430) | (100,1202) – (125,1454) | (205,1454) |
| Q-CHEM | (23,170) | (50,194) | (205,1454) |
| GAMESS | (96,288) | (110,1152) | (200,1404) |

[b]Requested integration accuracy

Table 2.3: "Exact" energies (Hartrees), computed as averages of energies from all programs with the "Large" grid quadratures. The expected absolute errors are no more than $5 \times 10^{-9}$ Hartrees

| Molecule | cc-pVDZ / BLYP | cc-pVTZ / BLYP | cc-pVDZ / B3LYP | cc-pVTZ / B3LYP |
|---|---|---|---|---|
| 0 | -324.532163855 | -324.663055279 | -324.569532629 | -324.696209446 |
| 2 | -542.148265922 | -542.298466460 | -542.186951743 | -542.332326484 |
| 3 | -1623.227854455 | -1623.303292449 | -1623.305639804 | -1623.377258682 |
| 4 | -437.463025038 | -437.625236468 | -437.506266057 | -437.661571429 |
| 5 | -1878.862714099 | -1878.945077115 | -1878.946046392 | -1879.023875433 |
| 6 | -511.539802748 | -511.593258887 | -511.566029601 | -511.616831715 |
| 7 | -834.494663420 | -834.538598384 | -834.530293237 | -834.572040732 |
| 8 | -313.002507166 | -313.116726653 | -313.031525527 | -313.140463978 |
| 9 | -689.061521009 | -689.276156974 | -689.112592179 | -689.322295840 |
| 10 | -2130.472659992 | -2130.571229074 | -2130.571099522 | -2130.665212604 |
| 11 | -184.669327415 | -184.726621130 | -184.675695077 | -184.730078527 |
| 12 | -590.107903820 | -590.165293246 | -590.120657650 | -590.174783897 |
| 13 | -354.081798500 | -354.213685762 | -354.096078609 | -354.222648010 |
| 14 | -640.942474643 | -641.104545397 | -640.978996553 | -641.136302200 |
| 15 | -225.438013848 | -225.513007230 | -225.422890363 | -225.495460086 |
| 16 | -274.669100906 | -274.771653033 | -274.669973214 | -274.767916639 |
| 17 | -759.484975362 | -759.645887257 | -759.502550309 | -759.656754650 |
| 18 | -475.486437511 | -475.660317752 | -475.534808279 | -475.701508624 |
| 19 | -1916.946752136 | -1917.041248625 | -1917.041327690 | -1917.130481786 |
| 22 | -116.602539438 | -116.649616147 | -116.663876879 | -116.706285476 |
| 23 | -116.560157375 | -116.605697043 | -116.624405481 | -116.665338721 |
| 24 | -117.831018481 | -117.882045177 | -117.911330137 | -117.956733444 |
| 25 | -117.813898011 | -117.864762641 | -117.897464968 | -117.942622752 |
| 26 | -119.045317000 | -119.100687334 | -119.143544227 | -119.192264447 |
| 27 | -155.910334085 | -155.971456563 | -156.000585840 | -156.055679934 |
| 29 | -155.875460837 | -155.936556809 | -155.968573300 | -156.023372584 |
| 30 | -155.857574069 | -155.916042196 | -155.953668157 | -156.006128510 |
| 31 | -155.885547102 | -155.943257313 | -155.979721253 | -156.031433700 |
| 32 | -157.103201495 | -157.165505786 | -157.215594335 | -157.270982535 |
| 33 | -157.121906441 | -157.188016060 | -157.230978477 | -157.289864034 |
| 34 | -158.331196666 | -158.401381892 | -158.458123824 | -158.520108084 |
| 36 | -195.151498013 | -195.226845517 | -195.276855102 | -195.344259129 |
| 37 | -232.143910944 | -232.221350596 | -232.262760189 | -232.333158809 |
| 38 | -238.947797548 | -239.045968201 | -238.989280411 | -239.081760161 |
| 39 | -338.207247943 | -338.338232309 | -338.249296386 | -338.373895778 |
| 40 | -959.675824256 | -959.730460270 | -959.739074812 | -959.789639916 |
| 42 | -95.798812941 | -95.845930267 | -95.857700835 | -95.899888378 |
| 43 | -132.709091995 | -132.758298531 | -132.760716324 | -132.805023868 |
| 44 | -244.983537234 | -245.070736260 | -245.026212374 | -245.108123529 |
| 45 | -244.983084036 | -245.067340450 | -245.024438698 | -245.103611579 |
| 46 | -331.149989248 | -331.192275402 | -331.223816402 | -331.261956456 |
| 47 | -189.736954284 | -189.808668873 | -189.773004930 | -189.840122477 |
| 48 | -229.011716876 | -229.098067242 | -229.075172336 | -229.155621261 |
| 49 | -209.150074915 | -209.232676768 | -209.226414346 | -209.302366173 |
| 50 | -133.853900140 | -133.908967343 | -133.925180668 | -133.974873103 |
| 51 | -185.637913913 | -185.693851578 | -185.666753311 | -185.718078390 |

| | | | | |
|---|---|---|---|---|
| 52 | -135.079370437 | -135.139363255 | -135.165996583 | -135.219787021 |
| 53 | -135.089206269 | -135.150544012 | -135.176465785 | -135.231336079 |
| 54 | -152.572534350 | -152.628235237 | -152.611558182 | -152.663062114 |
| 55 | -153.732935130 | -153.794444769 | -153.792092214 | -153.848753213 |
| 56 | -153.779815270 | -153.840410290 | -153.837590795 | -153.892969202 |
| 57 | -227.789407822 | -227.868471268 | -227.834686678 | -227.908488579 |
| 58 | -154.965836773 | -155.035106696 | -155.042896201 | -155.105782246 |
| 59 | -154.953711380 | -155.020201367 | -155.028922988 | -155.089726233 |
| 60 | -476.731859880 | -476.783153674 | -476.802939585 | -476.849745991 |
| 62 | -477.946398040 | -478.002805342 | -478.033356591 | -478.084234265 |
| 63 | -477.943966302 | -478.002253838 | -478.030165430 | -478.082995635 |
| 64 | -177.780822380 | -177.852089230 | -177.831666978 | -177.898073102 |
| 65 | -539.365169232 | -539.420218864 | -539.446437880 | -539.496003044 |
| 66 | -538.148070567 | -538.198360420 | -538.210686590 | -538.256629591 |
| 67 | -170.779970902 | -170.839642302 | -170.841313346 | -170.895487161 |
| 68 | -193.076979006 | -193.152789107 | -193.163755716 | -193.232685954 |
| 69 | -229.034276066 | -229.121512656 | -229.099849912 | -229.180680282 |
| 70 | -253.050700784 | -253.146485982 | -253.108270019 | -253.197809770 |
| 71 | -613.409597383 | -613.483611321 | -613.476697411 | -613.545203912 |
| 72 | -578.650911253 | -578.720982318 | -578.760901962 | -578.823911140 |
| 73 | -194.257690022 | -194.340978243 | -194.363323509 | -194.438830171 |
| 74 | -194.244904878 | -194.326545653 | -194.348844934 | -194.423118447 |
| 75 | -174.361254215 | -174.434569359 | -174.475890525 | -174.541815314 |
| 76 | -229.953803969 | -230.030913959 | -230.036799266 | -230.108452449 |
| 77 | -552.937639662 | -553.008825299 | -553.031889615 | -553.097833320 |
| 78 | -210.087326764 | -210.159313868 | -210.182810429 | -210.248814328 |
| 79 | -248.192648871 | -248.273021378 | -248.299318575 | -248.372860253 |
| 80 | -1.161575100 | -1.169526345 | -1.173189443 | -1.179976599 |
| 82 | -76.580844375 | -76.611175140 | -76.609186122 | -76.636846139 |
| 83 | -77.861307083 | -77.895030616 | -77.905687791 | -77.935806708 |
| 84 | -153.141037775 | -153.198299932 | -153.189873811 | -153.242342002 |
| 85 | -115.024137296 | -115.073826938 | -115.063885744 | -115.109649168 |
| 86 | -115.013855855 | -115.062359984 | -115.054946455 | -115.099003397 |
| 88 | -438.026923486 | -438.064177226 | -438.077985945 | -438.111739870 |
| 89 | -79.096787340 | -79.134579645 | -79.158938466 | -79.192130628 |
| 90 | -118.389242406 | -118.442057074 | -118.479585542 | -118.526112901 |
| 92 | -205.088518915 | -205.154135532 | -205.091811644 | -205.154296011 |

Figure 2.1: Gamess error curves. The x-axis is the absolute error relative to the "exact" results. The vertical position of a plotted curve for a given error is the percentage of molecules within a set that have that error or less.[c]

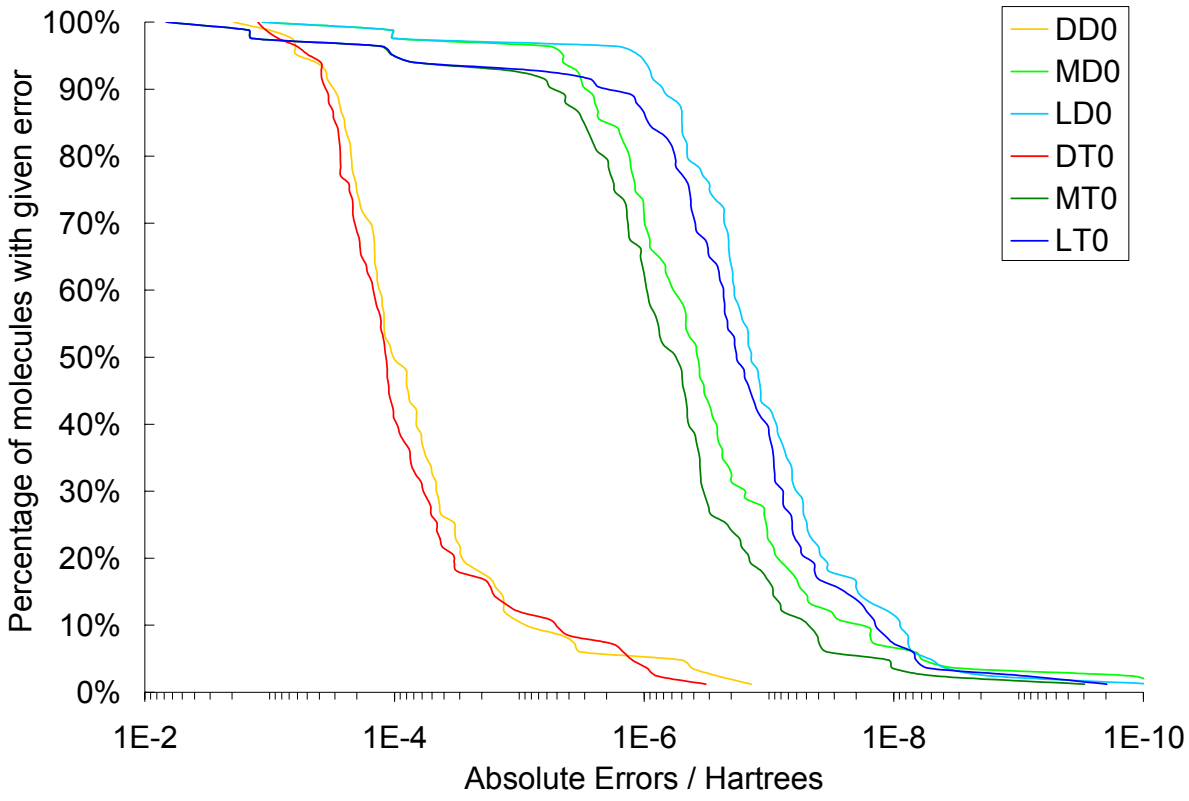


[c]In the legend, XYZ designations are used. X is grid quadrature (D=default, M=medium, L=large); Y is basis set (D=cc-pVDZ, T=cc-pVTZ); Z is functional (0=BLYP, 3=B3LYP)

Figure 2.2: Molpro error curves. The x-axis is the absolute error relative to the "exact" results. The vertical position of a plotted curve for a given error is the percentage of molecules within a set that have that error or less.[c]

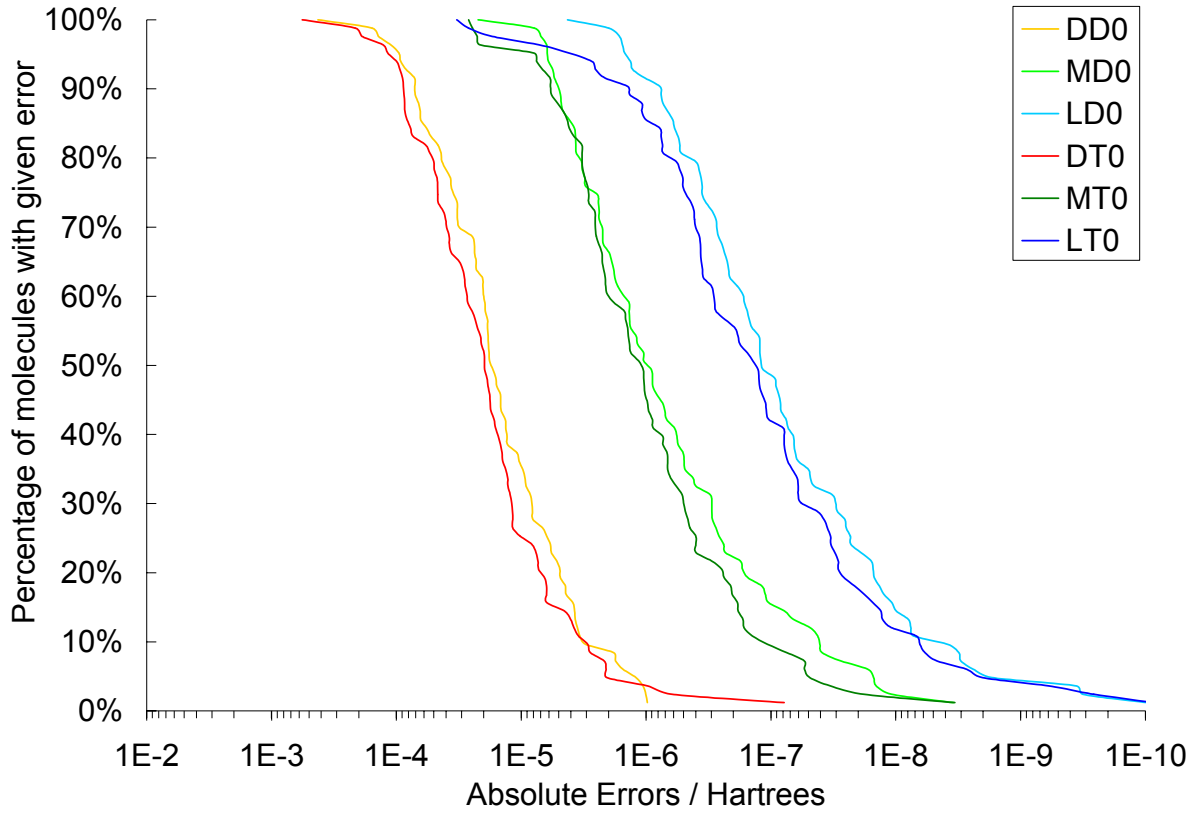


[c]See footnote, Figure 1.

Figure 2.3: NWChem error curves. The x-axis is the absolute error relative to the "exact" results. The vertical position of a plotted curve for a given error is the percentage of molecules within a set that have that error or less.[c]

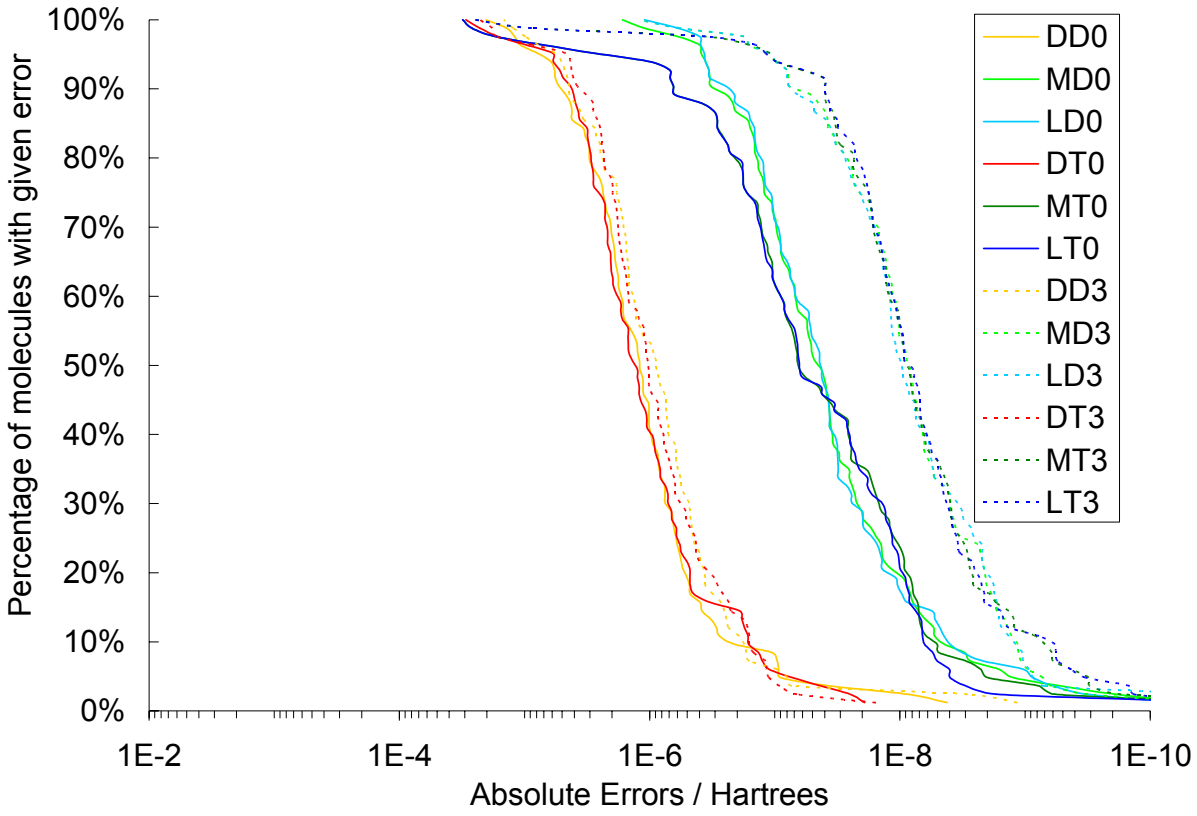


[c]See footnote, Figure 1.

Figure 2.4: QChem error curves. The x-axis is the absolute error relative to the "exact" results. The vertical position of a plotted curve for a given error is the percentage of molecules within a set that have that error or less.[c]

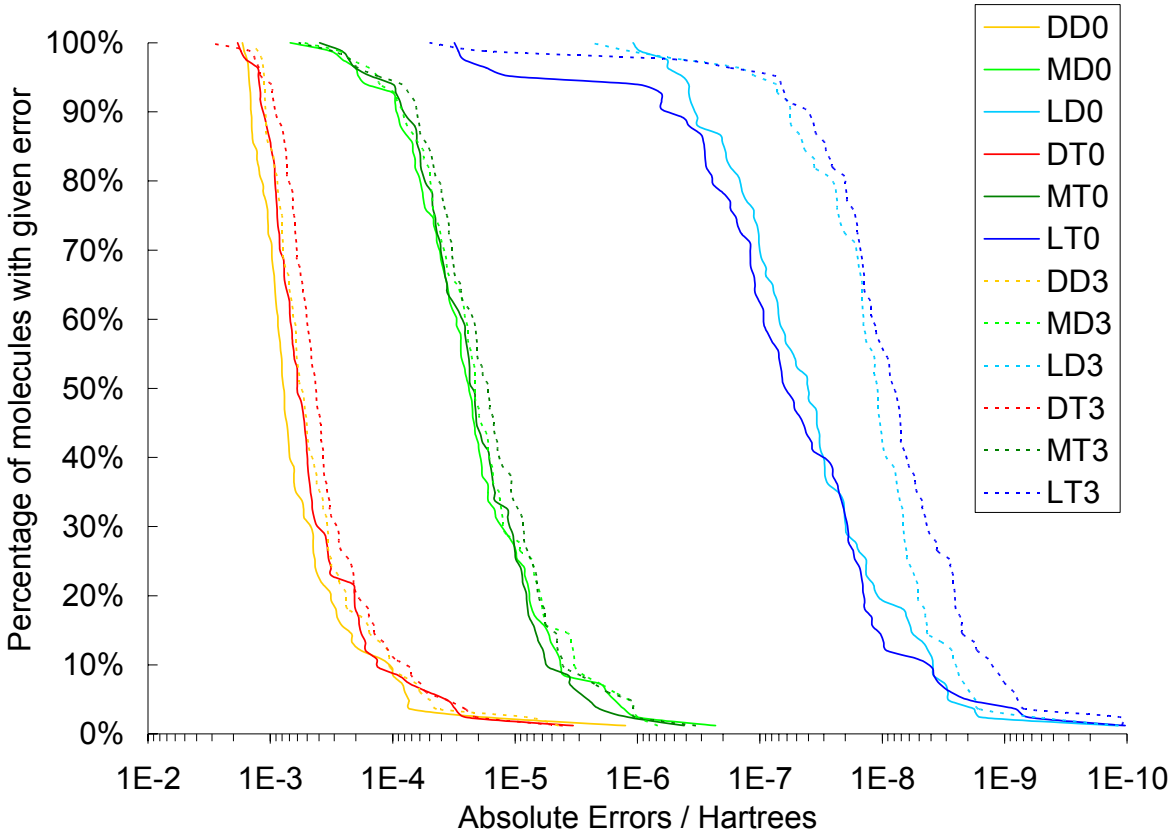


[c]See footnote, Figure 1.

Figure 2.5: Gaussian 94 error curves. The x-axis is the absolute error relative to the "exact" results. The vertical position of a plotted curve for a given error is the percentage of molecules within a set that have that error or less.[c]

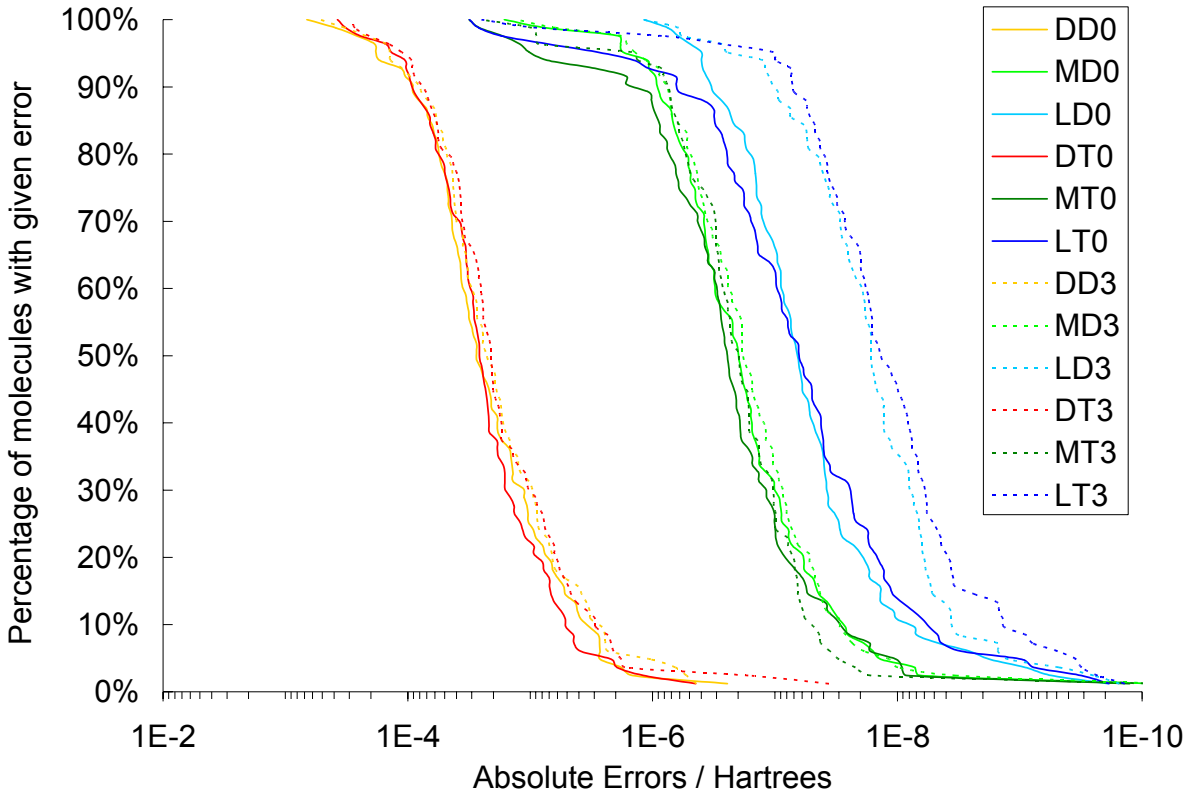


[c]See footnote, Figure 1.

Figure 2.6: BLYP results by molecule type. The x-axis is the absolute error relative to the "exact" results. The vertical position of a plotted curve for a given error is the percentage of molecules within a set that have that error or less. From left too right, the collections of curves are for the default, medium, and large grid settings.

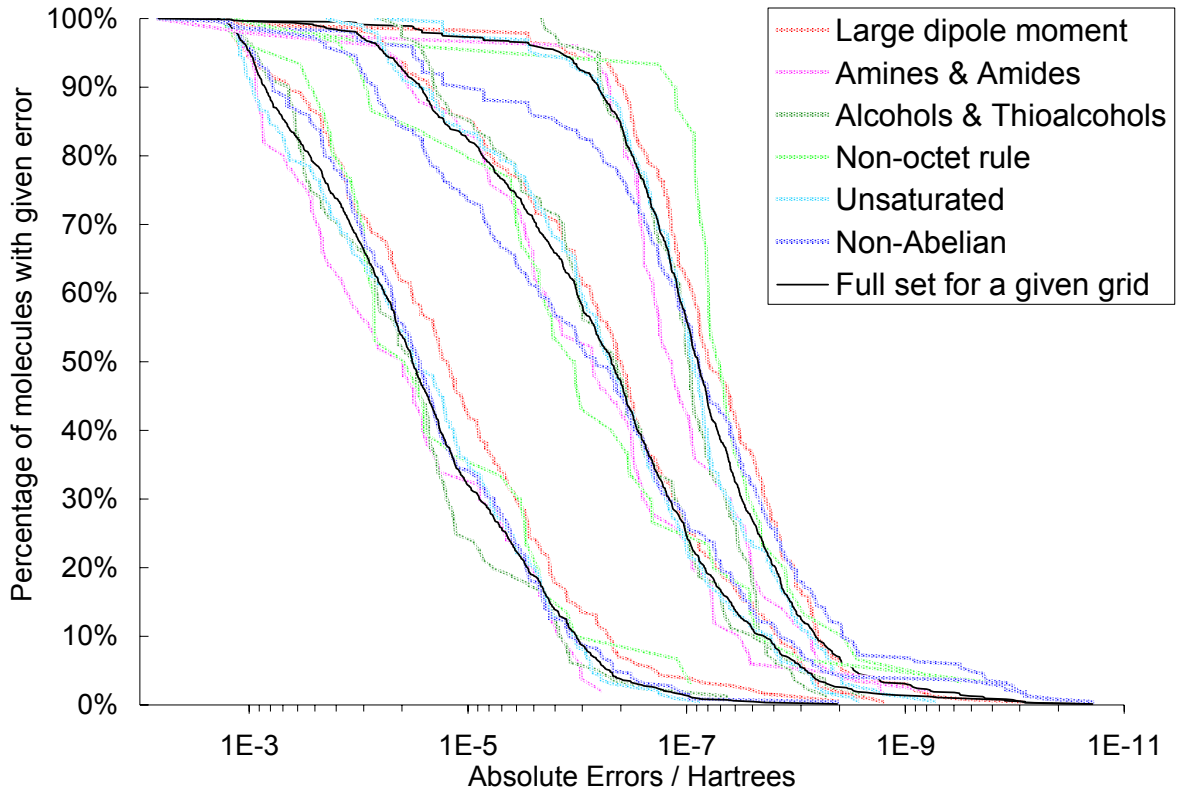

Figure 2.7: B3LYP results by molecule type. The x-axis is the absolute error relative to the "exact" results. The vertical position of a plotted curve for a given error is the percentage of molecules within a set that have that error or less. From left too right, the collections of curves are for the default, medium, and large grid settings.

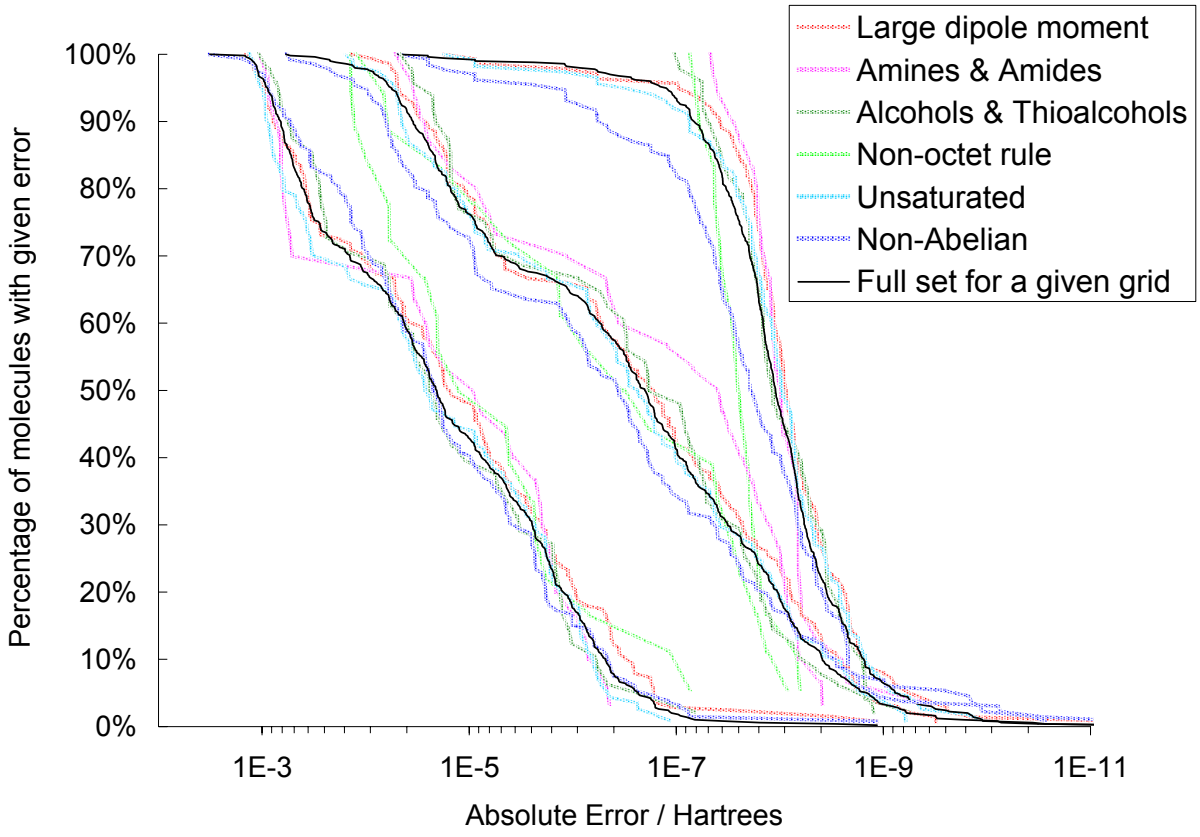

## 2.7 REFERENCES


[1] J. M. L. Martin, C. W. Bauschlicher, and A. Ricca, *Computer Phys. Comm.* **133**, 189 (2001).

[2] S. Dressler and W. Thiel, *Chem. Phys. Lett.* **273**, 71 (1997).

[3] C. Lee, W. Yang, and R. G. Parr, *Phys. Rev. B* **37**, 785 (1988).

[4] A. D. Becke, *Phys. Rev. A* **38**, 3098 (1988).

[5] A. D. Becke, *J. Chem. Phys.* **98**, 5648 (1993).

[6] Gaussian 94, Revision C.3, M. J. Frisch, G. W. Trucks, H. B. Schlegel, P. M. W. Gill, B. G. Johnson, M. A. Robb, J. R. Cheeseman, T. Keith, G. A. Petersson, J. A. Montgomery, K. Raghavachari, M. A. Al-Laham, V. G. Zakrzewski, J. V. Ortiz, J. B. Foresman, J. Cioslowski, B. B. Stefanov, A. Nanayakkara, M. Challacombe, C. Y. Peng, P. Y. Ayala, W. Chen, M. W. Wong, J. L. Andres, E. S. Replogle, R. Gomperts, R. L. Martin, D. J. Fox, J. S. Binkley, D. J. Defrees, J. Baker, J. P. Stewart, M. Head-Gordon, C. Gonzalez, and J. A. Pople, Gaussian, Inc., Pittsburgh PA, 1995.

[7] MOLPRO, a package of ab initio programs designed by H.-J. Werner and P. J. Knowles, version 2002.6, R. D. Amos, A. Bernhardsson, A. Berning, P. Celani, D. L. Cooper, M. J. O. Deegan, A. J. Dobbyn, F. Eckert, C. Hampel, G. Hetzer, P. J. Knowles, T. Korona, R. Lindh, A. W. Lloyd, S. J. McNicholas, F. R. Manby, W. Meyer, M. E. Mura, A. Nicklass, P. Palmieri, R. Pitzer, G. Rauhut, M. Schütz, U. Schumann, H. Stoll, A. J. Stone, R. Tarroni, T. Thorsteinsson, and H.-J. Werner.

[8] T.P. Straatsma, E. Aprà, T. L. Windus, E. J. Bylaska, W. de Jong, S. Hirata, M. Valiev, M. T. Hackler, L. Pollack, R. J. Harrison, M. Dupuis, D. M. A. Smith, J. Nieplocha, V. Tipparaju, M. Krishnan, A. A. Auer, E. Brown, G. Cisneros, G. I. Fann, H. Fruchtl, J. Garza, K. Hirao, R. Kendall, J. Nichols, K. Tsemekhman, K. Wolinski, J. Anchell, D. Bernholdt, P. Borowski, T. Clark, D. Clerc, H. Dachsel, M. Deegan, K. Dyall, D. Elwood, E. Glendening, M. Gutowski, A. Hess, J. Jaffe, B. Johnson, J. Ju, R. Kobayashi, R. Kutteh, Z. Lin, R. Littlefield, X. Long, B. Meng, T. Nakajima, S. Niu, M. Rosing, G. Sandrone, M. Stave, H. Taylor, G. Thomas, J. van Lenthe, A. Wong, Z. Zhang, "NWChem, A Computational Chemistry Package for Parallel Computers, Version 4.6" (2004), Pacific Northwest National Laboratory, Richland, Washington 99352-0999, USA.

[9] Q-Chem 2.0: A high-performance ab initio electronic structure program, J. Kong, C. A. White, A. I. Krylov, C. D. Sherrill, R. D. Adamson, T. R. Furlani, M. S. Lee, A. M. Lee, S. R. Gwaltney, T. R. Adams, C. Ochsenfeld, A. T. B. Gilbert, G. S. Kedziora, V. A. Rassolov, D. R. Maurice, N. Nair, Y. Shao, N. A. Besley, P. E. Maslen, J. P. Dombroski, H. Daschel, W. Zhang, P. P.

Korambath, J. Baker, E. F. C. Byrd, T. Van Voorhis, M. Oumi, S. Hirata, C.-P. Hsu, N. Ishikawa, J. Florian, A. Warshel, B. G. Johnson, P. M. W. Gill, M. Head-Gordon, and J. A. Pople, *J. Comput. Chem.* **21**, 1532 (2000).

[10] M. W. Schmidt, K. K. Baldridge, J. A. Boatz, S. T. Elbert, M. S. Gordon, J. H. Jensen, S. Koseki, N. Matsunaga, K. A. Nguyen, S. J. Su, T. L. Windus, M. Dupuis, and J. A. Montgomery, *J. Comput. Chem.* **14**, 1347 (1993).

[11] P. J. Stephens, F. J. Delvin, C. F. Chabalowski, and M. J. Frisch, *J. Phys. Chem.* **98**, 11623 (1994).

[12] T. H. Dunning Jr., *J. Chem. Phys.* **90**, 1007 (1989).

[13] L. A. Curtiss, K. Raghavachari, P. C. Redfern, and J. A. Pople, *J. Chem. Phys.* **106**, 1063 (1997).

[14] L. A. Curtiss, P. C. Redfern, K. Raghavachari, and J. A. Pople, *J. Chem. Phys.* **109**, 42 (1998).

# CHAPTER 3

# THE NAPHTHALENYL, ANTHRACENYL, TETRACENYL, AND PENTACENYL RADICALS, AND THEIR ANIONS*

* B. N. Papas, S. Y. Wang, N. J. DeYonker, H. L. Woodcock and H. F. Schaefer 2003. Journal of Physical Chemistry A 107: 6311-6316. Reproduced with permission of the American Chemical Society.

## 3.1 ABSTRACT

Electronic structure theory has been applied to the naphthalene, anthracene, tetracene, and pentacene based radicals and their anions. Five different density functional methods were used to predict adiabatic electron affinities for these radicals. A consistent trend was found, suggesting that the electron affinity at a site of hydrogen removal is primarily dependent upon steric effects for polycyclic aromatic hydrocarbons. The results for the 1-naphthalenyl and 2-naphthalenyl radicals were compared to experiment, and it was found that B3LYP appears to be the most reliable functional for this type of system. For the larger systems the predicted site specific adiabatic electron affinities of the radicals are 1.51 eV (1-anthracenyl), 1.46 eV (2-anthracenyl), 1.68 eV (9-anthracenyl); 1.61 eV (1-tetracenyl), 1.56 eV (2-tetracenyl), 1.82 eV (12-tetracenyl); 1.93 eV (14-pentacenyl), 2.01 eV (13-pentacenyl), 1.68 eV (1-pentacenyl), and 1.63 eV (2-pentacenyl). These electron affinities are 0.5 – 1.5 eV higher than those for the analogous closed-shell singlet polycyclic aromatic hydrocarbons (PAHs), i.e. EA(anthracene) = 0.53 eV. The global minimum for each radical does not have the same hydrogen removed as the global minimum for the analogous anion. With this in mind, the global (or most preferred site) AEAs are 1.37 eV (naphthalenyl), 1.64 eV (anthracenyl), 1.81 eV (tetracenyl), and 1.97 eV (pentacenyl).

## 3.2 INTRODUCTION

The great stability of polycyclic aromatic hydrocarbons (PAHs) makes them prevalent in our surroundings, and recent research has discussed their abundance in the interstellar medium as well.[1,2] Most notably, PAHs are formed in combustion,[3-5] where they may be precursors to soot[6] and fullerenes.[7] This makes them an important class of pollutants, many of which have been found to be mutagenic and carcinogenic.[8] To better understand their role, PAHs, their radicals, and their anions, have been the targets of many recent experimental and theoretical studies.[9-16]

The PAHs examined in this study are derived from naphthalene ($C_{10}H_8$), anthracene ($C_{14}H_{10}$), tetracene ($C_{18}H_{12}$), and pentacene ($C_{22}H_{14}$). All unique radicals formed by homolytically splitting a

carbon-hydrogen bond are studied, as well as the anions of those radicals. The primary focus of this paper is the electron affinities (EAs) of the aryl radicals. See Figure 1 for the standard numbering of the carbon atoms.

Recent experimental studies have determined EAs for the naphthalenyl radicals.[9-11] These results will be used as a basis for judging the accuracy of several density functionals. The PAHs and their radicals, but not their anions, have been the subject of important DFT studies by Cioslowski[13,14] and Wiberg.[15] Average theoretical errors in EAs for PAHs and other molecules, as found by Rienstra-Kiracofe, Tschumper, Schaefer, Nandi and Ellison,[16] shall be used for evaluating the reliability of our results.

## 3.3 METHODS

All computations employed a double-ζ basis set with polarization and diffuse functions, denoted DZP++. Previous work[17,18] has shown that this basis has the flexibility needed for accurate results, while maintaining a small size appropriate for larger molecular systems. It was constructed by augmenting the Huzinaga-Dunning[19,20] set of contracted double-ζ Gaussian functions with one set of p polarization functions for each hydrogen atom and one set of d polarization functions for each carbon atom [4s2p1d|2s1p] ( $\alpha_p$(H)=0.75, $\alpha_d$(C)=0.75 ). To complete the DZP++ basis, one diffuse s function was added to each hydrogen atom, and a set of diffuse s and p functions to each carbon atom. These diffuse "even-tempered" orbital exponents were determined according to the guidelines of Lee and Schaefer.[21] That is, the s- or p-type diffuse function exponent, $\alpha_{diffuse}$, for a given atom was determined by

$$\alpha_{diffuse} = \frac{1}{2}\left(\frac{\alpha_1}{\alpha_2} + \frac{\alpha_2}{\alpha_3}\right)\alpha_1 \tag{3.1}$$

where $\alpha_1$ is the smallest, $\alpha_2$ the second smallest, and $\alpha_3$ the third smallest Gaussian orbital exponent of the s- or p-type primitive functions of that atom [ $\alpha_S$(H)=0.04415, $\alpha_S$(C)=0.04302, $\alpha_P$(C)=0.03629 ]. All polarization and diffuse orbital exponents were unscaled. There are a total of six DZP++ contracted gaussian basis functions per hydrogen atom and nineteen per carbon atom.

Five different exchange-correlation density functionals were used to determine the electronic energies, equilibrium geometries, harmonic vibrational frequencies, and zero-point vibrational energies (ZPVEs) for the naphthalene, anthracene, and tetracene derived radicals and anions. The functionals that were used have been denoted B3LYP, BHLYP, BLYP, BP86, and LSDA. Only the B3LYP functional was used for pentacene. All but LSDA are generalized gradient approximations (GGAs) and employ either the dynamical correlation functional of Lee, Yang, and Parr (LYP)[22] or that of Perdew (P86)[23,24] in conjunction with one of Becke's exchange functionals: the three-parameter HF/DFT hybrid exchange functional (B3),[25] a modification of the half-and-half HF/DFT hybrid method (BH)[26] (the BH functional as implemented in Gaussian 94[27]), or the 1988 pure DFT exchange functional (B).[28] The final density functional scheme used in this study was the standard local-spin-density approximation (LSDA) which employs the 1980 correlation functional of Vosko, Wilk, and Nusair[29] along with the Slater exchange functional.[30-32]

The quantum chemical computations of the naphthalene and anthracene derived species were conducted using the Gaussian 94[26] computational package, while the tetracene and pentacene derived species were done using the Gaussian 98[33] computational package. Spin unrestricted Kohn-Sham orbitals were used for all computations. Both the neutral and anion geometries were fully optimized via analytic gradients with each of the density functionals. Numerical integration of the functions was carried out using the Gaussian 94[26] and 98[33] default grid consisting of 75 radial shells and 302 angular points per shell. The mass-weighted Hessian matrix, and hence the harmonic vibrational frequencies, were determined analytically for all DFT methods for the naphthalenyl, anthracenyl, and tetracenyl species. ZPVE corrections for pentacenyl energies were approximated by extrapolating a linear trend in ZPVE corrections with respect to number of rings from the results of the other PAHs.

The electron affinities (AEAs) in this report are all adiabatic, and have values determined by

$$AEA = E_{neutral} - E_{anion} \tag{3.2}$$

where the geometry of each species is optimized independently for local AEAs. Global AEAs are also determined, where the global energy minimum for each species is used. An alternate term for “global

EA" is "most preferred site EA." The global EA is the energy difference between the lowest energy isomer of the radical and the lowest energy isomer of the anion. Corrections for zero-point vibrational energies were computed by adding the ZPVE correction to each energy before determining the EA. A positive EA corresponds to a bound electron. In this study, all species were optimized with the "tight" convergence criterion in the DFT frame using the Gaussian 94[26] or Gaussian 98[33] packages.

### 3.4 Results and Discussion

It should first be noted that the addition of diffuse functions has a significant impact upon the energetics. Sample B3LYP calculations on the 9-anthracenyl species showed a lowering of about 6 kcal/mol for the radical and 13 kcal/mol for the anion when the diffuse functions were added. The geometries were not significantly different.

Another concern is that of comparing Gaussian 94[26] results with those from Gaussian 98.[33] To address this concern, a B3LYP computation was performed on the 9-anthracenyl species. ZPVE corrected EAs were found to be different by less than 0.005 eV. As such, comparisons of EAs between the two versions should be valid.

One possible gauge of the accuracy of the results is an evaluation of $<S^2>$. For the radicals studied, this would be 0.75 in a spin-restricted formalism. For anthracenyl, BHLYP gives the largest deviation, with the 9-anthracenyl radical value being 0.85. All $<S^2>$ values for the other radicals were below 0.77. This suggests reasonable results, though it should be noted, as by Pople, Gill, and Handy,[34] that the DFT determinant formed from spin orbitals is not a true wavefunction, and $<S^2>$ is not necessarily meaningful.

Vibrational frequencies were evaluated to confirm minimum energy structures, and to determine ZPVEs. In all cases, structures were found for stable energy minima. It is worth noting that several anthracenyl species broke the expected symmetry, as well as one of the pentacenyl (see Tables 1 and 2). Note that the 9-anthracenyl radical should have $C_{2v}$ symmetry, while the 2-anthracenyl radical should have $C_s$ symmetry, but several functionals gave lower symmetries. For instance, the B3LYP

computations gave a 9-anthracenyl anion geometry in which the hydrogens remain in one plane, but are not symmetric with respect to the bisecting plane which contains the 9 site. This $C_s$ symmetry, however, is energetically and geometrically very close to the nearest $C_{2v}$ symmetry. This suggests that the symmetry loss is not physical, but instead an artifact of the computation method, most probably due to the numerical integration procedures necessary in DFT methods.

The majority of the change in geometry upon the addition of the σ electron occurs at the site of the hydrogen removal. Relevant parameters are the carbon-carbon-carbon angle associated with the site of removal (the ipso angle) and the carbon-carbon bond lengths adjacent to the site. The 'left' and 'right' labels in Table 2 refer to the position of the bond relative to the site of the removed hydrogen in the IUPAC orientation. In the designation of symmetries, $C_s$ refers to a system where the plane of symmetry contains all of the atoms, while $C_s$' bisects the middle ring.

On average, the ipso bond angle decreases by 14º and the adjacent bond lengths increase by 0.04 Å with the addition of the last electron. The angle change is consistent with the results found by Ervin *et al.*[9] using Gaussian 98[33] and a B3LYP/aug-cc-pVDZ computation for the smaller naphthalenyl species. The geometry changes are highly consistent between different PAH derived radicals. In fact, when comparing similar radicals (1-naphthalenyl to 1-anthracenyl, and 2-naphthalenyl to 2-anthracenyl, etc) one finds that the ipso angle is usually different by at most 0.2º, and the bond lengths are different by 0.01 Å. The exceptions to this trend involve anthracenyl systems which broke symmetry. This suggests that the behavior of the radical and its anion are relatively independent of the total system – what matters is that it is part of a PAH.

Theoretical EAs are reported in Table 3. ZPVE corrected EAs appear in parentheses. The ZPVE correction is typically around 0.06 eV for the naphthalenyl radicals, 0.07 eV for the anthracenyl radicals, and 0.05 eV for the tetracenyl radicals (the BHLYP corrections are very small compared to the others). On average, the 1-naphthalenyl radical has an EA approximately 0.06 eV higher than the 2-naphthalenyl radical. This difference is in good agreement with the values reported from experiment.[9-11] The difference between the 1-anthracenyl radical EA and the 2-anthracenyl radical EA is on average 0.05 eV,

though the different functionals predict a wider range of values. The same separation for the tetracenyl radical EA is 0.06 eV. The highest EA for anthracenyl is that of the 9-anthracenyl radical structure, which is on average 0.16 eV higher than the value for the 1-anthracenyl radical. The highest EA for the tetracenyl radical is that of the 12-tetracenyl radical, which is 0.21 eV higher than the 1-tetracenyl radical EA. The highest EA for the pentacenyl radical is that of the 13-pentacenyl radical, which is 0.33 eV higher than the value for the 1-pentacenyl radical.

Combining the results of experiments by Reed and Kass,[10] Lardin *et al*.[11] and Ervin *et al*.[9] gives average values for the EAs of the naphthalenyl radicals. The EA of the 1-naphthalenyl radical is 1.40 eV, and that of the 2-naphthalenyl radical is 1.34 eV. Compared to these, the smallest average error amongst the functionals is that for B3LYP, an error of 0.03 eV. This is much smaller than the average error of 0.14 eV reported by Rienstra-Kiracofe *et al*.[15] in their systematic study of 91 EAs. Also close are BLYP and BP86, which have errors of 0.10 eV and 0.08 eV, respectively, for the naphthalenyl radicals. The remaining functionals, BHLYP and LSDA, compare poorly, with LSDA far off from experimental value by any means of comparison. This suggests that the B3LYP values for the anthracenyl radicals are the ones that should be considered the best, and this is the reason only B3LYP was used for the pentacene based species.

There are four main points to consider for the energetics studies: the energetic ordering of the radicals, the ordering of the anions, the ordering of the local EAs, and the ordering of the global EAs. In Table 4, each energy is reported relative to the minimum for the functional and the given parent PAH. For all but the BLYP calculation, the 2-naphthalenyl radical is more stable than the 1-naphthalenyl radical. However, ignoring the presumably inaccurate LSDA results, the largest radical separation is only 0.13 kcal/mol. This separation is so small that it should not be considered significant.

Amongst the anthracenyl radicals, the 9- species is consistently the highest in electronic energy. This is followed by the 1-anthracenyl radical, then the 2-anthracenyl radical. It should be noted, however, that (except for LSDA) the total range of energies for the radicals is at most 0.7 kcal/mol. Except for BLYP, the tetracenyl radicals show ordering similar to the anthracene based radicals. The difference is

that BLYP predicts the 1-tetracenyl radical to lie energetically lower than the 2-tetracenyl radical. Once again, the separation of the 1- and 2- radicals is so small (0.11 kcal/mol at most, ignoring LSDA) that we should view the two structures as energetically degenerate. The pentacenyl radicals are in an energy ordering comparable to anthracenyl and tetracenyl. The least stable radical is 13-pentacenyl, followed by 1-pentacenyl then 2- and 14- pentacenyl. The energies span a range of 0.62 kcal/mol for the anthracenyl radicals and 0.31 kcal/mol for the tetracenyl radicals (both ignoring LSDA), again very small numbers.

For the naphthalene based systems, the 1-naphthalenyl anion is consistently the most stable. It is, on average, 1.24 kcal/mol more stable than the 2- anion. The ordering of the anthracenyl anions is also consistent between all functionals: the 9-anthracenyl anion is the most stable, with the 1-anthracenyl anion more stable than the 2-anthracenyl anion. This ordering is sensible, since the electron cloud corresponding to the additional electron (which has no associated H-atom) experiences greater electron-electron repulsion from species with more hydrogens near the site of the hydrogen removal. Specifically, the 9- site of the anthracenyl radical has no hydrogens on adjacent carbons, the 1- site one, and the 2-site two. The tetracenyl anions show the same trend, with the 12- species the most stable, followed by the 1- than the 2-, and the pentacenyl anions are also consistent, falling in the order of 13-, 14-, 1-, then 2-.

One referee has proposed an alternate explanation. Since the hybridization of the anionic center must have more s character (s orbitals are closer to the nucleus) the ipso C-C bonds must have more p character. This means that the bond angle must decrease, as is seen in the theoretical predictions. This deformation causes significant strain, and it is the ability of the particular anionic site to accommodate this strain that determines the relative energies. While this certainly explains the change in the C-C-C angle, the neighboring hydrogen atoms in the 1- and 2-anthracenyl anions are bent away from the anionic site, in one case by 5 degrees. This suggests the presence of steric effects in addition to hybridization effects.

As noted, the radicals have small energetic separations. So small, in fact, that the ordering of the EAs of the various species is almost entirely dependent upon the ordering of the anions. The EAs, then, fall in order according to steric and hybridization effects, just like the anions.

Figure 2 details the changes in the EAs as the number of rings involved increases. The trends seem to be near linear, with the increase in EA decreasing slightly with each ring added. In general, larger ring systems have greater EAs for comparable radicals (the 1-radicals, 2-radicals, and 9-anthracenyl with 12-tetracenyl and 14-pentacenyl, and 13-pentacenyl by itself). It is likely that the larger ring systems allow the electron density around the site of the last electron to spread out more, thus stabilizing the anion.

Table 5 gives predicted values for the global EAs. In all cases the trend is simple – the global EA increases as the number of rings increases. This most likely occurs for the same reason as the trend in the local EAs – the larger ring system stabilizes the anions more. Since the radicals for each set of systems with the same number of rings are so close together in energy, the global EA depends almost exclusively upon this stabilization effect.

## 3.5 CONCLUSIONS

Potential surface minima, harmonic vibrational frequencies, and EAs have been computed for naphthalene-, anthracene- and tetracene-based radicals using five different density functionals. All except vibrational frequencies were found for pentacene based radicals using only B3LYP. Optimized geometries are reported, and the geometry changes with electron attachment are consistent for all functionals. It would also appear that the relative order of EAs for different sites within a given PAH is mainly dependent upon steric effects, and perhaps upon hybridization effects as well. Which is more significant could be pursued further by placing larger groups adjacent to the site of hydrogen removal. In addition, both the local EAs for equivalent radical sites, and the global EAs increased as the number of rings in the system increased.

Results for the 1- and 2-naphthalenyl radicals have been compared to experiment, and the most accurate functional was found to be B3LYP. BLYP and BP86 are also in good agreement with experiment. As such, those three functionals are recommended for use on future computational studies of PAHs.

## 3.6 ACKNOWLEDGMENTS

This research was supported by the U.S. Department of Energy Combustion and SciDAC programs. Computations using GAUSSIAN 98 were carried out at the NERSC (National Energy Research Supercomputing Center) at the Lawrence Berkeley Laboratory, also supported by the Department of Energy. We thank Dr. Zhi-Xiang Wang for many helpful discussions.

## 3.7 TABLES AND FIGURES

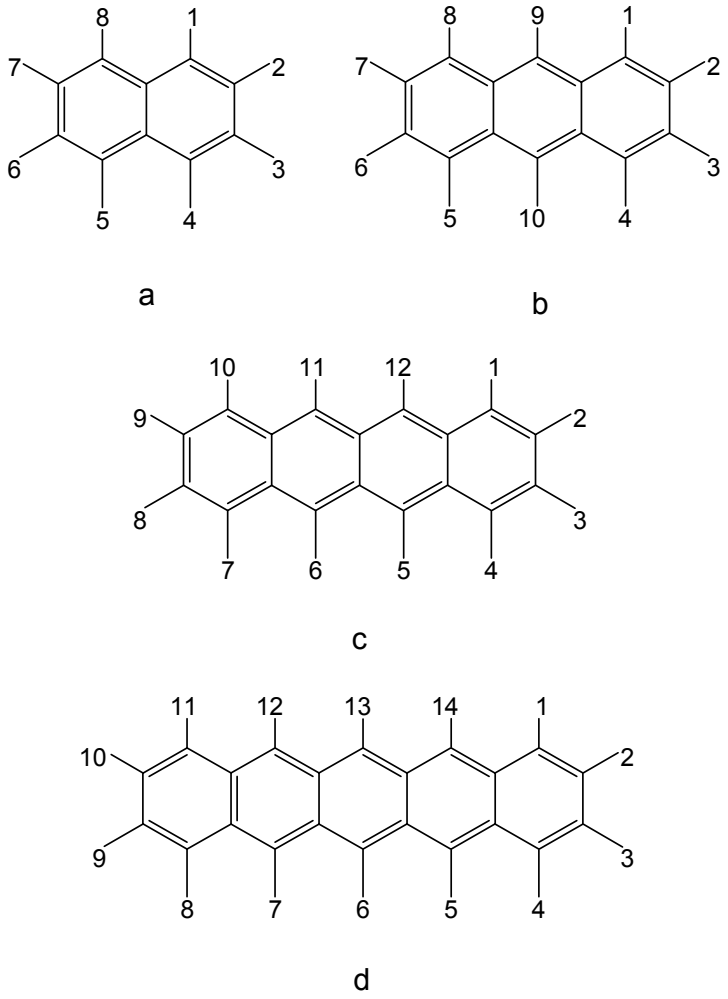


Figure 3.1: IUPAC numbering scheme for (a) naphthalene, (b) anthracene, (c) tetracene, and (d) pentacene.

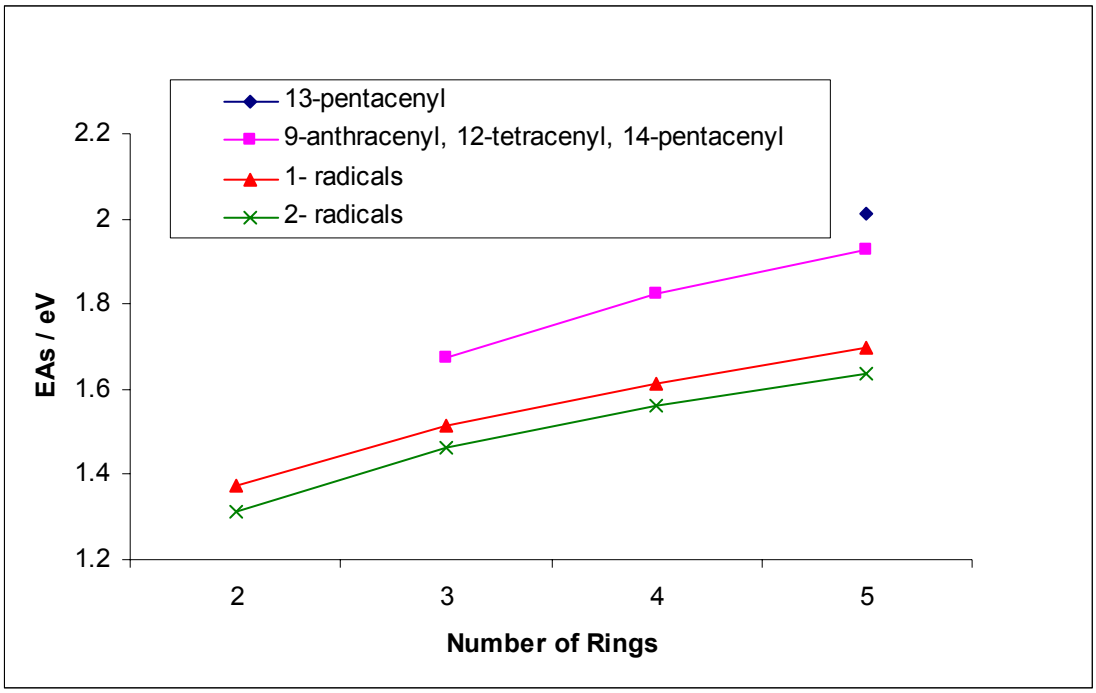


Figure 3.2: EAs vs Number of Rings

Table 3.1: Ipso C-C-C angles (in degrees) for the radicals and their anions.

| | | B3LYP | BLYP | BHLYP | BP86 | LSDA |
|---|---|---|---|---|---|---|
| 1-naphthalenyl | radical | 126.6 | 126.7 | 126.4 | 126.7 | 126.9 |
| | symmetry | $C_s$ | $C_s$ | $C_s$ | $C_s$ | $C_s$ |
| | anion | 112.6 | 112.8 | 112.6 | 112.5 | 112.8 |
| | symmetry | $C_s$ | $C_s$ | $C_s$ | $C_s$ | $C_s$ |
| 2-naphthalenyl | radical | 126.3 | 126.3 | 126.1 | 126.4 | 126.7 |
| | symmetry | $C_s$ | $C_s$ | $C_s$ | $C_s$ | $C_s$ |
| | anion | 111.9 | 112.0 | 111.9 | 111.7 | 112.2 |
| | symmetry | $C_s$ | $C_s$ | $C_s$ | $C_s$ | $C_s$ |
| 1-anthracenyl | radical | 126.8 | 126.9 | 126.5 | 126.9 | 127.1 |
| | symmetry | $C_s$ | $C_s$ | $C_s$ | $C_s$ | $C_s$ |
| | anion | 112.6 | 112.6 | 112.6 | 112.3 | 112.7 |
| | symmetry | $C_s$ | $C_s$ | $C_s$ | $C_s$ | $C_s$ |
| 2-anthracenyl | radical | 126.5 | 126.5 | 126.3 | 126.6 | 126.9 |
| | symmetry | $C_s$ | $C_s$ | $C_s$ | $C_s$ | $C_s$ |
| | anion | 111.9 | 112.5 | 112.0 | 112.7 | 114.3 |
| | symmetry | $C_s$ | $C_1$ | $C_s$ | $C_1$ | $C_1$ |
| 9-anthracenyl | radical | 127.3 | 127.6 | 127.0 | 127.5 | 127.7 |
| | symmetry | $C_s$ | $C_s'$ | $C_s'$ | $C_s'$ | $C_s'$ |
| | anion | 113.4 | 113.6 | 113.3 | 113.2 | 113.5 |
| | symmetry | $C_s$ | $C_{2v}$ | $C_{2v}$ | $C_{2v}$ | $C_{2v}$ |
| 1-tetracenyl | radical | 126.8 | 126.9 | 126.6 | 127.0 | 127.2 |
| | symmetry | $C_s$ | $C_s$ | $C_s$ | $C_s$ | $C_s$ |
| | anion | 112.5 | 112.7 | 112.6 | 112.3 | 112.7 |
| | symmetry | $C_s$ | $C_s$ | $C_s$ | $C_s$ | $C_s$ |

| | | | | | | | |
|---|---|---|---|---|---|---|---|
| 2-tetracenyl | radical | 126.5 | 126.6 | 126.2 | 126.7 | 126.9 |
| | symmetry | $C_s$ | $C_s$ | $C_s$ | $C_s$ | $C_s$ |
| | anion | 112.0 | 112.0 | 112.1 | 111.8 | 112.7 |
| | symmetry | $C_s$ | $C_s$ | $C_s$ | $C_s$ | $C_s$ |
| 12-tetracenyl | radical | 127.5 | 127.7 | 127.1 | 127.7 | 127.8 |
| | symmetry | $C_s$ | $C_s$ | $C_s$ | $C_s$ | $C_s$ |
| | anion | 113.4 | 113.5 | 113.4 | 113.2 | 113.4 |
| | symmetry | $C_s$ | $C_s$ | $C_s$ | $C_s$ | $C_s$ |
| 1-pentacenyl | radical | 126.9 | | | | |
| | symmetry | $C_s$ | | | | |
| | anion | 112.6 | | | | |
| | symmetry | $C_s$ | | | | |
| 2-pentacenyl | radical | 126.6 | | | | |
| | symmetry | $C_s$ | | | | |
| | anion | 112.1 | | | | |
| | symmetry | $C_s$ | | | | |
| 13-pentacenyl | radical | 127.6 | | | | |
| | symmetry | $C_{2v}$ | | | | |
| | anion | 113.3 | | | | |
| | symmetry | $C_s$ | | | | |
| 14-pentacenyl | radical | 127.6 | | | | |
| | symmetry | $C_s$ | | | | |
| | anion | 113.4 | | | | |
| | symmetry | $C_s$ | | | | |

Table 3.2: C-C bond lengths (in Å) adjacent to the removed hydrogen atom.

| | | | B3LYP | BLYP | BHLYP | BP86 | LSDA |
|---|---|---|---|---|---|---|---|
| 1-naphthalenyl | radical | left | 1.407 | 1.414 | 1.401 | 1.411 | 1.395 |
| | | right | 1.364 | 1.375 | 1.353 | 1.372 | 1.359 |
| | anion | left | 1.451 | 1.460 | 1.443 | 1.457 | 1.437 |
| | | right | 1.407 | 1.417 | 1.396 | 1.415 | 1.399 |
| 2-naphthalenyl | radical | left | 1.364 | 1.375 | 1.353 | 1.372 | 1.358 |
| | | right | 1.404 | 1.411 | 1.398 | 1.408 | 1.392 |
| | anion | left | 1.405 | 1.416 | 1.393 | 1.414 | 1.397 |
| | | right | 1.449 | 1.457 | 1.442 | 1.454 | 1.435 |
| 1-anthracenyl | radical | left | 1.415 | 1.421 | 1.411 | 1.417 | 1.401 |
| | | right | 1.357 | 1.369 | 1.346 | 1.367 | 1.353 |
| | anion | left | 1.461 | 1.469 | 1.455 | 1.464 | 1.444 |
| | | right | 1.400 | 1.412 | 1.388 | 1.410 | 1.394 |
| 2-anthracenyl | radical | left | 1.357 | 1.369 | 1.346 | 1.367 | 1.353 |
| | | right | 1.413 | 1.419 | 1.409 | 1.415 | 1.399 |
| | anion | left | 1.399 | 1.409 | 1.385 | 1.406 | 1.386 |
| | | right | 1.459 | 1.463 | 1.453 | 1.456 | 1.430 |
| 9-anthracenyl | radical | left | 1.386 | 1.395 | 1.379 | 1.393 | 1.378 |
| | | right | 1.386 | 1.395 | 1.379 | 1.393 | 1.378 |
| | anion | left | 1.431 | 1.441 | 1.421 | 1.438 | 1.420 |
| | | right | 1.431 | 1.441 | 1.421 | 1.438 | 1.420 |
| 1-tetracenyl | radical | left | 1.419 | 1.424 | 1.411 | 1.420 | 1.403 |
| | | right | 1.355 | 1.367 | 1.348 | 1.365 | 1.351 |
| | anion | left | 1.465 | 1.472 | 1.460 | 1.468 | 1.446 |

| | | | | | | | |
|---|---|---|---|---|---|---|---|
| | | right | 1.398 | 1.410 | 1.385 | 1.408 | 1.392 |
| 2-tetracenyl | radical | left | 1.354 | 1.367 | 1.348 | 1.365 | 1.351 |
| | | right | 1.417 | 1.423 | 1.410 | 1.419 | 1.402 |
| | anion | left | 1.397 | 1.410 | 1.382 | 1.407 | 1.446 |
| | | right | 1.464 | 1.472 | 1.460 | 1.467 | 1.392 |
| 12-tetracenyl | radical | left | 1.396 | 1.403 | 1.390 | 1.400 | 1.385 |
| | | right | 1.379 | 1.389 | 1.377 | 1.387 | 1.372 |
| | anion | left | 1.442 | 1.451 | 1.434 | 1.448 | 1.429 |
| | | right | 1.424 | 1.435 | 1.413 | 1.433 | 1.415 |
| 1-pentacenyl | radical | left | 1.420 | | | | |
| | | right | 1.354 | | | | |
| | anion | left | 1.466 | | | | |
| | | right | 1.397 | | | | |
| 2-pentacenyl | radical | left | 1.353 | | | | |
| | | right | 1.419 | | | | |
| | anion | left | 1.396 | | | | |
| | | right | 1.466 | | | | |
| 13-pentacenyl | radical | left | 1.389 | | | | |
| | | right | 1.389 | | | | |
| | anion | left | 1.435 | | | | |
| | | right | 1.436 | | | | |
| 14-pentacenyl | radical | left | 1.400 | | | | |
| | | right | 1.377 | | | | |
| | anion | left | 1.448 | | | | |
| | | right | 1.421 | | | | |

Table 3.3: EAs (in eV) with ZPVE corrected values in parentheses.

| | B3LYP | BHLYP | BLYP | BP86 | LSDA | Expt1 | Expt2 | Expt3 |
|---|---|---|---|---|---|---|---|---|
| 1-naphthalenyl | 1.31 | 1.06 | 1.24 | 1.40 | 1.97 | | | |
| | (1.37) | (1.11) | (1.30) | (1.47) | (2.03) | 1.37±0.02 | 1.43±0.06 | 1.403±0.015 |
| 2-naphthalenyl | 1.25 | 0.99 | 1.19 | 1.35 | 1.90 | | | |
| | (1.31) | (1.04) | (1.25) | (1.42) | (1.96) | 1.30±0.02 | 1.37±0.04 | $1.34^{+0.03}_{0.07}$ |
| 1-anthracenyl | 1.46 | 1.19 | 1.38 | 1.56 | 2.12 | | | |
| | (1.51) | (1.24) | (1.45) | (1.62) | (2.18) | | | |
| 2-anthracenyl | 1.39 | 1.12 | 1.33 | 1.51 | 2.07 | | | |
| | (1.46) | (1.17) | (1.41) | (1.58) | (2.15) | | | |
| 9-anthracenyl | 1.61 | 1.37 | 1.51 | 1.69 | 2.28 | | | |
| | (1.68) | (1.42) | (1.58) | (1.77) | (2.35) | | | |
| 1-tetracenyl | 1.55 | 1.25 | 1.48 | 1.66 | 2.22 | | | |
| | (1.61) | (1.27) | (1.53) | (1.71) | (2.27) | | | |
| 2-tetracenyl | 1.49 | 1.17 | 1.43 | 1.60 | 2.15 | | | |
| | (1.56) | (1.20) | (1.48) | (1.65) | (2.20) | | | |
| 12-tetracenyl | 1.75 | 1.47 | 1.65 | 1.84 | 2.43 | | | |
| | (1.82) | (1.49) | (1.72) | (1.91) | (2.49) | | | |
| 1-pentacenyl | 1.61 | | | | | | | |
| | (1.68) | | | | | | | |
| 2-pentacenyl | 1.55 | | | | | | | |
| | (1.63) | | | | | | | |

| | |
|---|---|
| 13-pentacenyl | 1.93 (2.01) |
| 14-pentacenyl | 1.84 (1.93) |

Table 3.4: ZPVE corrected energies (kcal/mol) relative to lowest energy species.

| | | B3LYP | BHLYP | BLYP | BP86 | LSDA |
|---|---|---|---|---|---|---|
| 1-naphthalenyl | radical | 31.647 | 25.663 | 29.995 | 33.874 | 46.717 |
| | anion | 0.000 | 0.000 | 0.000 | 0.000 | 0.000 |
| 2-naphthalenyl | radical | 31.569 | 25.530 | 30.005 | 33.824 | 46.325 |
| | anion | 1.273 | 1.499 | 1.131 | 1.159 | 1.144 |
| 1-anthracenyl | radical | 38.057 | 32.393 | 36.006 | 40.192 | 53.175 |
| | anion | 3.124 | 3.768 | 2.663 | 2.771 | 2.843 |
| 2-anthracenyl | radical | 37.925 | 32.224 | 35.958 | 40.089 | 52.732 |
| | anion | 4.219 | 5.156 | 3.413 | 3.555 | 3.124 |
| 9-anthracenyl | radical | 38.629 | 32.819 | 36.529 | 40.711 | 54.105 |
| | anion | 0.000 | 0.000 | 0.000 | 0.000 | 0.000 |
| 1-tetracenyl | radical | 41.822 | 34.383 | 39.244 | 43.551 | 56.543 |
| | anion | 4.597 | 5.153 | 3.935 | 4.083 | 4.094 |
| 2-tetracenyl | radical | 41.758 | 34.323 | 39.288 | 43.527 | 56.145 |
| | anion | 5.773 | 6.724 | 5.111 | 5.375 | 5.470 |
| 12-tetracenyl | radical | 42.077 | 34.383 | 39.660 | 43.984 | 57.409 |
| | anion | 0.000 | 0.000 | 0.000 | 0.000 | 0.000 |
| 1-pentacenyl | radical | 46.333 | | | | |
| | anion | 7.525 | | | | |
| 2-pentacenyl | radical | 46.325 | | | | |
| | anion | 8.674 | | | | |
| 13-pentacenyl | radical | 46.429 | | | | |
| | anion | 0.000 | | | | |
| 14-pentacenyl | radical | 45.814 | | | | |
| | anion | 1.319 | | | | |

Table 3.5: Global AEAs (eV), with ZPVE corrected values in parentheses.

| | B3LYP | BHLYP | BLYP | BP86 | LSDA |
|---|---|---|---|---|---|
| naphthalenyl | 1.31 (1.37) | 1.05 (1.11) | 1.24 (1.30) | 1.40 (1.47) | 1.95 (2.01) |
| anthracenyl | 1.59 (1.64) | 1.36 (1.40) | 1.50 (1.56) | 1.68 (1.74) | 2.24 (2.29) |
| tetracenyl | 1.74 (1.81) | 1.47 (1.49) | 1.64 (1.70) | 1.83 (1.89) | 2.38 (2.43) |
| pentacenyl | 1.89 (1.99) | | | | |

## 3.8 REFERENCES


[1] D. J. Cook and R. J. Saykally, *Astrophys. J.* **493**, 793 (1998).

[2] J. Szczepanski and M. Vala, *Nature* **363**, 699 (1993).

[3] H. Wang and M. Frenklach, *J. Phys. Chem.* **98**, 11465 (1994).

[4] H. Richter, O. A. Mazyar, R. Sumathi, W. H. Green, J. B. Howard, and J. W. Bozzelli, *J. Phys. Chem. A* **105**, 1561 (2001).

[5] C. Barckholtz, T. A. Barckholtz, and C. M. Hadad, *J. Am. Chem. Soc.* **121**, 491 (1999).

[6] H. F. Calcote, *Combust. Flame* **42**, 215 (1981).

[7] C. J. Pope, J. A. Marr, and J. B. Howard, *J. Phys. Chem.* **97**, 11001 (1993).

[8] J. L. Durant, W. F. Busby, A. L. Lafleur, B. W. Penman, and C. L. Crespi, *Mutat. Res.* (371), 123 (1996).

[9] K. M. Ervin, T. M. Ramond, G. E. Davico, R. L. Schwartz, S. Casey, M., and W. C. J. Lineberger, *Phys. Chem A* **105**, 10822 (2001).

[10] D. R. Reed and S. R. Kass, *J. Mass Spectrom.* **35**, 534 (2000).

[11] H. A. Lardin, R. R. Squires, and P. G. Wenthold, *J. Mass Spectrom.* **36**, 607 (2001).

[12] M. W. Wong, *Chem. Phys. Lett.* **256**, 391 (1996).

[13] J. Cioslowski, G. Liu, and D. Moncrieff, *J. Am. Chem. Soc.* **118**, 5261 (1996).

[14] J. Cioslowski, G. Liu, and D. Moncrieff, *J. Org. Chem* **61**, 4111 (1996).

[15] K. B. Wiberg, *J. Org. Chem* **62**, 5720 (1997).

[16] J. C. Rienstra-Kiracofe, G. S. Tschumper, H. F. Schaefer, III, S. Nandi, and G. B. Ellison, *Chem. Rev.* **102(1)**, 231 (2002).

[17] S. T. Brown, J. C. Rienstra-Kiracofe, and H. F. Schaefer III, *J. Phys. Chem A* **103**, 4065 (1999).

[18] J. C. Rienstra-Kiracofe, C. J. Barden, S. T. Brown, and H. F. Schaefer III, *J. Phys. Chem. A* **105**, 524 (2001).

[19] S. Huzinaga, *J. Chem. Phys.* **42**, 1293 (1965).

[20] T. H. Dunning, Jr., *J. Chem. Phys.* **53**, 2823 (1970).

[21] T. J. Lee and H. F. Schaefer, *J. Chem. Phys.* **83**, 1784 (1985).

[22] C. Lee, W. Yang, and R. G. Parr, *Phys. Rev. B* **37**, 785 (1998).

[23] J. P. Perdew, *Phys. Rev. B* **33**, 8822 (1986).

[24] J. P. Perdew, *Phys. Rev. B* **34**, 7406 (1986).

[25] A. D. Becke, *J. Chem. Phys.* **98**, 5648 (1993).

[26] A. D. Becke, *J. Chem. Phys.* **98**, 1372 (1992).

[27] R. E. Gaussian 94, M. J. Frisch, G. W. Trucks, H. B. Schlegel, P. M. W. Gill, B. G. Johnson, M. A. Robb, J. R. Cheeseman, T. Keith, G. A. Petersson, J. A. Montgomery, K. Raghavachari, M. A. Al-Laham, V. G. Zakrzewski, J. V. Ortiz, J. B. Foresman, J. Cioslowski, B. B. Stefanov, A. Nanayakkara, M. Challacombe, C. Y. Peng, P. Y. Ayala, W. Chen, M. W. Wong, J. L. Andres, E. S. Replogle, R. Gomperts, R. L. Martin, D. J. Fox, J. S. Binkley, D. J. Defrees, J. Baker, J. P. Stewart, M. Head-Gordon, C. Gonzalez, and J. A. Pople, Gaussian, Inc., Pittsburgh PA, 1995.

[28] A. D. Becke, *Phys. Rev. A* **38**, 3098 (1998).

[29] S. H. Vosko, L. Wilk, and M. Nusair, *Can. J. Phys.* **58**, 1200 (1980).

[30] P. Hohenberg and W. Kohn, *Phys. Rev. A* **136**, 864 (1964).

[31] W. Kohn and L. J. Sham, *Phys. Rev. A* **140**, 1133 (1965).

[32] J. C. Slater, *Quantum Theory of Molecules and Solids: The Self-Consistent Field for Molecules and Solids*. (McGraw-Hill, New York, 1974).

[33] M. J. F. Gaussian 98 (Revision A.11), G. W. Trucks, H. B. Schlegel, G. E. Scuseria, M. A. Robb, J. R. Cheeseman, V. G. Zakrzewski, J. A. Montgomery, Jr., R. E. Stratmann, J. C. Burant, S. Dapprich, J. M. Millam, A. D. Daniels, K. N. Kudin, M. C. Strain, O. Farkas, J. Tomasi, V. Barone, M. Cossi, R. Cammi, B. Mennucci, C. Pomelli, C. Adamo, S. Clifford, J. Ochterski, G. A. Petersson, P. Y. Ayala, Q. Cui, K. Morokuma, P. Salvador, J. J. Dannenberg, D. K. Malick, A. D. Rabuck, K. Raghavachari, J. B. Foresman, J. Cioslowski, J. V. Ortiz, A. G. Baboul, B. B. Stefanov, G. Liu, A. Liashenko, P. Piskorz, I. Komaromi, R. Gomperts, R. L. Martin, D. J. Fox, T. Keith, M. A. Al-Laham, C. Y. Peng, A. Nanayakkara, M. Challacombe, P. M. W. Gill, B. Johnson, W. Chen, M. W. Wong, J. L. Andres, C. Gonzalez, M. Head-Gordon, E. S. Replogle, and J. A. Pople, Gaussian, Inc., Pittsburgh PA, 2001.

[34] J. A. Pople, P. M. W. Gill, and N. C. Handy, *Int. J. Quant. Chem.* **56**, 303 (1995).

# CHAPTER 4

# HOMONUCLEAR TRANSITION METAL TRIMERS*

*B. N. Papas and H. F. Schaefer, 2005. The Journal of Chemical Physics 123 Article Number 074321. Reprinted here with permission of the American Institute of Physics.

## 4.1 ABSTRACT

Density functional theory has been used to determine the ground state geometries and electronic states for homonuclear transition metal trimers constrained to equilateral triangle geometries. This represents the first application of consistent theoretical methods to all of the ten 3d block transition metal trimers, from scandium to zinc. A search of the potential surfaces yields the following electronic ground states and bond lengths: $Sc_3$ ($^2A_1'$, 2.83 Å), $Ti_3$ ($^7E'$, 2.32), $V_3$ ($^2E''$, 2.06), $Cr_3$ ($^{17}E'$, 2.92), $Mn_3$ ($^{16}A_2'$, 2.73), $Fe_3$ ($^{11}E''$, 2.24), $Co_3$ ($^6E''$, 2.18), $Ni_3$ ($^3A_2''$, 2.23), $Cu_3$ ($^2E'$, 2.37), $Zn_3$ ($^1A_1'$, 2.93). Vibrational frequencies, several low-lying electronic states, and trends in bond lengths and atomization energies are discussed. The predicted dissociation energies $\Delta E$ ($M_3 \rightarrow M_2 + M$) are 49.4 kcal mol$^{-1}$ ($Sc_3$), 64.3 kcal mol$^{-1}$ ($Ti_3$), 60.7 kcal mol$^{-1}$ ($V_3$), 11.5 kcal mol$^{-1}$ ($Cr_3$), 32.4 kcal mol$^{-1}$ ($Mn_3$), 61.5 kcal mol$^{-1}$ ($Fe_3$), 78.0 kcal mol$^{-1}$ ($Co_3$), 86.1 kcal mol$^{-1}$ ($Ni_3$), 26.8 kcal mol$^{-1}$ ($Cu_3$), and 4.5 kcal mol$^{-1}$ ($Zn_3$).

## 4.2 INTRODUCTION

Since Anderson[1] examined small clusters of titanium, chromium, iron, and nickel using a low spin molecular orbital approximation in 1976 , interest in small transition metal clusters has led to an explosion in publications, specialized symposia,[2-8] and review papers[9-18] (In particular, note the review by Lombardi and Davis[15]). The fuel for this explosion is as diverse as the subject matter it studies. Small clusters bridge the gap between the discrete realm of Schrödinger's equation and the band structure of metal solids.[19a] On a fundamental level, chemists desire an intuitive understanding of small clusters in order to understand the formation of larger clusters; in order to understand the behavior of metals.[19b] Interest in such clusters is hardly purely academic, however. They show significant size-specificity in many properties, allowing specialized applications in: catalysis,[19c] chemisorption and substrate adsorbtion,[19d] crystal growth,[19e] lasers,[19f] magnetism,[19g] nucleation,[19h] photographic processes,[19i] and reactivity.[19j]

A quarter of a century has passed since Anderson's work, and even one of the simplest classes of transition metal clusters, the homonuclear trimers, are not well understood. The primary reasons for this

are the density of electronic states which these systems show, Jahn-Teller instabilities, and frequently flat potential surfaces. The result is that analysis of electronic spectra is difficult and often inconclusive, and the convergence of *ab initio* computations is tribulating at best. In most cases, previous theoretical studies have not identified the spatial symmetries of the electronic states under consideration.

Four years ago, Barden, Rienstra-Kiracofe, and Schaefer[20] systematically examined the homonuclear transition metal dimers using a variety of DFT methods. To proceed to cluster growth, the trimers have now been studied in a similar fashion, though only with the BP86 functional, as it was shown in the Barden work to provide the best agreement with experiment. The goal of this research is to provide systematic benchmarks for comparison to existing and future experiments and to future higher level theoretical studies.

## 4.3 METHODS

Stationary geometries for the ten molecules studied were predicted using Becke's pure 1988 DFT exchange functional (B)[21] with the correlation functional of Perdew (P86).[22,23] The BP86 method appears to be slightly more reliable than B3LYP for molecular systems incorporating transition metals.[24-27] It has been noted by a referee that the DFT methods used in this research cannot describe anti-ferromagnetic coupling. As such, only ferromagnetic states are considered, and special attention is given to previous studies which examine alternate magnetic couplings.

The above noted theoretical challenges may be discussed in terms of a particularly difficult case, the $Mn_3$ molecule. The DFT methods used in this research predict that the lowest electronic state of $Mn_3$ has 15 unpaired electrons and S = $^{15}/_2$. This suggests that all the molecular orbitals formed from atomic 4*s* orbitals are filled and the d electrons are all unpaired. Thus each atom may be represented as $3d^5$, S = $^5/_2$. If these are arranged in a perfect equilateral triangle, the Heisenberg model Hamiltonian is exactly soluble. This yields electronic states with S = $^{15}/_2$, $^{13}/_2$, $^{11}/_2$, $^9/_2$, $^7/_2$, $^5/_2$, $3/_2$, and $^1/_2$, with the lower S values having many distinct linearly independent spin eigenfunctions. The ground state will likely be either S = $^{15}/_2$ or S = $^1/_2$. However, the above described S = $^1/_2$ anti-ferromagnetic state (15 unpaired

spins) is not the S = $^1/_2$ state (one unpaired electron) state found here. Another way of stating this is to say that we are only considering strong coupling between the d shells. The extreme difficulty of carrying out a rigorous theoretical treatment of such low spin electronic states has been examined in detail in a series of papers by Davidson and coworkers.[28-32]

The basis sets used in this study were constructed from the Wachters (14*s*9*p*5*d*) sets,[33] which were supplemented with diffuse 3d functions by Hay[34] and additionally with 4p functions as given by Hood, Pitzer, and Schaefer.[35] The sets were loosely contracted to (10*s*8*p*3*d*) with the scheme of Hood et al.[35] Spherically harmonic angular momentum functions were employed.

Quantum chemical computations were carried out using the MOLPRO[36,37] computational suite, using the restricted Kohn-Sham based DFT method. The restricted paradigm was chosen because in most cases it converged more rapidly than the unrestricted case (if that case indeed converged). Self-consistent field convergence was determined by stringent criteria; the square sum of the density matrix element changes was less than $10^{-7}$ and the energy change was less than $10^{-10}$ Hartree ($E_h$). Geometry convergence was also determined with tightened criteria of $3x10^{-7}$ a.u. for the maximum component of the gradient and $1x10^{-6}$ hartrees for the energy change. Numerical integration of the functionals was carried out using the MOLPRO[36,37] adaptive quadrature to generate a grid on which the Slater-Dirac functional should be integrated to $10^{-10}$ $E_h$ accuracy. Analytic first derivatives were used to help determine state designations in cases where there are multiple possibilities, i.e. when the Cartesian forces are not close to zero at the optimized geometry (where the gradient along the bond length coordinate is zero) then it is assumed that the state is of degenerate E′ or E″ symmetry.

Unfortunately, at this time analytic second derivatives are not implemented for DFT in MOLPRO.[36] As a result, harmonic vibrational frequencies were computed using INTDIF2004[38] through numerical differentiation of analytic gradients. This alternate program was used because MOLPRO[36] uses only Cartesian displacements in numerically computing vibrational frequencies, which cause unphysical mixing of states when the symmetry is broken. Intdif2004 allows the use of internal coordinates, in this case the symmetric stretch (SS), antisymmetric stretch (AS), and bend (B). Since only

the antisymmetric stretch breaks the $C_{2v}$ computational point group, it is the only internal coordinate that should be considered suspicious. In the event that the ground state is degenerate and should undergo Jahn-Teller distortion, symmetry was relaxed to $C_{2v}$ and an optimized geometry was found for the two states arising from the degenerate state in $D_{3h}$ symmetry. In each case, there should be a symmetric stretch ($a_1'$) and degenerate bending and antisymmetric stretch ($e'$) vibrational modes (these three modes are of $a_1$, $a_1$, and $b_2$ irreducible representations, respectively, in $C_{2v}$ symmetry). For such structures, the potential surface is highly anharmonic along the antisymmetric stretch, and the resulting harmonic frequencies should be considered highly suspect, especially since the loss of $C_{2v}$ symmetry means that interaction with other low-lying states may produce anomalous energies.

It must also be noted that the BP86 implemented in Molpro[36] is different than those implemented in some other popular programs, including that used to produce the results of Barden.[20] Since $\Delta E$ ($M_3 \rightarrow M_2 + M$) requires the dimer energy, the dimers had to be computed in Molpro.[36] The BP86 ground states reported by Barden[20] were assumed. Optimized bond lengths found in this study where on average 0.003 Å different than those he reported, while the harmonic frequencies differed by 2.25 $cm^{-1}$ and $D_e$ values by 0.27 eV. Some of these differences may be accounted for by his use of unrestricted Kohn-Sham formalism.

## 4.4 RESULTS

### 4.4.1 $Sc_3$

Both experimental and theoretical studies exist for $Sc_3$. Experimentally, Knight, Woodward, Van Zee and Weltner[39] have studied this species using electron spin resonance, and a resonance Raman study was reported by Moskovits, DiLella and Limm.[40] Theoretically, Walch and Bauschlicher[41,42] have performed CASSCF/CCI computations, while Pápai and Castro,[43] Bérces,[44] and Wu, Zhang, Meng, Dai, Han, and Jin[45] have examined it with DFT.

In 1983 Knight et al.[39] reported a $^2A_1'$ ground state and in 1984 Moskovits et al.[40] postulated a $^2E'$ ground state. A year later Walch and Bauschlicher[41] attempted to resolve this conflict using high-level multi-reference computations and found a $^2A_2''$ ground state with a bond length of 3.04 Å. Pápai and Castro's 1997 paper[43] reported a $^2A_1'$ ground state bond length of 2.83 Å, while Bérces[44] examined the same state with a bond length of 2.81 Å. Contrary to all previous results, Wu et al.[45] reported a $C_{2v}$ quartet ground state, which for BP86 is distorted from an equilateral triangle by 6.2 degrees and is 0.26 eV more stable than the lowest doublet (also of $C_{2v}$ symmetry).

In the present research, spin states ranging from doublets to decets were examined. These computations support the $Sc_3$ results of Pápai and Castro[43] and Bérces.[44] Specifically the $^2A_1'$ ground state ([Core] $6a_1'^2\ 8e'^4\ 1a_2''^2\ 7a_1'$ ) and the 2.83 Å bond length are reproduced, suggesting that its status as ground state is not merely a result of the basis set employed. A low-lying $^2A_2''$ state (4.7 kcal/mol) was also found, having a bond length similar to that reported by Pápai and Castro[43] (2.84 Å). Other low-lying electronic states and their bond lengths are reported in Table 1.

The harmonic vibrational frequencies for ground state $Sc_3$ are 267 $cm^{-1}$ (symmetric stretch), 139 $cm^{-1}$ (antisymmetric stretch), and 140 $cm^{-1}$ (bend). As can be seen in Table 2, these values are in qualitative agreement with other DFT results, all of which indicate that the $^2A_1'$ state is a true minimum on the potential energy surface. These also agree well with the experimental results found by Moskovits, DiLella, and Limm.[40]

Assuming dissociation into $^2D_g$ scandium atoms, an atomization energy of 3.89 eV is predicted. This is comparable to the value 3.75 eV determined by Pápai and Castro[43] and suggests that $Sc_3$ is a well-bound molecule. Dissociation into the dimer and an atom is predicted to take 2.14 eV.

### 4.4.2 $Ti_3$

Only one experimental study of the titanium trimer exists: the 1996 photoelectron spectroscopy (PES) study performed by Wu, Desai and Wang.[46] Applications of theory, however, abound. In his early study, Anderson[1] used a low-spin model to examine several transition metal clusters, including $Ti_3$. Eight

years later, the structure was examined using configuration interaction (CI) by Cremaschi and Whitten.[47] Wei, Zeng, You, Yan, and Gong[48]; Zhao, Qiu, Wang, Wang, and Wang[49]; Oymak and Erkoç[19]; Castro, Liu, Zhai, and Wang[50]; and Wu et al.[45] have all studied this trimer using DFT.

Anderson[1] reported a 3.1 Å bond length for the equilateral triangle geometry of the titanium trimer. Cremaschi and Whitten[47] report an unspecified electronic ground state with ten unpaired electrons. Wei et al.[48] report an equilateral triangle triplet with a bond length of 2.35 Å as the minimum, while Zhao et al.[49] report a bond length of 2.28 Å. The ground state reported by Oymak and Erkoç[19] is of $C_{2v}$ structure, though only 8 degrees away from an equilateral triangle, with a bond length of 2.3 Å. Castro et al.[50] report peculiar scalene ($C_S$ symmetry) triangles, with a septet ground spin state. Wu et al.[45] report a quintet $C_{2v}$ ground state, as determined by B3LYP, though they only examined spin multiplicities ranging from one to seven.

In the present research all spin states from singlet to S = 6 were computed. A $^7E'$ ground state ([Core] $6a_1'^2\ 1a_2''^2\ 7a_1'^2\ 8e'^2\ 3e''^2\ 8a_1'\ 9e'$) was found for the titanium trimer in $D_{3h}$ symmetry, with a bond length of 2.32 Å. There are four excited electronic states of $Ti_3$ within 10 kcal/mol of the ground state, a $^5E'$ state (2.2 kcal/mol above the ground state), a $^3A_2'$ state (8.1 kcal/mol), a $^3E''$ state(8.4 kcal/mol), and a $^9A_2'$ state (9.8 kcal/mol). These have bond lengths of 2.34, 2.39, 2.38 and 2.43 Å, respectively. This energetic ordering of septet, quintet, and triplet is the same as that reported by Castro et al.[50]

Since the ground state is degenerate, additional optimizations were performed in $C_{2v}$ symmetry in order to obtain frequencies. This relaxation caused a decrease in energy of 2.53 kcal/mol for the $^7A_1$ state, and 2.48 kcal/mol for the $^7B_2$ state. The first is a triangle with a central angle of 52º and a bond length of 2.44 Å, while the latter has a central angle of 68º and a bond length of 2.24 Å. These structures are consistent with those reported by Oymak and Erkoç.[19] The $^7A_1$ state has predicted harmonic vibrational frequencies of 369 $cm^{-1}$ (SS), 35 $cm^{-1}$ (AS), and 190 $cm^{-1}$ (B). The $^7B_2$ state has frequencies of 363 $cm^{-1}$ (SS), 44i $cm^{-1}$ (AS) and 200 $cm^{-1}$ (B). Table 2 compares these with the one previous DFT result for a septet from Wu et al.[45] The results of Wu were computed with B3LYP, the use of which is usually somewhat less effective than BP86 for transition metal systems.

Dissociation into three $^3F_g$ titanium atoms gives our predicted atomization energy of 6.09 eV. This is smaller than the binding energies reported by Wei et al.[48] (7.11 eV) and Zhao et al.[49] (8.79 eV), but similar to that reported by Oymak and Erkoç[19] (5.84 eV). The single atom dissociation energy is predicted to be 2.79 eV.

### 4.4.3 $V_3$

As for $Ti_3$, Wu, Desai, and Wang[51] have measured a PES spectrum for the vanadium trimer. In 1993 Su, Hales, and Armentrout[52] determined a binding energy experimentally by CID. Grönbeck and Rosén;[53] Sun, Luo, Zhao, and Wang;[54] and Wu and Ray[55] have attempted to describe the ground state using theoretical methods. Calaminici, Köster, Carrington, Roy, Russo, and Salahub[56] used DFT and the result of a PFI-ZEKE experiment performed by Yang, James, Rayner, and Hackett[57] to examine the electronic structure of $V_3$, while Varga, Bolton, Grönbeck, Snis, Rosén, and Fricke[58] examine the effect of DFT functional choice upon theoretical results. Most recently, in unpublished research, Doreen Leopold has used anion photoelectron spectroscopy to measure vibrational frequencies and excitation energies for $V_3$.

In every case for which the $V_3$ spin multiplicity is examined, a doublet ground state is reported,[53,55,56,58] though controversy does exist for the geometry. The DFT studies by Grönbeck and Rosén[53] and by Wu and Ray[55] both report $C_{2v}$ structures, while Sun et al.[54] and Calaminici et al.[56] report equilateral triangles. The latter have bond lengths of 2.38 and 2.169 Å respectively. Calaminici et al.[56] also report that the ground state is of $^2A_1'$ symmetry and that there is a low-lying $C_{2v}$ quartet. Calminici noted, however, that DFT stabilization of d orbitals may have caused the frontier $a_1'$ orbital to be artificially lower than the frontier e″, and that the true ground state may be $^2E''$.

Electronic states ranging from doublets to S = $^{15}/_2$ were examined, and the ground state of $V_3$ was found to be $^2E''$ ([Core] $6a_1'^2\ 8e'^4\ 1a_2''^2\ 7a_1'^2\ 8a_1'^2\ 3e''^3$), with an equilibrium bond length of 2.06 Å. This state is 5.9 kcal/mol lower in energy than the $^2A_1'$ state and 5.8 kcal/mol below a $^4E'$ state. Since the $^2E''$ state is doubly degenerate, it will distort to the $C_{2v}$ structures reported in other DFT papers.[53,55] Doreen Leopold

(unpublished) has found excitations at 5.404±0.086 and 11.551±0.086 kcal/mol. We predict two excited states near the first of those peaks, namely the $^4E'$ (5.8 kcal/mol) and $^2A_1'$ (5.9 kcal/mol) states. Likewise, there are two states which could correspond to the higher exitation: $^4E''$ (14.2 kcal/mol), and $^6A_1'$ (16.0 kcal/mol).

As with the titanium trimer, the $^2E''$ ground state of $V_3$ is Jahn-Teller unstable. When symmetry is relaxed to $C_{2v}$ (isosceles) the $^2A_2$ state angle shrinks to 52º and a bond length increases to 2.14 Å. The $^2B_1$ state changes in the opposite manner, having a central angle of 67º and a bond length of 1.99 Å. These states are stabilized compared to the parent $^2E''$ state by 3.52 and 2.12 kcal/mol, respectively. The symmetric stretch vibrational frequency ($\omega_1$ = 467 $cm^{-1}$ for $^2A_2$, 476 $cm^{-1}$ for $^2B_1$) and bending frequency ($\omega_2$ = 244 and 270) are in reasonable agreement with other DFT results (Table 2).[56,58] The $^2A_2$ antisymmetric stretch ($\omega_3$ = 203 $cm^{-1}$) is similar to those computed previously, both for the $D_{3h}$ ground state[56] and $C_{2v}$ structures.[58] An antisymmetric stretch frequency of 481i $cm^{-1}$ is found for the $^2B_1$ state. Our predictions for the $^2A_2$ state compare well with unpublished results supplied by Doreen Leopold (460±20 $cm^{-1}$ and 200±20 $cm^{-1}$), though those are for an equilateral triangle.

The vanadium trimer is predicted to lie 7.21 eV lower in energy than three $^4F_g$ vanadium atoms. This is a larger dissociation energy than that reported by Calaminici et al.[56] (5.57 eV), which is in turn greater than the experimental zero-point corrected atomization energy value (4.17).[52] This difference is much larger than can be accounted for by vibrational zero-point energy. The energy to dissociate $V_3$ into $V_2$ and V is predicted to be 2.63 eV.

### 4.4.4 $Cr_3$

While somewhat controversial, the chromium trimer is well studied. It was first examined in 1975 theoretically by Anderson[1], and experimentally by DiLella, Limm, Lipson, Moskovits, and Taylor[59] in 1982. Wang, Wu, and Cheng[60] and Fang, Davis, Lu, and Lombardi[61] have also studied it experimentally; while Cheng and Wang,[62] Bérces,[44] Kohl and Bertsch,[63] and Hobbs and Hafner[64] have used various DFT methods to model $Cr_3$.

Anderson's[1] low-spin trimer has a bond length of 2.7 Å for the equilateral triangle. Argon matrix Raman spectra obtained by DiLella et al.[59] suggest that the structure should be distorted slightly to $C_{2v}$. The DFT research by Bérces[44] finds a ground state fitting this description, a $^5B_2$ state (which corresponds to $^5E'$ in the $D_{3h}$ point group) with a bond angle of only 65.8º. The lowest non-distorted equilateral triangle Bérces[44] reports is the singlet, which is 2.50 eV higher in energy than the ground state. DFT computations by Wang et al.[60] reported a $C_{2v}$ $^7A_1$ ground state, which corresponds to a complex of a chromium dimer with a ground state atom. This state was also found by Hobbs et al.[64] Most recently Fang et al.[61] have done another argon matrix resonance Raman experiment, and found evidence that the chromium trimer has a $D_{3h}$ symmetry electronic ground state.

The present research predicts a $^{17}E'$ ([Core] $6a_1'^2$ $8e'^2$ $1a_2''$ $7a_1'$ $3e''^2$ $8a_1'$ $9e'^2$ $10e'^2$ $4e''^2$ $3a_1''$ $3a_2'$ $11e'$) ground state for $Cr_3$ with a bond length of 2.92 Å. This state is 16 kcal/mol lower in energy than the nearest excited state ($^{17}E''$), and 40 kcal/mol lower than the lowest singlet state (all spin-states in between were also computed). A bond length of 1.98 Å was found for the $^1A_1'$ state, comparable to that reported by Bérces.[44] The $^{17}E'$ ground state necessarily shows Jahn-Teller coupling. In light of the very high spin predicted by BP86, we would encourage the use of higher level theoretical methods for $Cr_3$. Both Hobbs et al.[64] and Kohl and Bertsch[63] have examined $Cr_3$ spin couplings more extensively. Both report frustrated noncollinear anti-ferromagnetic ground states derived from six unpaired electrons. It is unclear if the 16 unpaired electron systems were considered.

Compared to $Ti_3$ and $V_3$, $Cr_3$ shows only small Jahn-Teller distortions. This is evident from our predicted stabilization energies: 0.69 kcal/mol for $^{17}A_1$, and 0.60 kcal/mol for $^{17}B_2$. This is not merely the result of symmetry breaking caused by the integration grid used by DFT, since these states have angles of 66º and 56º, respectively. The bond length changes by about 0.08 Å compared to the parent state, with the $^{17}A_1$ state having a bond distance of 2.85 Å and the $^{17}B_2$ state one of 3.00 Å. The $^{17}A_1$ state has predicted vibrational frequencies of 197 $cm^{-1}$ (SS), 103 $cm^{-1}$ (B), and 79 $cm^{-1}$ (AS), while for the $^{17}B_2$ state these are 200, 134, and 61i, respectively. These are significantly different from previous theoretical[61] (which correspond to a different state) frequencies (see Table 2). The similarity between the bending vibrational

frequency and that measured by DiLella et al.[59] suggests that the $^{17}A_1$ state may be what was observed in their experiments. The symmetric stretch (197 versus 308 $cm^{-1}$) is low, but, given the flatness of the potential surface predicted by DFT, not surprising. Since the stabilization energy and the barrier to pseudo-rotation (0.09 kcal/mol) are both small, $Cr_3$ may move freely over a large area of its potential surface. This should complicate the evaluation of the vibrational spectrum.

Assuming dissociation into three $^7S_g$ chromium atoms, this trimer has a dissociation energy of only 1.15 eV. Fang et al.[61] report an experimental $D_e$(atomization) value of 0.36 eV, while Cheng and Wang[62] report a DFT binding energy of 2.21 eV for the equilateral triangle structure. The experimental value (1.15 eV) was determined through use of a Morse potential fit. As discussed in the nickel trimer section, this may not be an entirely appropriate means for deducing binding energies for these systems.

### 4.4.5 $Mn_3$

A 1988 Raman study performed by Bier, Haslett, Kirkwood, and Moskovits[65] concluded that $Mn_3$ is a weakly Jahn-Teller distorted equilateral triangle of possibly $^2E'$ or $^2E''$ electronic state. The DFT study of Bérces[44] reports a sextet state with an angle of 61 degrees as the ground state, and a $D_{3h}$ structure with $^4E'$ electronic state 68 kcal/mol higher in energy. Bérces'[44] sextet has a bond length of 2.48 Å and the quartet 2.05 Å. A DFT examination of the magnetic properties of $Mn_3$ performed by Pederson, Reuse, and Khanna[66] found a magnetic moment per atom of 5.0 $\mu_B$ for an isosceles triangle ground state, as do studies by Nayak and Jena[67] and by Nayak, Rao, and Jena.[68] This result implies that $S = {}^{15}/_2$. These results confirm those measured in matrix isolation by Baumann, Van Zee, Bhat, and Weltner.[69] Most recently Sekine, Kondo, Yamamoto, and Onoe[70] used DFT and found an equilateral triangle as the ground state, with a bond length of 2.76 Å, a spin multiplicity of 16, and unspecified spatial symmetry.

Our examination of electronic states with spins ranging from doublet to $S = {}^{15}/_2$ predicts a $^{16}A_2'$ ([Core] $6a_1'^2\ 8e'^4\ 1a_2''\ 7a_1'\ 3e''^2\ 8a_1'\ 9e'^2\ 10e'^2\ 4e''^2\ 3a_1''\ 3a_2'\ 11e'^2$) ground state with a bond length of 2.73 Å, supporting the spin multiplicity of Pederson, Reuse, and Khanna,[66] Jena and coworkers,[67,68] Baumann et al.,[69] and Sekine et al.[70] The nearest exited electronic state predicted here is a $^{16}E''$ state with a bond

length of 2.67 Å, lying 5.6 kcal/mol above the ground state. Both quartet and sextet states lay over 50 kcal/mol above the ground state. Nayak et al.[68] report finding an S = $^{13}/_{2}$ equilateral triangle state 16 kcal/mol above the ground state. The present research predicts a $^{14}$E″ state 15.2 kcal/mol above the $Mn_3$ ground state. The spin states of $Mn_3$ have been examined by Nayak and Jena,[67] Nayak et al.,[68] and Pederson et al.[66] The two papers by Nayak both report a ferromagnetic (S = $^{15}/_{2}$) ground state, while Pederson et al. find little separation between the ferromagnetic and anti-ferromagnetic (S = $^{5}/_{2}$) coupled systems. In fact, the ordering is method dependent and warrants further investigation.

Harmonic vibrational frequencies predicted for the manganese trimer are 202 $cm^{-1}$ (SS), 146 $cm^{-1}$ (AS), and 147 $cm^{-1}$ (B). These are in good agreement with the experimental values reported by Bier et al.[65] (Table 2), though it should be noted that the symmetric stretch frequency they report necessarily includes anharmonicity, so the harmonic frequency is expected to be slightly higher.

This high spin multiplicity of $Mn_3$ suggests that the trimer is a complex of three ground state ($^6S_g$) manganese atoms; however, atomization of $Mn_3$ would require 2.33 eV. This is greater than that reported by Nayak, Rao, and Jena[68] (0.75 or 0.96 eV, depending upon the method) but very close to the 2.43 eV reported by Pederson, Reuse, and Khanna.[66] Sekine et al.[70] report a binding energy of 6.42 eV, significantly higher than any computed previously for $Mn_3$. The trimer to diatomic plus atom dissociation energy is predicted to be 0.50 eV.

### 4.4.6 $Fe_3$

Experimentally, in 1985 Micklitz, Pasternak, and Sanchez[71] reported a triangular structure for $Fe_3$, while Cox et al.[72] found it to be a nonet (S = 4). Other studies prior to 2000[1,71-91] will not be explicitly discussed, except to say that most agree upon a $C_{2v}$ symmetry nonet as the ground state of $Fe_3$. Studying only equilateral triangles and linear chains in 2000, Hobbs, Kresse, and Hafner[64] reported a $D_{3h}$ ground state with ten unpaired electrons. That same year Gutsev, Khanna, and Jena[92] report an "unambiguous" ground state of $^{11}A_1$ ($C_{2v}$ symmetry) using DFT in conjunction with an electron photodetachment experiment. Shortly afterwards, Diéguez, Alemany, Rey, Ordejón, and Gallego[93]

reported a $D_{3h}$ nonet as the DFT ground state. Following this, Gutsev[94] and then Gutsev and Bauschlicher[26] confirmed their earlier findings[92] with more extensive DFT studies. In between these two papers, Chrétien et al.[95] performed a DFT study that reports the lowest near-equilateral triangle as an $^{11}B_2$ state only 5.0 kcal/mol above the ground state, with a low-lying $^{13}A_2$ state. The most recent work on the iron trimer was done by Calaminici,[96] who reports this same $^{11}B_2$ ground state.

For the most part it is difficult to compare results between the current and previous studies, since the latter report $C_{2v}$ symmetries. Three direct comparisons which can be made, however, are with the work of Castro, Jamorski, and Salahub[89], who found a septet equilateral triangle with bond length of 2.10 Å as the ground state using DFT methods; the S = 5 state found by Hobbs, Kresse, and Hafner[64] which has a bond length of 2.22 Å; and the nonet with a bond length of 2.14 Å found by Diéguez et al.[93] Also, Chrétien and Salahub[95] found four near equilateral triangle states, the lowest being the $^{11}B_2$ state (2.25 Å bond length), followed by $^{13}A_2$ (2.33 Å, 0.38 kcal/mol higher in energy), another $^{11}B_2$ (2.25 Å, 1.60 kcal/mol), and a $^{9}A_2$ state (2.19 Å, 3.75 kcal/mol). In addition to these, the ground state reported by Chrétien and Salahub[95] appears to be a part of a Jahn-Teller distorted $^{11}E''$ state (also reported by Calaminici[96]). These contrast with the work done by Gutsev et al.,[26,92,94] which consistently reports what appears to be part of an $^{11}E'$ pair as the ground state. In addition to this, Gutsev et al.[92] report a low-lying $^{9}A_2$ state (possibly $^{9}E''$) only 5.5 kcal/mol above the ground state with a bond length of 2.18 Å (this appears to be the state found by Diéguez et al.[93]).

Spin states of $Fe_3$ from the singlet to S = 6 were examined in this study, and an $^{11}E''$ ([Core] $6a_1'^2\ 8e'^4\ 1a_2''^2\ 7a_1'^2\ 3e''^4\ 8a_1'\ 9e'^2\ 10e'^2\ 4e''^2\ 3a_1''\ 3a_2'\ 11e'$) electronic ground state was found. The equilibrium bond length is 2.24 Å. Three low-lying excited states were found (see Table 1). The excited state descriptions and their ordering are comparable to those reported by Chrétien and Salahub.[95] Our $^{9}E''$ state, which lies 6.19 eV above the ground state (bond length 2.15 Å), compares favorable with that found by Gutsev, Khanna, and Jena.[92] Furthermore, the energy separation is consistent with the $^{11}A_1$ ground state being a Jahn-Teller distortion of the $^{11}E'$ state found 2.9 kcal/mol above the ground state in this study. In addition, the $^{11}B_2$ state reported by Chrétien and Salahub[95] as a low-lying state (~5 kcal/mol)

should be the other state resulting from such a distortion. The septets (as found by Castro et al.[89]) have bond lengths around 2.15 Å, and are more than 30 kcal/mol higher in energy than the ground state. Gutsev[94] and Hobbs et al.[64] examined different spin states of $Fe_3$ and found ferromagnetic (S = 5) ground states with 10 unpaired electrons. Castro[90] also reports a ferromagnetic ground state, but it is a nonet state (S = 4).

Distortion into $C_{2v}$ symmetry results in $^{11}B_1$ and $^{11}A_2$ states of $Fe_3$. These have angles of 64º and 56º, bond lengths of 2.19 Å and 2.29 Å, and stabilization energies (with respect to the $D_{3h}$ $^{11}E''$ state) of 0.99 and 0.94 kcal/mol, all respectively. These results agree very well with those reported by Chrétien and Salahub[95] and by Gutsev, Khanna, and Jena[92] Table 2 shows the comparison of our symmetric stretch (362 $cm^{-1}$ for $^{11}B_1$, 364 $cm^{-1}$ for $^{11}A_2$), antisymmetric stretch (78 $cm^{-1}$ and 66i $cm^{-1}$), and bend (198 $cm^{-1}$ and 232 $cm^{-1}$) frequencies with previous theoretical[26,89,95] and experimental[77,91] results. These comparisons demonstrate that the states reported by some previous papers[26,92-94] are likely derived from the $^{11}E''$ state found in this study. Assuming that the antisymmetric stretch has been contaminated by low-lying states, the results found here agree very well with those found experimentally by Haslett, Bosnik, Fedrigo, and Moskovits.[91] It should be noted that the latter authors only tentatively assigned the symmetric stretch to 249 $cm^{-1}$. Nour, Alfaro-Franco, Gingerich, and Laane[77] isolated argon-trapped $Fe_3$ and reported an antisymmetric stretch of 180 $cm^{-1}$ and a symmetric stretch of 220 $cm^{-1}$. These experimental results seem considerably different than the theoretical findings reported here. However Nour et al.[77] found a band at 386 $cm^{-1}$ which they ascribed to a reaction of iron atoms with impurities in the argon matrix. It may be that this is the symmetric stretch band for $Fe_3$ and that the bending mode has a frequency of 220 $cm^{-1}$. If this is the case, the agreement with the values computed here (assuming that the antisymmetric stretch is unphysically low due to the high anharmonicity of the potential surface along the antisymmetric stretch mode) are quite good. As with $Cr_3$, there is a very low barrier to pseudo-rotation (0.05 kcal/mol) and this may have complicated the analysis of experimental spectra.

Iron is the first of two atoms for which BP86 combined with the Wachters basis set incorrectly promotes a 4s electron into the d shell for the atom, resulting in an $sd^{n-1}$ configuration rather than the

correct $s^2d^{n-2}$ configuration. Forcing the atomic occupation to correspond to a $^5D_g$ state we find a binding energy of 5.70 eV for $Fe_3$. Using the atomic minima found by BP86, this drops to 4.68 eV. Two experimental values for $D_0$ are reported in the literature: 2.91 eV found by Loh, Hales, Lian, and Armentrout[79] and 3.08 eV reported by Armentrout.[97] Using the vibrational frequencies measured by Haslett et al.[91] these correspond to $D_e$ values of 2.95 and 3.12 eV, respectively. DFT values vary widely, from 3.95 eV[95] to 8.26 eV[89]. Since the Jahn-Teller stabilization energy is small (less than 1 kcal/mol) the $D_{3h}$ binding energies should be comparable to the experimental results. Curiously, this suggests that the $D_e$ value found using the DFT ground state atom may be the appropriate value to use, as it is closer to the two experimental $D_e$ values, though still far larger than expected. The 'real' and 'DFT' values for the single atom dissociation are predicted to be 2.67 and 2.33 eV, respectively.

### 4.4.7 $Co_3$

Three experimental studies examined the cobalt trimer in the early nineties. First, Van Zee, Hamrick, Li, and Weltner[98] measured its electron spin resonance spectra, and concluded that the ground state was either a sextet or an octet. Following this Hales, Su, Lian, and Armentrout[99] measured the collision-induced dissociation of the cation and from this estimated a binding energy of 2.77 eV for the neutral species. Finally, Ho, Parks, Zhu, and Riley[100] measured the coordination of $N_2$ with small cobalt clusters. Their results led them to conclude that the cobalt trimer has a triangular structure. Thus experiment tells us that the cobalt trimer should be a well-bound triangle with five or seven unpaired electrons.

Shortly thereafter the DFT studies began. In 1997 Jamorski, Martinez, Castro, and Salahub[101] report a local minimum $D_{3h}$ structure as having a spin multiplicity of six, and a bond length of 2.11 Å with the PW86P86 functional. They were unable to find a potential minimum for a $D_{3h}$ octet, but the $C_{2v}$ octet they found is only 0.2 kcal/mol below their reported sextet. The potential minimum they report is a $C_{2v}$ sextet derived from the $D_{3h}$ structure mentioned above. The distortion (with respect to $D_{3h}$) energy is only 1.8 kcal/mol. These results are repeated in the paper by Castro, Jamorski, and Salahub.[89] Also in

1997, Fan, Liu, and Liao[102] predicted that the ground state of the cobalt trimer is an equilateral triangle with a spin multiplicity of eight. Fan also reported slightly distorted decet ($S = {}^{9}/_{2}$) and sextet states, which were predicted to lie 5.5 and 6.9 kcal/mol above the ground state, respectively. In 2001 two more papers were added to the list of computational studies of $Co_3$. Pereiro, Baldomir, Iglesias, Rosales, and Castro[103] reported a $C_{2v}$ symmetry ground state which is significantly distorted from an equilateral triangle. It is a sextet with its parent $D_{3h}$ state lying 9.0 kcal/mol higher in energy. The lowest octet they predict is 5.1 kcal/mol above the ground state. In the second paper, Pereiro, Man'kovsky, Baldomir, Iglesias, Młynarski, Valladares, Suarez, Castro, and Arias[104] confine themselves to high-symmetry structures and predict an octet state to be the ground state. Dennler, Morillo, and Pastor[105] also report a triangular minimum that appears from their diagram to be equilateral.

In the present research computations on all states for spins ranging from the doublet to the decet predict a $^{6}E''$ ([Core] $6a_1'^2\ 8e'^4\ 1a_2''^2\ 7a_1'^2\ 3e''^4\ 8a_1'^2\ 9e'^4\ 10e'^3\ 4e''^2\ 3a_1''\ 3a_2'$ ) equilateral triangle ground state. It has a predicted bond length of 2.18 Å, and lies 0.4 kcal/mol lower in energy than an $^{8}E''$ state with bond length 2.20 Å. This separation is too small to allow an unambiguous designation of the ground state. There are several other low-lying states (see Table 1). In particular, note that a $^{6}E'$ exists at a similar excitation energy as that reported by Fan, Liu, and Liao[102]

The cobalt trimer shows only small Jahn-Teller distortions. Our geometrical distortions were small (57º and 62º for the angles, 2.20 Å and 2.16 Å for the bond lengths of the $^{6}B_1$ and $^{6}A_2$ states, respectively) and the relaxation energies were only 0.5 and 0.2 kcal/mol, respectively, when allowed to distort to $C_{2v}$ symmetry. Jamorski et al.[101] and Castro et al.[89] report identical sextet $C_{2v}$ ground states with a bond length of 2.12 Å and an angle of 65º, in reasonable agreement with the $^{6}A_2$ state found here. Table 2 shows the frequencies found in this study as well as those mentioned above. For the $^{6}B_1$ state these are 361 $cm^{-1}$ (SS), 171 $cm^{-1}$ (AS), and 261 $cm^{-1}$ (B). For the $^{6}A_2$ state these vibrational frequencies are 357, 493i, and 194 $cm^{-1}$, respectively. Since the differences in geometries are so small, it is likely that the energy used to compute the antisymmetric stretch of the $^{6}A_2$ state actually corresponds to the $^{6}B_1$ state, causing it to be overly large in magnitude.

As with iron, BP86 incorrectly reports an $sd^{n-1}$ ground state configuration for the cobalt atom. The energy difference between the ground state trimer and three $^4F_g$ atoms is 6.12 eV. For dissociation with respect to three artifactual DFT ($^6F_g$) ground state atoms, the difference is 4.13 eV. The experimental value determined by Hales et al.[99] ($D_0$ = 2.77 eV) compares more favorably with the DFT binding energy, though is still much smaller. Previously computed values range from 1.78 eV to 11.00 eV,[89,101,102,104] an indication of the challenges presented by transition metal trimers. The $Co_3$ to $Co_2$ plus Co($^4F_g$) dissociation energy is predicted to be 3.38 eV, while that with the DFT ground state atomic description ($^6F_g$) is 2.72 eV.

### 4.4.8 $Ni_3$

The nickel trimer has been extensively studied. For a review of most of the research prior to 1998,[1,44,77,88,89,106-123] readers should consult the study by Michelini, Diez, and Jubert.[124] Highlights include the experimental structure suggested by Moskovits and DiLella,[109] which has a bond angle between 90 and 100 degrees, a visible spectrum and resultant frequencies measured by Woodward, Cobb, and Gole,[114] and the DFT study by Bérces.[89] In the Bérces study a $^3A_1$ (this should either be a prime or double-prime state, but is not reported in the paper) ground state is reported, with a $^3E'$ Jahn-Teller pair only 3 kcal/mol higher in energy. Other states are more than 10 kcal/mol higher in energy than the ground state. Michelini, Diez, and Jubert[124] report a $^3A_2''$ ground state, with a quintet (4.6 kcal/mol) and a singlet (5.1 kcal/mol) as low-lying excited states. While studying ionization of the nickel trimer anion, Weber and Jena[125] report a triplet-quintet separation of 10.6 kcal/mol.

Several subsequent papers[19,126-130] report equilateral triangle (and when reported, triplet spin) or near equilateral triangle ground state geometries. Aside from these, there are five other papers of particular note. First, Cisneros, Castro, and Salahub[131] report a triplet $C_{2v}$ ground state with the quintet only 4.4 kcal/mol higher in energy. Viitala, Häkkinen, Manninen, and Timonen[132] report an $S_z$ = 1 ferromagnetically coupled equilateral ground state, along with $S_z$ = 0 (7.9 kcal/mol), $S_z$ = 2 (8.1 kcal/mol), and $S_z$ = 3 (26.3 kcal/mol) excited states using an effective spin Hamiltonian. Using a parallel

generalized LSD method, Calvayrac[133] found a triplet $C_s$ structure with a bond angle of about 105º. This is significant, as it is the first time a theoretical value for the bond angle agreed with the argon matrix results published by Moskovits and DiLella.[109] Revisiting $Ni_3$, Michelini, Diez, and Jubert[134] find the same ground state as they did three years previously,[124] with excited singlet, quintet, and septet states all more than 3.5 kcal/mol higher in energy. Derosa, Seminario, and Balbuena[135] use DFT with effective core potentials and find a $C_{2v}$ quintet as the ground state, with a triplet state only 1.4 kcal/mol higher in energy. This is the only DFT study which reports a quintet ground state.

In the present research, including states from singlet to septet in spin multiplicity, the BP86 optimized $D_{3h}$ ground state for the nickel timer is a $^3A_2''$ ([Core] $6a_1'^2$ $8e'^4$ $1a_2''^2$ $7a_1'^2$ $3e''^4$ $8a_1'^2$ $9e'^4$ $10e'^4$ $4e''^4$ $3a_1''$ $3a_2'$ ) state with a bond length of 2.23 Å. It must be noted that it was possible to converge on a state slightly (0.07 kcal/mol) lower in energy than this, but the Cartesian forces for this state were unphysical, considering that the orbital occupations (the same as the ground state) should not exhibit Jahn-Teller character. Only 2.96 kcal/mol above this is a $^3A_1''$ state and just above that a $^3E'$ (2.99 kcal/mol) excited state (see Table 1). These results are different than those found by Michelini, Diez, and Jubert[124,134] as the lowest quintet is 10 kcal/mol above the ground state (which is in good agreement with the value computed by Weber and Jena[125]). The 2.99 kcal/mol energy of the $^3E'$ state agrees well with that reported by Bérces,[89] despite the difference in ground state symmetry.

The values of the symmetric stretch (329 $cm^{-1}$), antisymmetric stretch (225 $cm^{-1}$), and bend (225 $cm^{-1}$) vibrational frequencies compare favorably (Table 2) with previous results. In particular, there is reasonable agreement with the value for the antisymmetric stretch measured by Nour et al.[77]

The atomization energy of $Ni_3$ presents a difficulty. The absolute ground state of the nickel atom is the $^5F_g$ state; however, if energies are J averaged, the $^3D_g$ state has the lowest energy. As such, only this state was considered when computing the atomization energy of 5.00 eV. Recently computed values[19,89,120,124,125,128,130,134-136] range from 3.23 to 11.22 eV. Experimentally, an estimate of 1.7 eV, based upon harmonic and anharmonic stretch frequencies, exists.[109] As pointed out by Cheng and Ellis,[115] $Ni_3$

likely has a wide "flat" region for $R > R_e$. As such, a Morse potential fit may be insufficient to derive dissociation energy from frequencies. This is supported by the collision induced spectroscopy value of $D_0 = 4.33$ eV found by Ervin, Ho, and Lineberger,[137] which agrees well with the result predicted here. The energy required to remove a single Ni atom from $Ni_3$ is predicted here to be 3.74 eV.

### 4.4.9 $Cu_3$

Copious research[15,44,127,135,138-183] has been carried out on the copper trimer. A review of all of these results is impractical; as such the reader is referred to the works by Walch and Laskowski,[158] and by Bérces[44] for discussions of much of the previous work. Following is a discussion of the most pertinent results.

Previous DFT work[44,172,181] generally agree on a $^2B_2$ ground state (note that Jug et al. and Calaminici et al. both report $^2B_1$ states, but this is merely a difference in axes designations), slightly distorted from its $^2E'$ parent such that the angle is greater than 60º. Bérces[44] reports a bond length of 2.39 Å for this $D_{3h}$ state, while Calaminici, Köster, Russo, and Salahub[172] report a value of 2.32 Å. Only Bérces[44] reports an excited state: a $^4A_1'$ state 40.1 kcal/mol above the $^2E'$ state.

A $^2E'$ ([Core] $6a_1'^2$ $8e'^4$ $1a_2''^2$ $7a_1'^2$ $3e''^4$ $8a_1'^2$ $9e'^4$ $10e'^4$ $4e''^4$ $3a_1''^2$ $3a_2'^2$ $11e'$) ground state was found in this study, lower in energy that the other doublets and all of the quartets. The bond length of 2.37 Å agrees reasonably well with previous DFT results, and the lowest excited state found by Bérces[44] is supported, with an excitation energy of 37 kcal/mol. Knickelbein[167] has reported two experimental excitations, one at 53.0 kcal/mol and one approximately 3.0 kcal/mol higher than that. Comparison with *ab initio* results from Walch and Laskowski[158] suggests that these are $^2A_1'$ and $^2E''$ states, respectively. Unfortunately, it is not possible to examine the first of these states in this study, as its symmetry is the same as that of the ground state in the $C_{2v}$ point group. A $^2A_2''$ state (49.6 kcal/mol) is found in the present study near the excitation energies reported by Knickelbein.[167] The $^2E''$ state is predicted to lie 63 kcal/mol above the ground state.

$Cu_3$ relaxes significantly when allowed to deform from $D_{3h}$ into $C_{2v}$ symmetry. This is not surprising, as the 11e′ orbital is singly occupied. Each set of equivalent atomic orbitals (e.g. $3d_{xy}$) gives rise to a set of three molecular orbitals, one 'a'-type orbital ($a_1'$, $a_2''$, $a_1''$, or $a_2'$) and a pair of 'e'-type orbitals (e′ or e″). When one of these sets of three is fully occupied, the resulting net bonding is zero. With almost all such sets of three orbitals fully occupied, the copper trimer has its binding character determined by only three electrons. Two electrons are in an 'a'-type orbital, which energetically favors $D_{3h}$ symmetry. The last electron goes into an 'e'-type orbital which will favor distortion into $C_{2v}$ symmetry. In this case, the $^2B_2$ state expands, with a central angle of 68º, a bond length of 2.31 Å, and relaxation energy of 1.50 kcal/mol. The $^2A_1$ state has an angle of 56º, a bond length of 2.43 Å, and relaxation energy of 1.0 kcal/mol. These two states have vibrational frequencies of 253 $cm^{-1}$ (SS), 159 $cm^{-1}$ (AS), and 107 $cm^{-1}$ (B); and 260 $cm^{-1}$ (SS), 145i $cm^{-1}$ (AS) and 179 $cm^{-1}$ (B), respectively. As shown in Table 2, these results are in good agreement with most previous theoretical[44,172,181] and experimental[155,168] frequencies. In particular, the symmetric stretch supports the measurement by Rohlfing and Valentini,[155] and the $\omega_e$ value reported by Koizumi and Sugano[168] falls in between the bending mode frequencies for both states.

Dissociation into three $^2S_g$ copper atoms is predicted here to require 3.22 eV of energy. This is in reasonable agreement with the value of 3.19 eV computed by Jaque and Toro-Labbé[180] for the slightly distorted system. Recent experimental results are from collision induced dissociation spectroscopy. Spasov, Lee, and Ervin[179] used the anion to determine a $D_0$ value of 3.19 eV. Ingólfsson, Busolt, and Sugawara[178] deduced this value to be 2.57 eV using the cation thermochemistry. Assuming the experimental frequencies[156,159] (those suggested by Lombardi and Davis[15] are not different enough to cause a change within the significant figures used) these correspond to $D_e$ values of 3.22 and 2.60 eV, respectively. To form a copper dimer and atom from the trimer, it is predicted that 1.16 eV of energy is required.

### 4.4.10 $Zn_3$

The zinc trimer, a weakly bound van der Waals system, presents systemic difficulties for DFT. In 1984 Tomonari, Tatewaki, and Nakamura[184] used simple *ab initio* methods and found that the system is not bound. Later they improved their theory to configuration interaction and still found a negative atomization energy.[185] The first coupled cluster study, by Flad, Schautz, Wang, Dolg, and Savin[186] reports an optimized bond length of 3.75 Å, a low atomization energy (0.09 eV) and harmonic vibrational frequencies below 30 $cm^{-1}$. In 1999 Park, Lee, and Lee[187] examined zinc clusters with DFT and found a much more tightly bound (0.73 eV) complex with a zinc to zinc distance of 2.63 Å. Using DFT to study zinc-sulfur clusters, Katırcıoğlu and Erkoç[188] predicted a bond length of 3.20 Å, harmonic frequencies around 50 $cm^{-1}$ and a binding energy of 0.0857 eV, much smaller than that found by Park et al. These results were confirmed by Erkoç[189] in a later paper which examines zinc – cadmium clusters. Wang, Wang, and Zhao[190] have applied the PW92C functional to this system and found a bond length of 3.08 Å and a binding energy of 0.22 eV.

The ground state for this system is, as expected, $^1A_1'$ ([Core] $6a_1'^2\ 8e'^4\ 1a_2''^2\ 7a_1'^2\ 3e''^4\ 8a_1'^2\ 9e'^4\ 10e'^4\ 4e''^4\ 3a_1''^2\ 3a_2'^2\ 11e'^4$). Our predicted bond length, 2.93 Å, is similar to the previous DFT results, and shorter than the coupled cluster number. The lowest triplet, corresponding to exciting an electron from the highest e′ orbital into the $a_2''$ orbital consisting of $4p_z$ orbitals (where the z-axis is perpendicular to the molecular plane) on each zinc atom, is 61 kcal/mol above the ground state.

The symmetric stretch, antisymmetric stretch, and bend vibrational frequencies of $Zn_3$ are 80, 73, and 73 $cm^{-1}$, respectively. These are of the same magnitude as previous DFT values,[188,189] but far larger than the coupled-cluster results.[186]

The binding energy is computed to be 0.24 eV, in good agreement with that found by Wang, Wang, and Zhao.[190] As noted in the latter paper, the discrepancy between this value and that found by Flad et al.[186] is expected due to the difficulties DFT has with van der Waals systems. A large portion of

the atomization energy, 0.20 eV, is accounted for by the removal of a single zinc atom, meaning that the trimer has a much higher binding energy per atom than the dimer.

## 4.5 CONCLUSIONS

One of the primary goals of the present research was to obtain consistent theoretical results for all of the transition metal trimers, so that comparisons can be safely made. In this section such comparisons shall be attempted. First, it is important to note the ground-state spin multiplicities (Table 3). Going from left to right from scandium, these BP86 multiplicities are seemingly somewhat haphazard: 2, 7, 2, 17, 16, 11, 6, 3, 2, and 1. To a certain extent, the multiplicities can be expected to represent the degree of bonding of the molecule, and this structure should be reflected in the bond lengths and binding energies; this hypothesis only proves partially true. For the bond lengths (see Figure 1) there is one discrepancy. Equilibrium bond lengths fall monotonically from the scandium trimer to the vanadium trimer, despite the fact that the titanium trimer has a much higher spin. This is likely a result of orbital occupation of the titanium trimer: all of the fully occupied valence orbitals are three-center, two-electron, cyclic-bonding orbitals. In both the scandium and vanadium trimers, at least one filled orbital has a node across a bond. Changes in atomization and single-atom dissociation energies (Figures 2 and 3) exactly mirror the changes in bond length, with $V_3$ having both the shortest bond and highest binding energy.

The orbital ordering in Table 3 was chosen to represent the order in which the orbitals were most commonly filled. This ordering appears to work well as an *aufbauprinzip*, with the main exception being the 8e′ orbital in $Ti_3$. In particular, there appear to be three categories of molecular orbitals. The first is the $6a_1'$ orbital, which is a cyclic bonding orbital consisting of atomic 3 $d_{z^2}$ (oriented such that each atom's z axis points towards the center of the molecule) mixed with s-like orbitals on each atom. The next shell contains orbitals formed from all of the other d orbitals. The final, and by far highest in energy among these is the 11e′ orbital. This doubly-degenerate orbital is composed of linear combinations of the same orbitals as make up the $6a_1'$ orbital, but the 11e′ components have a single nodal surface. As the atomic number of the metal in the trimer increases, the d orbitals contract. At chromium, this contraction is such

that it becomes more favorable to half-occupy the valence orbitals rather than fully occupy only the lower-lying ones. Beyond chromium, as the number of electrons increases, they must occupy the lower, bonding-type orbitals. This decreases the bond length, and for a while ($Fe_3$ to $Ni_3$) it becomes more favorable to fully occupy additional low-lying orbitals rather than partially occupy the more diffuse 11e′ orbital.

## 4.6 ACKNOWLEDGEMENTS

This research was supported by the National Science Foundation, Grant CHE-0451445.

## 4.7 TABLES AND FIGURES

Table 4.1: Low-lying electronic states of first row transition metal trimers.

| Molecule | $r_e$ / Å | Relative Energy (kcal/mol) | State |
|---|---|---|---|
| $Sc_3$ | 2.826 | 0.0 | $^2A_1'$ |
| | 2.726 | 3.1 | $^2E'$ |
| | 2.903 | 3.8 | $^4A_2''$ |
| | 2.841 | 4.7 | $^2A_2''$ |
| | 2.911 | 5.9 | $^4E'$ |
| | 2.886 | 6.4 | $^6E''$ |
| | 2.857 | 8.4 | $^8E''$ |
| | 2.841 | 9.3 | $^8E'$ |
| $Ti_3$ | 2.321 | 0.0 | $^7E'$ |
| | 2.336 | 2.2 | $^5E'$ |
| | 2.394 | 8.2 | $^3A_2'$ |
| | 2.380 | 8.4 | $^3E''$ |
| | 2.432 | 9.8 | $^9A_2'$ |
| $V_3$ | 2.062 | 0.0 | $^2E''$ |
| | 2.104 | 5.8 | $^4E'$ |
| | 2.074 | 5.9 | $^2A_1'$ |
| $Cr_3$ | 2.915 | 0.0 | $^{17}E'$ |
| | 2.965 | 16.2 | $^{17}E''$ |
| | 2.781 | 22.6 | $^{15}E'$ |
| $Mn_3$ | 2.734 | 0.0 | $^{16}A_2'$ |
| | 2.672 | 5.6 | $^{16}E''$ |
| | 2.523 | 15.2 | $^{14}E''$ |
| $Fe_3$ | 2.236 | 0.0 | $^{11}E''$ |
| | 2.232 | 2.9 | $^{11}E'$ |
| | 2.309 | 4.4 | $^{13}A_1''$ |
| | 2.153 | 6.2 | $^9E''$ |
| | 2.323 | 6.7 | $^{13}E'$ |
| $Co_3$ | 2.182 | 0.0 | $^6E''$ |
| | 2.201 | 0.4 | $^8E''$ |
| | 2.198 | 1.3 | $^6A_2'$ |
| | 2.232 | 1.5 | $^8E'$ |
| | 2.189 | 6.4 | $^6E'$ |
| | 2.278 | 8.9 | $^{10}E'$ |
| $Ni_3$ | 2.227 | 0.0 | $^3A_2''$ |
| | 2.245 | 3.0 | $^3A_1''$ |
| | 2.247 | 3.0 | $^3E'$ |
| $Cu_3$ | 2.367 | 0.0 | $^2E'$ |
| | 2.379 | 37.5 | $^4A_1'$ |
| | 2.450 | 44.9 | $^4E'$ |
| | 2.421 | 44.9 | $^4E''$ |
| $Zn_3$ | 2.934 | 0.0 | $^1A_1'$ |
| | 2.524 | 61.3 | $^3E''$ |
| | 2.812 | 81.6 | $^3E'$ |

Table 4.2: Harmonic vibrational frequencies (in $cm^{-1}$) for transition metal trimers. The abbreviations used are symmetric stretch ($\omega_1$, SS), antisymmetric stretch ($\omega_3$, AS), and bend ($\omega_2$, B).

| Molecule | Source | SS | AS | B |
|---|---|---|---|---|
| $Sc_3$ | $^2A_1'$ | 267 | 139 | 140 |
| | Ref. [43] | 272 | 153 | 153 |
| | Ref. [44] | 292 | 238 | 238 |
| | Ref. [45b,c] | 259 | 238 | 185 |
| | Ref. [40a] | 246 | 151 | 145 |
| $Ti_3$ | $^7A_1$ | 369 | 35 | 190 |
| | $^7B_2$ | 363 | 44i | 200 |
| | Ref. [45b,c] | 206 | 136 | 609i |
| $V_3$ | $^2A_2$ | 467 | 203 | 244 |
| | $^2B_1$ | 476 | 481i | 270 |
| | Ref. [56] | 421 | 255 | 255 |
| | Ref. [58b,c] | 466 | 237 | 191 |
| | (unpub) | 460 | 200 | 200 |
| $Cr_3$ | $^{17}A_1$ | 197 | 79 | 103 |
| | $^{17}B_2$ | 200 | 61i | 134 |
| | Ref. [59a] | 308 | 226 | 123 |
| | Ref. [61a] | 432 | 302 | 302 |
| $Mn_3$ | $^{16}A_2'$ | 202 | 146 | 147 |
| | Ref. [65a] | 197 | 130 | 130 |
| $Fe_3$ | $^{11}B_1$ | 362 | 78 | 198 |
| | $^{11}A_2$ | 364 | 66i | 232 |
| | Ref. [95b] $^{11}A_2$ | 347 | 56 | 235 |
| | Ref. [95b] $^{11}B_1$ | 345 | 73 | 198 |
| | Ref. [26b] $^{11}B_1$ | 353 | 20i | 198 |
| | Ref. [77a] | 386[d] | 180 | 220[d] |
| | Ref. [91a,c] | 249 | 185 | 178 |
| $Co_3$ | $^6B_1$ | 361 | 171 | 261 |
| | $^6A_2$ | 357 | 493i | 194 |
| | Ref. [89,101b] | 372 | 235 | 220 |
| $Ni_3$ | $^3A_2''$ | 329 | 225 | 225 |
| | Ref. [44b] | 356 | 142 | 142 |
| | Ref. [77a] | - | 198 | - |
| | Ref. [89b] | 307 | 198 | 197 |
| | Ref. [114a,b] | 230 | - | 100 |
| | Ref. [131b] | 307 | 218 | 189 |
| | Ref. [134] | 359 | 229 | 229 |
| $Cu_3$ | $^2B_2$ | 253 | 159 | 107 |
| | $^2A_1$ | 260 | 145i | 179 |
| | Ref. [44b] $^2B_2$ | 293 | 158 | 142 |
| | Ref. [44b] $^2A_1$ | 217 | 130i | 299 |
| | Ref. [181b] | 290 | 177 | 118 |
| | Ref. [172b] | 251 | 172 | 139 |
| | Ref. [155a] | 245 | - | - |
| | Ref. [168a] | - | 130 | 130 |
| $Zn_3$ | $^1A_1'$ | 80 | 73 | 73 |
| | Ref. [186] | 26 | 30 | 30 |
| | Ref. [188c] | 53 | 51 | 49 |
| | Ref. [189c] | 53 | 51 | 49 |

a: Experimental
b: $C_{2v}$ geometry
c: Order of AS,B not certain.
d: Designations differ from those suggested by original author.

Table 4.3: Summary of electronic ground states for the transition metal trimers in $D_{3h}$ symmetry. The ordering of orbitals is chosen to be consistent across the periodic table to illustrate the successes and failures of the *aufbauprinzip*.

| Mol. | $r_e$ / Å | $D_e$ / eV | Occupation | State |
|---|---|---|---|---|
| $Sc_3$ | 2.83 | 3.89 | [Core] $6a_1'^2$ $8e'^4$ $1a_2''^2$ $7a_1'$ | $^2A_1'$ |
| $Ti_3$ | 2.32 | 6.10 | [Core] $6a_1'^2$ $8e'^2$ $1a_2''^2$ $7a_1'^2$ $8a_1'$ $3e''^2$ $9e'$ | $^7E'$ |
| $V_3$ | 2.06 | 7.21 | [Core] $6a_1'^2$ $8e'^4$ $1a_2''^2$ $7a_1'^2$ $8a_1'^2$ $3e''^3$ | $^2E''$ |
| $Cr_3$ | 2.92 | 1.15 | [Core] $6a_1'^2$ $8e'^2$ $1a_2''$ $7a_1'$ $3e''^2$ $8a_1'$ $9e'^2$ $10e'^2$ $4e''^2$ $3a_1''$ $3a_2'$ $11e'$ | $^{17}E'$ |
| $Mn_3$ | 2.73 | 2.33 | [Core] $6a_1'^2$ $8e'^4$ $1a_2''$ $7a_1'$ $3e''^2$ $8a_1'$ $9e'^2$ $10e'^2$ $4e''^2$ $3a_1''$ $3a_2'$ $11e'^2$ | $^{16}A_2'$ |
| $Fe_3$ | 2.24 | 4.68 | [Core] $6a_1'^2$ $8e'^4$ $1a_2''^2$ $7a_1'^2$ $3e''^4$ $8a_1'$ $9e'^2$ $10e'^2$ $4e''^2$ $3a_1''$ $3a_2'$ $11e'$ | $^{11}E''$ |
| $Co_3$ | 2.18 | 4.13 | [Core] $6a_1'^2$ $8e'^4$ $1a_2''^2$ $7a_1'^2$ $3e''^4$ $8a_1'^2$ $9e'^4$ $10e'^3$ $4e''^2$ $3a_1''$ $3a_2'$ | $^6E''$ |
| $Ni_3$ | 2.23 | 5.00 | [Core] $6a_1'^2$ $8e'^4$ $1a_2''^2$ $7a_1'^2$ $3e''^4$ $8a_1'^2$ $9e'^4$ $10e'^4$ $4e''^4$ $3a_1''$ $3a_2'$ | $^3A_2''$ |
| $Cu_3$ | 2.37 | 3.22 | [Core] $6a_1'^2$ $8e'^4$ $1a_2''^2$ $7a_1'^2$ $3e''^4$ $8a_1'^2$ $9e'^4$ $10e'^4$ $4e''^4$ $3a_1''^2$ $3a_2'^2$ $11e'$ | $^2E'$ |
| $Zn_3$ | 2.93 | 0.24 | [Core] $6a_1'^2$ $8e'^4$ $1a_2''^2$ $7a_1'^2$ $3e''^4$ $8a_1'^2$ $9e'^4$ $10e'^4$ $4e''^4$ $3a_1''^2$ $3a_2'^2$ $11e'^4$ | $^1A_1'$ |

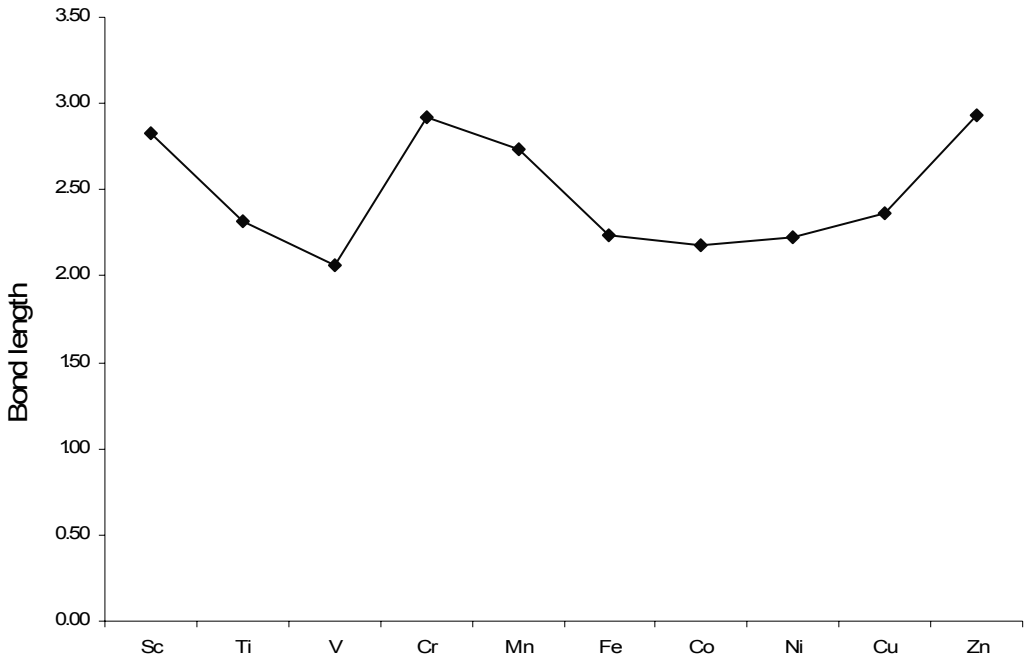


Figure 4.1: Bond lengths (Å) of $D_{3h}$ transition metal trimers computed with the BP86 method.

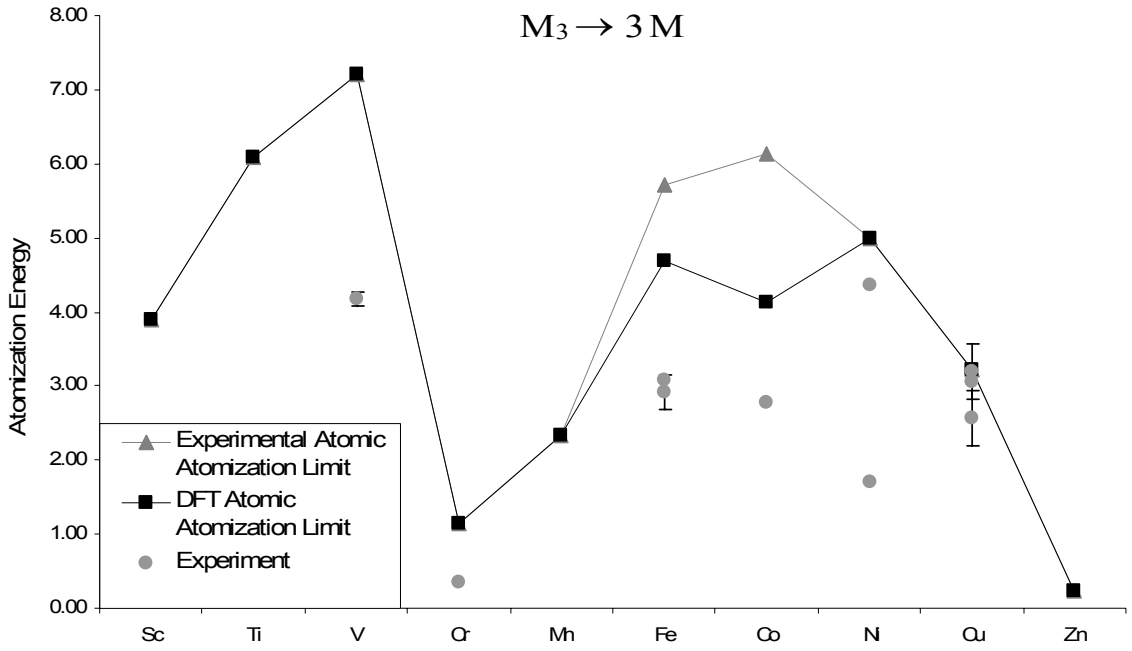


Figure 4.2: Atomization energies (eV) of $D_{3h}$ transition metal trimers computed with the BP86 method. 'Experimental Atomic Atomization Limit' refers to dissociation to three transition metal atoms in their experimental atomic ground states. 'DFT Atomic Atomization Limit' refers to dissociation into three transition metal atoms in the atomic ground states predicted by BP86.

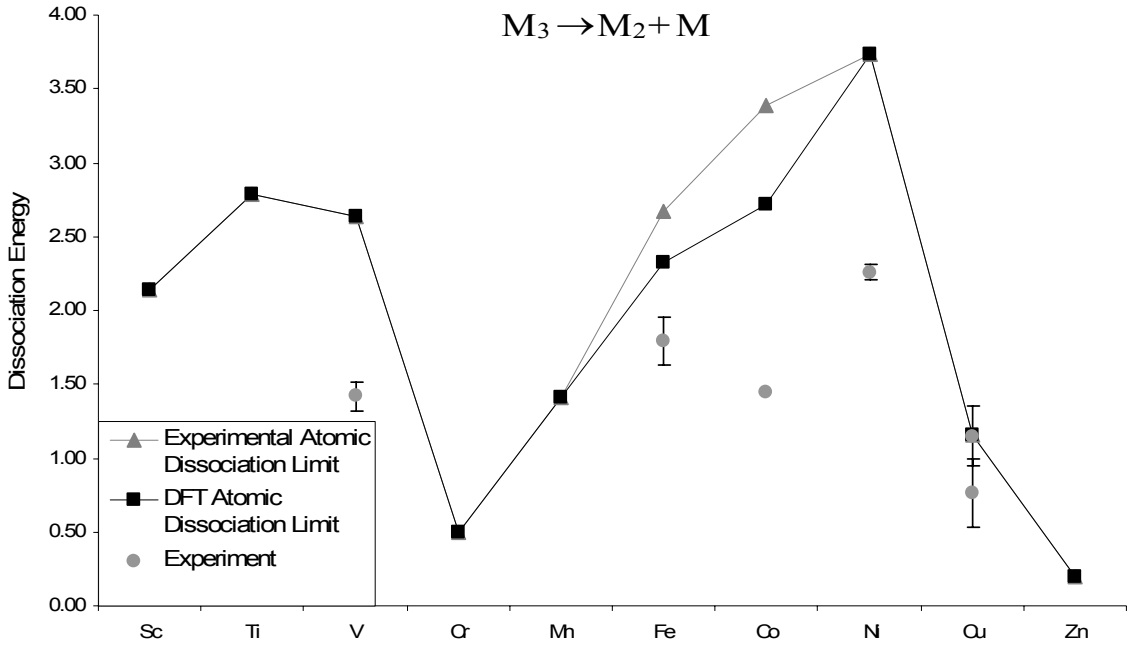


Figure 4.3: $M_3 \rightarrow M_2 + M$ dissociation energies (eV) of $D_{3h}$ transition metal trimers computed with the BP86 method. 'Experimental Atomic Dissociation Limit' refers to dissociation into a dimer and a transition metal atom its experimental atomic ground state. 'DFT Atomic Dissociation Limit' refers to dissociation into a dimer and a transition metal atom in the atomic ground state predicted by BP86.

## 4.7 REFERENCES


[1] A. B. Anderson, *J. Chem. Phys.* **64**, 4046 (1976).

[2] *E. Sicily Thirteenth International School; 1987. See: G. Benedek et al. Elemental and Molecular Clusters (Springer-Verlag: New York, 1988).*

[3] *Fifth International on Small Particles and Metal Clusters, Konstanz, Germany, 1990. See Z. Phys.* ***1991****, D19. Sixth International on Small Particles and Metal Clusters, Chicago, IL, 1992. See Z. Phys.* ***1993****, D26.*

[4] *Sicily, E. Thirteenth International School; 1987. See: G. Benedek et al. Elemental and Molecular Clusters; Springer-Verlag: New York, 1988.*

[5] *Symposia on Clusters and Cluster Assembled Materials, Materials Research Society Meeting, Boston, MA, 1990. See: MRS Symposium Series 206, 1991.*

[6] *International Symposium on the Physics and Chemistry of Small Clusters, NATO Advanced Workshop, Richmond, VA, 1991. See: Physics and Chemistry of Finite Systems: From Clusters to Crystals; P. Jena, S. N. Khanna, B. K. Rao, Eds. (Kluwer: Dordrecht, 1992).*

[7] *First International Conference on Nuclear and Atomic Clusters, Turku, Finland, 1991. Second International Conference on Nuclear and Atomic Clusters, Santorini, Greece, 1993.*

[8] *Proceedings of the 10$^{th}$ International IUPAC Conference. High Temp. Mater. Chem.* ***2000****, 15.*

[9] K. Balasubramanian, *Chem. Rev.* **90**, 93 (1990).

[10] M. Brack, *Rev. Mod. Phys.* **65**, 677 (1993).

[11] W. A. de Heer, *Rev. Mod. Phys.* **65**, 611 (1993).

[12] M. A. Duncan, *Advances in Metal and Semiconductor Clusters*. (JAI Press, Greenwich, CT, 1993).

[13] T. Halıcıoğlu and C. W. Bauschlicher, *Rep. Prog. Phys.* **51**, 883 (1988).

[14] J. Koutecký and P. Fantucci, *Chem. Rev.* **86**, 539 (1986).

[15] J. R. Lombardi and B. Davis, *Chem. Rev.* **102**, 2431 (2002).

[16] M. D. Morse, *Chem. Rev.* **86**, 1049 (1986).

[17] M. Moskovits, *Metal Clusters*. (Wiley, New York, 1986).

[18] W. Weltner and R. J. Van Zee, *Annu. Rev. Phys. Chem.* **35**, 291 (1984).

[19] H. Oymak and S. Erkoç, *Phys. Rev. A* **66**, 033202 (2002). Oymak & Erkoç give a splendid review of the metal cluster literature. In the present paper we refer back to many references contained in Oymak & Erkoç. For example, our reference 19a includes references 16 & 17 of Oymak & Erkoç. See the references therein:
a: 16,17;
b: 3, 30, 41, 58, 59, 70, 75, 76, 90, 92-101;
c: 14, 20, 24-36;
d: 28-31, 35, 37-50;
e: 2, 51-56;
f: 31;
g: 47, 66, 69, 70, 75-84;
h: 26, 27, 31, 50, 55, 57, 85-88;
i: 27, 31, 36;
j: 14, 36, 89-91.

[20] C. J. Barden, J. C. Rienstra-Kiracofe, and H. F. Schaefer, *J. Chem. Phys.* **113**, 690 (2000).

[21] A. D. Becke, *Phys. Rev. A* **38**, 3098 (1988).

[22] J. P. Perdew, *Phys. Rev. B* **33**, 8822 (1986).

[23] J. P. Perdew, *Phys. Rev. B* **34**, 7046 (1986).

[24] V. Jonas and W. Thiel, *J. Chem. Phys.* **102**, 8474 (1995).

[25] J. H. Jang, J. G. Lee, H. Lee, Y. Xie, and H. F. Schaefer, *J. Phys. Chem. A* **102**, 5298 (1998).

[26] G. L. Gutsev and C. W. Bauschlicher, *J. Phys. Chem. A* **107**, 7013 (2003).

[27] Y. Xie, R. B. King, and H. F. Schaefer, *Spec. Chim. Acta Part A* **61**, 1693 (2005).

[28] C. Cañada-Vilalta, T. A. O'Brien, E. K. Brechin, M. Pink, E. R. Davidson, and G. Christou, *Inorg. Chem.* **43**, 5505 (2004).

[29] A. E. Clark and E. R. Davidson, *J. Chem. Phys.* **115**, 7382 (2001).

[30] E. R. Davidson and A. E. Clark, *Mol. Phys.* **100**, 373 (2002).

[31] E. R. Davidson and A. E. Clark, *J. Phys. Chem. A* **106**, 7456 (2002).

[32] T. A. O'Brien and E. R. Davidson, *Int. J. Quantum Chem.* **92**, 294 (2003).

[33] A. J. H. Wachters, *J. Chem. Phys.* **52**, 1033 (1970).

[34] P. J. Hay, *J. Chem. Phys.* **66**, 4377 (1977).

[35] D. M. Hood, R. M. Pitzer, and H. F. Schaefer, *J. Chem. Phys.* **71**, 705 (1979).

[36] MOLPRO, a package of *ab initio* programs designed by H.-J. Werner and P. J. Knowles, version 2002.6, R. D. Amos, A. Bernhardsson, A. Berning, P. Celani, D. L. Cooper, M. J. O. Deegan, A. J. Dobbyn, F. Eckert, C. Hampel, G. Hetzer, P. J. Knowles, T. Korona, R. Lindh, A. W. Lloyd, S. J. McNicholas, F. R. Manby, W. Meyer, M. E. Mura, A. Nicklass, P. Palmieri, R. Pitzer, G. Rauhut, M. Schütz, U. Schumann, H. Stoll, A. J. Stone, R. Tarroni, T. Thorsteinsson, and H.-J. Werner.

[37] R. Lindh, U. Ryu, and B. Liu, *J. Chem. Phys.* **95**, 5889 (1991).

[38] INTDIF2004 is an abstract program written by Wesley D. Allen for *Mathematica* (Wolfram Research.

[39] L. B. Knight, R. J. Woodward, R. J. Van Zee, and W. Weltner, *J. Chem. Phys.* **79**, 5820 (1983).

[40] M. Moskovits, D. P. DiLella, and W. Limm, *J. Chem. Phys.* **80**, 626 (1984).

[41] S. P. Walch and C. W. Bauschlicher, *J. Chem. Phys.* **83**, 5735 (1985).

[42] S. P. Walch, *Theor. Chim. Acta* **71**, 449 (1987).

[43] I. Pápai and M. Castro, *Chem. Phys. Lett.* **267**, 551 (1997).

[44] A. Bérces, *Spectrochim. Acta Part A* **53**, 1257 (1997).

[45] Z. J. Wu, H. J. Zhang, J. Meng, Z. W. Dai, B. Han, and P. C. Jin, *J. Chem. Phys.* **121**, 4699 (2004).

[46] H. Wu, S. R. Desai, and L. Wang, *Phys. Rev. Lett.* **76**, 212 (1996).

[47] P. Cremaschi and J. L. Whitten, *Chem. Phys. Lett.* **111**, 215 (1984).

[48] S. H. Wei, Z. Zeng, J. Q. You, X. H. Yan, and X. G. Gong, *J. Chem. Phys.* **113**, 11127 (2000).

[49] J. Zhao, Q. Qui, B. Wang, J. Wang, and G. Wang, *Solid State Commun.* **118**, 157 (2001).

[50] M. Castro, S. Lui, H. Zhai, and L. Wang, *J. Chem. Phys.* **118**, 2116 (2003).

[51] H. Wu, S. R. Desai, and L.-S. Wang, *Phys. Rev. Lett.* **77**, 2436 (1996).

[52] C.-X. Su, D. A. Hales, and P. B. Armentrout, *J. Chem. Phys.* **99**, 6613 (1993).

[53] H. Grönbeck and A. Rosén, *J. Chem. Phys.* **107**, 10620 (1997).

[54] H. Sun, Y.-H. Luo, J. Zhao, and G. Wang, *Phys. Stat. Sol.* **215**, 1127 (1999).

[55] X. Wu and A. K. Ray, *J. Chem. Phys.* **110**, 2437 (1999).

[56] P. Calaminici, A. M. Köster, T. Carrington, P. Roy, N. Russo, and D. R. Salahub, *J. Chem. Phys.* **114**, 4036 (2001).

[57] D. S. Yang, A. M. James, D. M. Rayner, and P. A. Hackett, *Chem. Phys. Lett.* **231**, 177 (1994).

[58] S. Varga, K. Bolton, H. Grönbeck, A. Snis, A. Rosén, and B. Fricke, *Eur. Phys. J. D* **16**, 29 (2001).

[59] D. P. DiLella, W. Limm, R. H. Lipson, M. Moskovits, and K. V. Taylor, *J. Chem. Phys.* **77**, 5263 (1982).

[60] L.-S. Wang, H. Wu, and H. Cheng, *Phys. Rev. B* **55**, 12884 (1997).

[61] L. Fang, B. Davis, H. Lu, and J. R. Lombardi, *J. Phys. Chem. A* **105**, 9375 (2001).

[62] H. Cheng and L.-S. Wang, *Phys. Rev. Lett.* **77**, 51 (1996).

[63] C. Kohl and G. F. Bertsch, *Phys. Rev. B* **60**, 4205 (1999).

[64] D. Hobbs, G. Kresse, and J. Hafner, *Phys. Rev. B* **62**, 11556 (2000).

[65] K. D. Bier, T. L. Haslett, A. D. Kirkwood, and M. Moskovits, *J. Chem. Phys.* **89**, 6 (1988).

[66] M. R. Pederson, F. A. Reuse, and S. N. Khanna, *Phys. Rev. B* **58**, 5632 (1998).

[67] S. K. Nayak and P. Jena, *Chem. Phys. Lett.* **289**, 473 (1998).

[68] S. K. Nayak, B. K. Rao, and P. Jena, *J. Phys.: Condens. Matter* **10**, 10863 (1998).

[69] C. A. Baumann, R. J. Van Zee, S. Bhat, and W. Weltner, *J. Chem. Phys.* **78**, 190 (1983).

[70] R. Sekine, R. Kaldor, T. Yamamoto, and J. Onoe, *Radiochemistry* **45**, 233 (2003).

[71] H. Micklitz, M. Pasternak, and J. P. Sanchez, *Solid State Commun.* **55**, 667 (1985).

[72] D. M. Cox, D. J. Trevor, R. L. Whetton, E. A. Rohlfing, and A. Kaldor, *Phys. Rev. B* **32**, 4779 (1985).

[73] L. Zhou, Y. Hashi, Q. Sun, J. Yu, D. Wang, and Y. Kawazoe, *Phys. Rev. B* **59**, 1028 (1999).

[74] S. Shamai, M. Pasternak, and H. Micklitz, *Phys. Rev. B* **26**, 3031 (1982).

[75] E. A. Rohlfing, D. M. Cox, A. Kaldor, and K. H. Johnson, *J. Chem. Phys.* **81**, 3846 (1984).

[76] E. A. Rohlfing, D. M. Cox, and A. Kaldor, *J. Chem. Phys.* **81**, 3846 (1984).

[77] E. M. Nour, C. Alfaro-Franco, K. A. Gingerich, and J. Laane, *J. Chem. Phys.* **86**, 4779 (1987).

[78] H. Tatewaki, M. Tomonari, and T. Nakamura, *J. Chem. Phys.* **88**, 6419 (1988).

[79] S. K. Loh, D. A. Hales, L. Li, and P. B. Armentrout, *J. Chem. Phys.* **90**, 5466 (1989).

[80] J. L. Chen, C. S. Wang, K. A. Jackson, and M. R. Pederson, *Phys. Rev. B* **44**, 6558 (1991).

[81] M. Castro and D. R. Salahub, *Phys. Rev. B* **47**, 10955 (1993).

[82] O. B. Christensen and M. L. Cohen, *Phys. Rev. B* **47**, 13643 (1993).

[83] F. Gao, R. L. Johnston, and J. N. Murell, *J. Phys. Chem.* **97**, 12073 (1993).

[84] A. Vega, J. Dorantes-Davila, L. C. Balbas, and G. M. Pastor, *Phys. Rev. B* **47**, 4742 (1993).

[85] M. Castro and D. R. Salahub, *Phys. Rev. B* **49**, 11842 (1994).

[86] P. Ballone and R. O. Jones, *Chem. Phys. Lett.* **233**, 632 (1995).

[87] N. A. Besley, R. L. Johnston, A. J. Stace, and J. Uppenbrink, *J. Mol. Struct. (Theochem)* **341**, 75 (1995).

[88] A. N. Andriotis, N. Lathiotakis, and M. Menon, *Chem. Phys. Lett.* **260**, 15 (1996).

[89] M. Castro, C. Jamorski, and D. R. Salahub, *Chem. Phys. Lett.* **271**, 133 (1997).

[90] M. Castro, *Int. J. Quantum Chem.* **64**, 223 (1997).

[91] T. L. Haslett, K. A. Bosnick, S. Fedrigo, and M. Moskovits, *J. Chem. Phys.* **111**, 6456 (1999).

[92] G. L. Gutsev, S. N. Khanna, and P. Jena, *Phys. Rev. B* **62**, 1604 (2000).

[93] O. Diéguez, M. M. G. Alemany, C. Rey, P. Ordejón, and L. J. Gallego, *Phys. Rev. B* **63**, 205407 (2001).

[94] G. L. Gutsev, *Phys. Rev. B* **65**, 132417 (2002).

[95] S. Chrétien and D. R. Salahub, *Phys. Rev. B* **66**, 155425 (2002).

[96] P. Calaminici, *Chem. Phys. Lett.* **387**, 253 (2004).

[97] *Metal-Ligand Interactions: Structure and Reactivity*, edited by P. B. Armentrout (Kluwer Academic Publishers, Amsterdam, 1996).

[98] R. J. Van Zee, Y. M. Hamrick, S. Li, and W. Weltner, *Chem. Phys. Lett.* **195**, 214 (1992).

[99] D. A. Hales, C.-X. Su, L. Lian, and P. B. Armentrout, *J. Chem. Phys.* **100**, 1049 (1994).

[100] J. Ho, E. K. Parks, L. Zhu, and S. J. Riley, *Chem. Phys.* **201**, 245 (1995).

[101] C. Jamorski, A. Martinez, M. Castro, and D. R. Salahub, *Phys. Rev. B* **55**, 10905 (1997).

[102] H.-J. Fan, C.-W. Liu, and M.-S. Liao, *Chem. Phys. Lett.* **273**, 353 (1997).

[103] M. Pereiro, D. Baldomir, M. Iglesias, C. Rosales, and M. Castro, *Int. J. Quantum Chem.* **81**, 422 (2001).

[104] M. Pereiro, S. Man'kovsky, D. Baldomir, M. Iglesias, P. Mlynarski, M. Valladares, D. Suarez, M. Castro, and J. E. Arias, *Comp. Mat. Sci.* **22**, 118 (2001).

[105] S. Dennler, J. Morillo, and G. M. Pastor, *Surface Science* **532-535**, 334 (2003).

[106] A. B. Anderson, *J. Chem. Phys.* **66**, 5108 (1977).

[107] M. Moskovits and J. E. Hulse, *J. Chem. Phys.* **66**, 3988 (1977).

[108] H. Bash, M. D. Newton, and J. W. Moskowitz, *J. Chem. Phys.* **73**, 4492 (1980).

[109] M. Moskovits and D. P. DiLella, *J. Chem. Phys.* **72**, 2267 (1980).

[110] M. D. Morse, *Chem. Rev.* **86**, 1049 (1986).

[111] M. Tomonari, H. Tatewaki, and T. Nakamura, *J. Chem. Phys.* **85**, 2875 (1986).

[112] S. P. Walch, *J. Chem. Phys.* **86**, 5082 (1987).

[113] D. E. Ellis, J. Guo, and H.-P. Cheng, *J. Phys. Chem.* **92**, 3024 (1988).

[114] J. R. Woodward, S. H. Cobb, and J. L. Gole, *J. Phys. Chem.* **92**, 1404 (1988).

[115] H.-P. Cheng and D. E. Ellis, *J. Chem. Phys.* **94**, 3735 (1991).

[116] R. Fournier, M. S. Stave, and A. E. DePristo, *J. Chem. Phys.* **96**, 1530 (1992).

[117] C. Bureau, M. Defranceschi, and J. Delhalle, *Int. J. Quantum Chem.* **46**, 87 (1993).

[118] M. Madhu and J. Connolly, *Phys. Rev. B* **50**, 8903 (1994).

[119] E. K. Parks, L. Zhu, J. Ho, and S. J. Riley, *J. Chem. Phys.* **100**, 7206 (1994).

[120] F. A. Reuse and S. N. Khanna, *Chem. Phys. Lett.* **234**, 77 (1995).

[121] P. B. Balbuena and J. M. Seminario, *J. Theor. Comp. Chem.* **4**, 649 (1996).

[122] A. Posada-Amarillas and I. L. Garzon, *Phys. Rev. B* **54**, 10362 (1996).

[123] S. K. Nayak, S. N. Khanna, B. K. Rao, and P. Jena, *J. Phys. Chem. A* **101**, 1072 (1997).

[124] M. C. Michelini, R. P. Diez, and A. H. Jubert, *Int. J. Quantum Chem.* **70**, 693 (1998).

[125] S. E. Weber and P. Jena, *Chem. Phys. Lett.* **281**, 401 (1997).

[126] F. A. Reuse and S. N. Khanna, *Eur. Phys. J. D* **6**, 77 (1999).

[127] W. T. Chan and R. Fournier, *Chem. Phys. Lett.* **315**, 257 (1999).

[128] B. V. Reddy, S. K. Nayak, S. N. Khanna, B. K. Rao, and P. Jena, *J. Phys. Chem. A* **102**, 1748 (1998).

[129] E. Curotto, A. Matro, D. L. Freeman, and J. D. Doll, *J. Chem. Phys.* **108**, 729 (1998).

[130] C. Ashman, S. N. Khanna, and M. R. Pederson, *Chem. Phys. Lett.* **368**, 257 (2002).

[131] G. A. Cisneros, M. Castro, and D. R. Salahub, *Int. J. Quantum Chem.* **75**, 847 (1999).

[132] E. Viitala, H. Häkkinen, M. Manninen, and J. Timonen, *Phys. Rev. B* **61**, 8851 (2000).

[133] F. Calvayrac, *Comp. Mat. Sci.* **17**, 164 (2000).

[134] M. C. Michelini, R. P. Diez, and A. H. Jubert, *Int. J. Quantum Chem.* **85**, 22 (2001).

[135] P. A. Derosa, J. M. Seminario, and P. B. Balbuena, *J. Phys. Chem. A* **105**, 7917 (2001).

[136] B. Chen, A. W. Castleman, and S. N. Khanna, *Chem. Phys. Lett.* **304**, 423 (1999).

[137] K. M. Ervin, J. Ho, and W. C. Lineberger, *J. Chem. Phys.* **89**, 4514 (1988).

[138] A. B. Anderson, *J. Chem. Phys.* **68**, 1744 (1978).

[139] C. Bachmann, J. Demuynck, and A. Veillard, *Faraday Symp. Roy. Soc. Chem.* **14**, 170 (1980).

[140] A. R. Miedema, *Faraday Symp. Roy. Soc. Chem.* **14**, 136 (1980).

[141] G. del Conde, P. S. Bagus, and O. Novaro, *Phys. Rev. B* **25**, 7842 (1982).

[142] D. Post and E. J. Baerends, *Chem. Phys. Lett.* **86**, 176 (1982).

[143] H. Tatewaki, E. Miyoshi, and T. Nakamura, *J. Chem. Phys.* **76**, 5073 (1982).

[144] D. P. DiLella, K. Taylor, and M. Moskovits, *J. Phys. Chem.* **87**, 524 (1983).

[145] J. A. Howard, K. F. Preston, R. Sutcliffe, and B. Mile, *J. Phys. Chem.* **87**, 536 (1983).

[146] G. H. Jeung, M. Pelissier, and J. C. Barthelat, *Chem. Phys. Lett.* **97**, 369 (1983).

[147] E. Miyoshi, H. Tatewaki, and T. Nakamura, *J. Chem. Phys.* **78**, 815 (1983).

[148] E. Miyoshi, H. Tatewaki, and T. Nakamura, *Int. J. Quantum Chem.* **23**, 1201 (1983).

[149] M. D. Morse, J. B. Hopkins, P. R. R. Langridge-Smith, and R. E. Smalley, *J. Chem. Phys.* **79**, 5316 (1983).

[150] W. Weltner and R. J. Van Zee, *Ann. Rev. Phys. Chem.* **35**, 291 (1984).

[151] M. Moskovits, *Chem. Phys. Lett.* **118**, 111 (1985).

[152] S.-W. Wang, *J. Chem. Phys.* **82**, 4633 (1985).

[153] W. H. Crumley, J. S. Hayden, and J. L. Gole, *J. Chem. Phys.* **84**, 5250 (1986).

[154] S. R. Langhoff, C. W. Bauschlicher, S. P. Walch, and B. C. Laskowski, *J. Chem. Phys.* **85**, 7211 (1986).

[155] E. A. Rohlfing and J. J. Valentini, *Chem. Phys. Lett.* **126**, 113 (1986).

[156] D. G. Truhlar, T. C. Thompson, and C. A. Mead, *Chem. Phys. Lett.* **127**, 287 (1986).

[157] S. P. Walch, C. W. Bauschlicher, and S. R. Langhoff, *J. Chem. Phys.* **85**, 5900 (1986).

[158] S. P. Walch and B. C. Laskowski, *J. Chem. Phys.* **84**, 2734 (1986).

[159] J. W. Zwanziger, R. L. Whetten, and E. R. Grant, *J. Phys. Chem.* **90**, 3298 (1986).

[160] D. M. Lindsay, G. A. Thompson, and Y. Wang, *J. Phys. Chem.* **91**, 2630 (1987).

[161] M. D. Morse, *Chem. Phys. Lett.* **133**, 8 (1987).

[162] A. Ramírez-Solís, O. Novaro, and M. E. Ruiz, *Phys. Rev. B* **35**, 4082 (1987).

[163] C. W. Bauschlicher, S. R. Langhoff, and P. R. Taylor, *J. Chem. Phys.* **88**, 1041 (1988).

[164] C. W. Bauschlicher, S. R. Langhoff, and H. Partridge, *J. Chem. Phys.* **91**, 2412 (1989).

[165] A. O'Keefe, J. J. Scherer, A. L. Cooksy, R. Sheeks, J. Heath, and R. J. Saykally, *Chem. Phys. Lett.* **172**, 214 (1990).

[166] M. B. Knickelbein, *J. Chem. Phys.* **100**, 4729 (1994).

[167] M. B. Knickelbein, *J. Chem. Phys.* **100**, 2388 (1994).

[168] H. Koizumi and S. Sugano, *J. Chem. Phys.* **102**, 4472 (1995).

[169] C. Massobrio, A. Pasquarello, and R. Car, *Chem. Phys. Lett.* **238**, 215 (1995).

[170] Q. Sun, X. G. Gong, Q. Q. Zheng, and G. H. Wang, *Phys. Lett. A* **209**, 249 (1995).

[171] L. Triguero, U. Wahlgren, P. Boussard, and P. Siegbahn, *Chem. Phys. Lett.* **237**, 550 (1995).

[172] P. Calaminici, A. M. Koester, N. Russo, and D. R. Salahub, *J. Chem. Phys.* **105**, 9546 (1996).

[173] F. Illas, J. M. Ricart, and M. Fernández-García, *J. Chem. Phys.* **104**, 5647 (1996).

[174] C. Massobrio, A. Pasquarello, and A. Dal Corso, *J. Chem. Phys.* **109**, 6626 (1998).

[175] S. Erkoç and R. Shaltaf, *Phys. Rev. A* **60**, 3053 (1999).

[176] P. Fuentealba and Y. Simón-Manso, *Chem. Phys. Lett.* **314**, 108 (1999).

[177] P. Calaminici, A. M. Köster, and A. Vela, *J. Chem. Phys.* **113**, 2199 (2000).

[178] O. Ingólfsson, U. Busolt, and K.-I. Sugwara, *J. Chem. Phys.* **112**, 4613 (2000).

[179] V. A. Spasov, T.-H. Lee, and K. M. Ervin, *J. Chem. Phys.* **112**, 1713 (2000).

[180] P. Jaque and A. Toro-Labbé, *J. Chem. Phys.* **117**, 3208 (2002).

[181] K. Jug, B. Zimmerman, P. Calaminici, and A. M. Köster, *J. Chem. Phys.* **116**, 4497 (2002).

[182] K. Jug, B. Zimmerman, and A. M. Köster, *Int. J. Quantum Chem.* **90**, 594 (2002).

[183] M. I. Belinsky, *Inorg. Chem.* **43**, 739 (2004).

[184] M. Tomonari, H. Tatewaki, and T. Nakamura, *J. Chem. Phys.* **80**, 344 (1984).

[185] H. Tatewaki, M. Tomonari, and T. Nakamura, *J. Chem. Phys.* **82**, 5608 (1985).

[186] H.-J. Flad, F. Schautz, Y. Wang, M. Dolg, and A. Savin, *Eur. Phys. J. D* **6**, 243 (1999).

[187] S. Park, K. Lee, and C. Lee, *J. Korean Phys. Soc.* **34**, 310 (1999).

[188] S. Katırcıoğlu and S. Erkoç, *J. Mol. Struct. (Theochem)* **546**, 99 (2001).

[189] S. Erkoç, *Chem. Phys. Lett.* **369**, 605 (2003).

[190] J. Wang, G. Wang, and J. Zhao, *Phys. Rev. A* **68**, 013201 (2003).

# CHAPTER 5

# CONCLUSIONS

Application of DFT to large or complicated molecular systems continues to expand out knowledge of the world around us. Its scaling and inclusion of some correlation effects makes it an extremely versatile methodology in computational chemistry. Despite issues relating to both accuracy and precision, this versitality ensures its continued use and development.

The nature of current functionals necessitates the use of a numerical integration quadrature. This is a source of potential error that many researchers neglect. Figures 2.1 to 2.7 were created to provide a precision guide which users new to the field may refer to when using DFT in computations. In the worst of cases, loss of precision due to poor grid quadrature choice was on the order of 1 kcal $mol^{-1}$.

The scaling of DFT allows its use on biologically significant systems. In Chapter 3 linear PAH derived systems were studied, including pentacenyl. PAH systems become reactive upon hydrogen abstraction, creating the –enyl radicals which were examined. Once a radical, these systems can either react chemically with other molecules, or pull an electron away from another system. For every radical examined, the electron affinity was a positive number, indicating that electron attachment is favorable.

Transition metals represent a special challenge to both theory and experiment. Complex electronic structures and a large number of valence electrons makes electronic structure based correlation methods difficult to apply. With care and persistence, DFT can yield chemically significant results for these complicated systems, as shown in the study of homonuclear trimers presented in Chapter 4.

In the physical sciences, it is often desired to strive for perfection, to find the absolute truth. This can be a trap. In our desire to understand out surroundings, we often study systems which are currently technologically infeasible to describe flawlessly. It is often necessary to accept errors in the name of finding an answer, but care must be taken to understand the consequences of these errors. So long as the weaknesses of DFT are considered during an investigation, the answers it provides can further scientific knowledge.